

**THE IDENTIFICATION OF NOVEL REGULATORY ELEMENTS IN
THE PROMOTERS OF HEAT SHOCK RESPONSE GENES**

SIFELANI NCUBE



A thesis submitted in partial fulfilment of the requirements of Magister Scientiae
in the Faculty of Science, University of the Western Cape.

Supervisor: Dr Mervin Meyer

November 2010

ABSTRACT

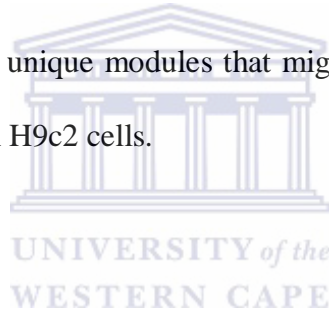
THE IDENTIFICATION OF NOVEL REGULATORY ELEMENTS IN THE PROMOTERS OF HEAT SHOCK RESPONSE GENES

S. Ncube

M.Sc. thesis, Department of Biotechnology, Faculty of Science, University of the Western Cape, South Africa.

Mammalian cells have evolved self-protective mechanisms that are activated in response to cellular stress, including non-lethal heat shock (heat shock response-HSR). These adaptive and cytoprotective mechanisms are mediated by heat shock factors that bind to cognate sequences in the promoters of heat shock responsive genes. The main objective of this study was to investigate promoter sequences of putative HSR genes for the presence of unique regulatory elements and modules that might be involved in the regulation of HSR. In order to achieve this objective, an *in silico* promoter analysis strategy was devised, which focused on the identification of promoter sequences and regulatory elements, and modelling of promoter modules by using Genomatix software tools such as MatInspector and ModelInspector. Results showed that two modules (EGRF_SP1F_01 and SP1F_CEBP_01) were conserved in the promoter sequences of three well-known Hsp-genes (*Hsp90*, *Hsp105 β* and *$\alpha\beta$ -crystallin*). Screening the 60 target gene promoters for the presence of the two modules revealed that 12 genes (20 %) contained both modules. These included *Moesin*, *Proline-4 hydroxylase*, *Poly(A) binding protein* and *Formin-binding protein*. None of these genes had been previously associated with heat shock response.

As a result, the expression of the 12 putative HSR genes in response to heat shock was further investigated using experimental analyses. This included optimisation of a heat shock system using cultured H9c2 cells, toxicity testing, Western blot analysis and qRT-PCR. Results obtained showed that pre-conditioned H9c2 cell cultures were significantly protected ($p < 0.05$) from pro-apoptotic effects of ethanol compared to control cells. Real-time quantitative reverse transcription polymerase chain reaction revealed that *Atic*, *Pabpc1* and *Cacybp* were slightly up-regulated in cultured H9c2 cells after heat shock treatment. Known functions of these genes include mRNA processing, Ca^{2+} metabolism and regulation of the cytoskeleton. Thus the conclusion drawn from this study was that EGRF_SP1F_01 and SP1F_CEBP_01 are unique modules that might be involved in the regulation of heat shock response in H9c2 cells.



KEY WORDS

Apoptosis

Cardiomyocytes

Cytoprotection

Heat shock proteins

Heat shock response

Inducible gene expression

Molecular chaperones

Real-time quantitative PCR

Regulatory elements

Unfolded protein response



DEDICATION

For Nozi and Nyasha...



DECLARATION

I declare that “THE IDENTIFICATION OF NOVEL REGULATORY ELEMENTS IN THE PROMOTERS OF HEAT SHOCK RESPONSE GENES” is my own work that has not been submitted for any degree or examination in any other university and that all the sources I have used or quoted have been indicated and acknowledged by complete references.

Sifelani Ncube



Signed:.....

November 2010

TABLE OF CONTENTS

| | |
|---|-------------|
| ABSTRACT | ii |
| KEY WORDS | iv |
| DEDICATION | v |
| DECLARATION | vi |
| TABLE OF CONTENTS | vii |
| LIST OF FIGURES | xi |
| LIST OF TABLES | xiii |
| ABBREVIATIONS | xiv |
| ACKNOWLEDGEMENTS | xvi |
| CHAPTER 1.0: LITERATURE REVIEW | 1 |
| 1.1 Introduction | 1 |
| 1.2 The effects of stress on cellular function | 5 |
| 1.3 Apoptosis | 8 |
| 1.3.1 Mitochondrial stress-induced apoptotic signalling pathway | 9 |
| 1.3.2 The endoplasmic reticulum (ER) stress-mediated apoptotic signalling pathway | 9 |
| 1.4 Cellular defence mechanism against stress and cell death | 12 |
| 1.5 Stress or “Heat shock” proteins: Definitions and nomenclature | 14 |
| 1.6 The role of stress proteins in diseases | 16 |
| 1.7 Expression of stress proteins in the cardiovascular tissues | 17 |
| 1.8 The protective effect of stress proteins in the myocardium | 18 |
| 1.9 Hsps function as molecular chaperones | 20 |
| 1.9.1 Cytosolic and nuclear chaperones | 21 |
| 1.9.2 Molecular chaperones in cellular organelles | 23 |
| 1.10 Hsps associate with key apoptotic proteins | 24 |
| 1.11 Hsps as potential therapeutic targets to modulate apoptosis | 28 |
| 1.12 Methods used to active the stress response | 28 |
| 1.12.1 Pharmacological methods | 29 |
| 1.12.2 Gene therapy methods | 31 |
| 1.13 Principles of transcriptional regulation | 31 |
| 1.14 Transcriptional regulation of heat shock genes (Hsp-genes) | 32 |

| | |
|---|-----------|
| 1.15 Bioinformatics tools and the principle of transcriptional co-regulation | 34 |
| 1.16 Progress in <i>in silico</i> promoter analysis..... | 35 |
| CHAPTER 2.0: MATERIALS AND METHODS..... | 39 |
| 2.1 General chemicals and suppliers | 39 |
| 2.2 Kits | 41 |
| 2.3 Enzymes..... | 41 |
| 2.4 General stock solutions and buffers..... | 41 |
| 2.5 Bacterial culture | 44 |
| 2.5.1 Bacterial strain..... | 44 |
| 2.5.2 Culturing MC1061 | 44 |
| 2.5.3 Storage of bacterial strain and clones..... | 44 |
| 2.6 Cloning vector..... | 44 |
| 2.6.1 pcDNA3.1(+)/zeocin..... | 44 |
| 2.7 Preparation of <i>E. coli</i> competent cells for transformation..... | 48 |
| 2.8 Bacterial transformation | 48 |
| 2.9 Preparation of plasmid DNA..... | 49 |
| 2.9.1 Small-scale preparation of plasmid DNA..... | 49 |
| 2.9.2 Large-scale recovery of plasmid DNA from transformed MC1061 <i>E. coli</i> bacterial cells by double cesium chloride/ethidium bromide fractionation | 50 |
| 2.10 Restriction enzyme digestion of plasmid DNA | 52 |
| 2.11 Dephosphorylation of digested plasmid DNA..... | 53 |
| 2.12 Design of cloning primers..... | 54 |
| 2.13 Amplification of target fragments by PCR..... | 58 |
| 2.14 Agarose gel electrophoresis of DNA | 60 |
| 2.14.1 DNA molecular weight markers | 60 |
| 2.14.2 Agarose gel purification of DNA..... | 61 |
| 2.14.3 Restriction enzyme digestion of PCR fragments | 61 |
| 2.15 Construction of expression vectors..... | 62 |
| 2.16 Colony PCR | 63 |
| 2.17 DNA Sequencing..... | 63 |
| 2.18 Cell culture..... | 63 |
| 2.18.1 Cell line..... | 63 |

| | | |
|----------------------------------|--|-----------|
| 2.18.2 | Culturing of cells | 64 |
| 2.18.3 | Trypsinisation of cultured cells..... | 64 |
| 2.18.4 | Freezing cells..... | 65 |
| 2.18.5 | Transfection of cells..... | 65 |
| 2.19 | Isolation of total cellular proteins from cell cultures | 66 |
| 2.20 | Sodium dodecylsulphate polyacrylamide gel electrophoresis (SDS-PAGE) and protein transfer..... | 67 |
| 2.21 | Probing the blot with antibodies | 68 |
| 2.22 | Detection and exposure..... | 68 |
| 2.23 | Isolation of total ribonucleic acid (total RNA) from cells | 69 |
| 2.23.1 | Homogenisation..... | 69 |
| 2.23.2 | Phase separation | 69 |
| 2.23.3 | RNA precipitation..... | 70 |
| 2.23.4 | RNA wash | 70 |
| 2.23.5 | Re-dissolving the RNA | 70 |
| 2.23.6 | Assessing RNA quality | 70 |
| 2.24 | Reverse transcription (RT)..... | 73 |
| 2.24.1 | Target RNA and oligo(dT) primer combination and denaturation | 73 |
| 2.24.2 | Reverse transcription reaction | 74 |
| 2.25 | Real-time quantitative reverse transcription polymerase chain reaction | 75 |
| 2.25.1 | Primer design for qRT-PCR | 75 |
| 2.25.2 | Generation of standard curves | 80 |
| 2.25.3 | Amplification efficiency (E)..... | 80 |
| 2.25.4 | Relative gene expression | 80 |
| 2.25.5 | Quantification of relative gene expression in H9c2 cells by qRT-PCR..... | 82 |
| 2.26 | Cytoprotection Assays | 82 |
| 2.27 | The APOPercentage™ apoptosis Assay..... | 83 |
| 2.28 | <i>In silico</i> analysis of gene regulation..... | 84 |
| 2.28.1 | Identifying promoter sequences..... | 86 |
| 2.28.2 | Screening promoter sequences for the HSE (V\$HEAT) | 86 |
| 2.28.3 | Screening HSR genes for the presence of common promoter modules..... | 86 |
| CHAPTER 3.0: RESULTS..... | | 87 |

| | |
|--|------------|
| 3.1 Establishing heat shock response in H9c2 cells..... | 87 |
| 3.2 Characterisation of heat shock induced cytoprotection..... | 88 |
| 3.3 | 88 |
| 3.4 <i>In silico</i> analysis of promoter sequences..... | 91 |
| 3.5 Investigating the expression levels of genes containing conserved sequence motifs..... | 98 |
| 3.6 The over-expression of heat shock responsive genes in H9c2 genes..... | 110 |
| CHAPTER 4.0: DISCUSSION | 121 |
| 4.1 Heat shock optimisation and cytoprotection | 121 |
| 4.2 <i>In silico</i> analysis of gene regulation | 123 |
| 4.3 Real-time qRT-PCR analyses..... | 126 |
| CONCLUSIONS AND FUTURE DIRECTIONS | 130 |
| REFERENCES | 132 |



LIST OF FIGURES

| | |
|---|----|
| Figure 1.1: Images of a whole heart and coronary arteries showing damage (dead heart muscle) caused by blockage of the coronary artery. | 2 |
| Figure 1.2: A schematic illustration of major cellular pathways that are activated in response to stress. | 6 |
| Figure 1.3: A schematic illustration of the mitochondrial stress-induced apoptotic signalling pathway. | 10 |
| Figure 1.4: ER stress-mediated apoptotic signalling pathways. | 11 |
| Figure 1.5: A schematic model illustrating the coordinated action of the ESR through the UPR and ERAD. | 13 |
| Figure 1.6: Schematic illustration of interactions between the chaperones Hsc70 and nascent peptide chains or unfolded proteins. | 22 |
| Figure 1.7: Summary of regulation of apoptosis signalling pathways in cardiomyocytes. | 26 |
| Figure 1.8: Nucleotide sequence of the Hsp70 HSE (nt -130 to -81). | 32 |
| Figure 1.9: General structure and regulatory features of HSFs. | 33 |
| Figure 1.10: Graphic output from MatInspector showing the location of various TFBS in the promoter sequences of <i>Hsph1</i> and <i>Cryab</i> | 36 |
| Figure 2.1: Restriction maps of pcDNA3.1 vectors and the MCS of pcDNA3.1(+) (adapted from www.google.com). | 46 |
| Figure 2.2: Full coding sequence of <i>Atic</i> showing the position of the forward primer (yellow) and the reverse primer (purple). | 56 |
| Figure 2.3: Full coding sequence of <i>Pabpc1</i> showing the position of the forward primer (yellow) and the reverse primer (purple). | 57 |
| Figure 2.4: Full coding sequence of <i>Hsp27</i> showing the position of the forward primer (yellow) and the reverse primer (purple). | 57 |
| Figure 2.5: DNA molecular weight markers that were used to estimate the size of DNA fragments. | 60 |
| Figure 2.6: H9c2 cells viewed using a Nikon inverted light microscope (Magnification: 20x). | 64 |
| Figure 2.7: An example of electropherograms of different RNA samples with varying RIN (adapted from http://openwetware.org). | 72 |
| Figure 2.8: A schematic illustration of the strategy devised for <i>in silico</i> promoter analysis. | 85 |
| Figure 3.1: Western immunoblot of Hsc70/Hsp70 in H9c2 cells (a) and a polyacrylamide gel that was used as a sample loading control (b). | 87 |
| Figure 3.2: Histograms showing the shift in the position of the absorbance peak and percentage cell distribution as measured by the APOPercentage™ apoptosis assay. | 88 |
| Figure 3.3: The effects of ethanol concentration and time of exposure on H9c2 cells. | 89 |

| | |
|--|-----|
| Figure 3.4: The APOPercentage™ apoptosis assay showing the exposure time-dependent effect of 10 % ethanol on H9c2 cells. | 90 |
| Figure 3.5: The cytoprotective effect of heat shock treatment against subsequent pro-apoptotic effects of ethanol in H9c2 cells. | 91 |
| Figure 3.6: Graphic output from MatInspector showing the location of V\$HEAT in the promoters of known Hsps. | 93 |
| Figure 3.7: Electropherogram summary of an RNA sample extracted from H9c2 cells (a) and Gel electrophoresis image showing the 18S and 28S subunits of rRNA (b). | 98 |
| Figure 3.8: Real-time qRT-PCR amplification curves showing expression levels of <i>HPRT1</i> and <i>Hsp90</i> in non heat shocked (NHS) and heat shocked (HS) H9c2 cells. | 99 |
| Figure 3.9: Melting curves (a) and melting peaks (b) for <i>Karyopherin α-3</i> , <i>Clathrin</i> , <i>Hypoxanthine phosphoribosyltransferase 1</i> and <i>Filamin</i> | 100 |
| Figure 3.10: Amplification curves of standards (a) and the generated standard curve for <i>Atic</i> (b). | 101 |
| Figure 3.11: Amplification curves of standards (a) and the generated standard curve for <i>Cacybp</i> (b). | 102 |
| Figure 3.12: Amplification curves of standards (a) and the generated standard curve for <i>HPRT1</i> (b). | 103 |
| Figure 3.13: Amplification curves of standards (a) and the generated standard curve for <i>Hsp27</i> (b). | 104 |
| Figure 3.14: Amplification curves of standards (a) and the generated standard curve for <i>Pabpc1</i> (b). | 105 |
| Figure 3.15: Amplification curves of standards (a) and the generated standard curve for <i>RhoE</i> (b). | 106 |
| Figure 3.16: Expression levels of known Hsps in H9c2 cells following heat shock treatment. ... | 108 |
| Figure 3.17: Expression levels of various target genes in H9c2 cells following heat shock treatment. | 109 |
| Figure 3.18: PCR amplification of full coding sequences of <i>Atic</i> (1 779 bp) (a), <i>Pabpc1</i> (1 911 bp) (b) and <i>Hsp27</i> (618 bp) (c) from cDNA. | 110 |
| Figure 3.19: Agarose gel electrophoresis images of the undigested pcDNA3.1(+) vector (5 015 bp) and after digestion with <i>Bam</i> HI and <i>Not</i> I restriction enzymes. | 111 |
| Figure 3.20: Colony PCR screen of bacterial colonies for clones containing <i>Hsp27</i> | 112 |
| Figure 3.21: Graphic illustration of DNA sequence trace. | 113 |
| Figure 3.22: BLAST search results for the <i>Hsp27</i> sequence. | 114 |
| Figure 3.23: Colony PCR screen of bacterial colonies for clones containing <i>Atic</i> | 115 |
| Figure 3.24: BLAST search results for the <i>Atic</i> sequence. | 116 |
| Figure 3.25: Colony PCR screen of bacterial colonies for clones containing <i>Pabpc1</i> | 118 |
| Figure 3.26: BLAST search results for the <i>Pabpc1</i> sequence. | 119 |
| Figure 3.27: Relative expression of various target genes in transiently transfected H9c2 cells. ... | 120 |

LIST OF TABLES

| | |
|---|-----|
| Table 1.1: A list of abnormal proteins that are targeted for degradation by ERAD (adapted from Sherman and Goldberg, 2001)..... | 14 |
| Table 1.2: Pharmacological modifiers of Hsp action (Sreedhar and Csermely, 2004). | 29 |
| Table 2.1: Restriction enzyme digestion mix..... | 53 |
| Table 2.2: Dephosphorylation reaction set-up using shrimp alkaline phosphatase (SAP)..... | 54 |
| Table 2.3: Primers that were designed to amplify full-length coding sequences of <i>Atic</i> (1 779 bp), <i>Pabpc1</i> (1 911 bp) and <i>Hsp27</i> (618 bp) by PCR. | 55 |
| Table 2.4: PCR components. | 59 |
| Table 2.5: Components of the ligation reaction. | 62 |
| Table 2.6: Experimental reaction mix. | 73 |
| Table 2.7: Reverse transcription reaction mix. | 74 |
| Table 2.8: Forward and reverse primer sequences designed to amplify each of the 16 target genes and the endogenous reference gene <i>HPRT 1</i> using qRT-PCR. | 76 |
| Table 2.9: Real-time qRT-PCR cocktail using the LightCycler® FastStart DNA Master SYBR Green I kit. | 77 |
| Table 2.10: General qRT-PCR cycling program..... | 79 |
| Table 3.1: Functional classification of up- and down-regulated genes identified by SSH..... | 92 |
| Table 3.2: Presence of the heat shock response element (V\$HEAT) in the promoter regions of genes identified by SSH. | 94 |
| Table 3.3: The presence of EGRF_SP1F_01 and SP1F_CEBP_01 promoter modules and their position on the – and + DNA strands of putative HSR genes. | 96 |
| Table 3.4: Amplification efficiencies (<i>E</i>) of six target gene fragments that were amplified by qRT-PCR..... | 107 |

ABBREVIATIONS

| | |
|-------|--|
| AIF | Apoptosis-inducing factor |
| Apaf1 | Apoptosis protease activating factor 1 |
| ASK1 | Apoptosis signal-regulating kinase 1 |
| CARE | <i>cis</i> -acting regulatory elements |
| CDNA | complementary deoxyribonucleic acid |
| DNA | Deoxyribonucleic acid |
| ER | Endoplasmic reticulum |
| ERAD | ER-associated degradation |
| ESR | ER stress response |
| GDNA | genomic deoxyribonucleic acid |
| Grp | Glucose-related proteins |
| HS | Heat shock |
| HSE | Heat shock element |
| HSF | Heat shock factor |
| Hsp | Heat shock protein |
| Hsps | Heat shock proteins |
| HSR | Heat shock response |

| | |
|--------|-----------------------------------|
| I/R | Ischemia-reperfusion |
| JNK | c-Jun-N-terminal kinase |
| mt-Hsp | Mitochondrial heat shock protein |
| NHS | Non heat shock |
| PCR | Polymerase chain reaction |
| RNA | Ribonucleic acid |
| ROS | Reactive oxygen species |
| TFBS | Transcription factor binding site |
| UPR | Unfolded protein response |



ACKNOWLEDGEMENTS

I would like to worship the Almighty God for blessing me with life, resources and determination to accomplish this work. I would like to thank my supervisor Dr Mervin Meyer, Biotechnology Department, University of the Western Cape, for his mentorship throughout this study. I am very grateful to my dear wife Nozipho, my boy Nyasha M., my parents and my brothers for their sacrifice and support. I would also like to thank Ms Cleo Dodgen, Dr Faghri February, Mr Zukile Mbitha, Dr Joseph Mafofo, Dr Rudo Ngara and Dr Amanda Skepu for their valuable contributions and advice which made my work less strenuous. I am also very grateful to Dr Craig J. Kinner and Ms Jomien Mouton, both from the MRC/SU Centre for Molecular and Cellular Biology, University of Stellenbosch, for allowing me to use their tissue culture laboratory. I am thankful to my friends Dr Modreck Chibi, Mr Stonard Kanyanda, Dr Claudius Maronedze, and Mr Zedias Chikwambi for being there for me when I needed a helping hand. I would like to thank each and every member of the Apoptosis Research Group, Biotechnology Department, University of the Western Cape, for their support, one way or another, and everyone who made a positive contribution to this study. I am grateful to the National Research Foundation, South Africa, for funding this research.

CHAPTER 1.0: LITERATURE REVIEW

1.1 Introduction

Myocardial infarction, a clinical manifestation of ischemic heart injury, is one of the leading causes of death in modern society (World Health Organisation, 2010). Myocardial ischaemic injury is usually caused by severe impairment of the coronary blood supply, mostly as a result of occlusion of blood vessels by coronary atherosclerotic plaque or clamping during a surgical procedure, which cuts off the supply of oxygen and nutrients to the heart tissue (Hamacher-Brandy *et al.*, 2006). The resulting condition of low oxygen and nutrient supply is called ischaemia and is associated with decreased intracellular ATP and low pH due to accumulation of lactate and retention of carbon dioxide (Gill *et al.*, 2000). If the supply of oxygen and nutrients to the heart muscle is not rapidly restored, massive postischaemic cell death and tissue destruction may occur in the affected area (Figure 1.1).

In order to restore blood flow and prevent irreversible damage to the myocardium, reperfusion of blood must be done following ischaemia. Unfortunately, reperfusion has also been shown to cause various injuries to the heart tissue, including membrane permeation, contractile abnormalities, calcium influx, and depletion of high-energy phosphates, which ultimately leads to cell death (Umansky and Tomei, 1997; Gottlieb *et al.*, 1994). The damage inflicted to the myocardium as a result of the combined effects of ischaemia and reperfusion is referred to as ischaemic/reperfusion (I/R) injury. Additionally, increased production of reactive oxygen species (ROS) has been reported in cardiomyocytes

following I/R injury (Fleury *et al.*, 2002; Cook *et al.*, 1999; Von Harsdorf *et al.*, 1999; Zweier *et al.*, 1987). Excessive intracellular generation of ROS causes peroxidation of membrane lipids, damage proteins and inactivate enzymes (Yellon and Hausenloy, 2007; Butterfield *et al.*, 1997), which eventually results in cell death.

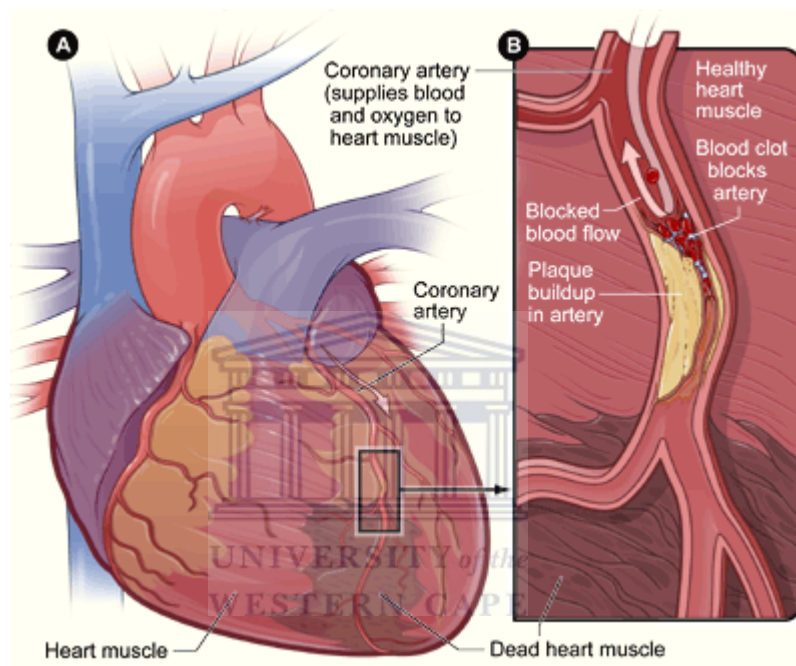


Figure 1.1: Images of a whole heart and coronary arteries showing damage (dead heart muscle) caused by blockage of the coronary artery.

A. Damaged heart muscle as a result of blockage of the coronary arteries that supply oxygen and nutrients to the heart muscle.

B. A cross section of the coronary artery showing a build-up of plaque and a blood clot that block blood flow resulting in death of heart muscle cells in the affected area (adapted from <http://www.speakingofresearch.files.wordpress.com/>).

In spite of the controversy surrounding the role of apoptosis in myocardial infarction, cumulative evidence suggests that indeed apoptosis contributes to loss of cardiomyocytes following I/R injury (Freude *et al.*, 2000; Schunkert and Riegger, 2000; Zhao *et al.*, 2000; Gottlieb and Engler, 1999; James, 1998; Kajtsura *et al.*, 1996). Mitochondrial stress, ER stress, oxidative stress, calcium overload, and other stimulators of pro-apoptotic factors are believed to be the pathophysiological triggers of apoptosis in the myocardium (Opie, 1993). Cardiomyocytes are terminally differentiated cells and once dead are rarely replaced (Kimes and Brandt, 1976). Thus loss of cardiomyocytes as a result of I/R injury contributes to reduced function of the heart muscle, which eventually manifests as myocardial infarction.

Cellular effects of hyperthermia are similar to those caused by ischaemia/reperfusion. These include inhibition of cap-dependent (i.e., general) protein synthesis, disintegration of the cytoskeleton, disruption of numerous metabolic processes, mitochondrial damage and uncoupling of oxidative phosphorylation (Cuesta *et al.* 2000; Liu *et al.*, 1992). These often lead to cell death when the stress is persistent and/or excessive. However, exposure of living cells, including cardiomyocytes, to a mild, non-lethal thermal stress (5 °C above normal growth temperature) has been shown to activate adaptive and protective cellular mechanisms that are collectively known as the stress response (SR). The SR increases the ability of a cell to cope with stress and to withstand fatal subsequent stress events (Quigney *et al.*, 2003). This phenomenon is referred to as heat shock preconditioning. Although originally discovered as a response to thermal stress (Ritossa, 1962), the SR is triggered by a variety of stressful

conditions that interfere with protein folding, transport and function (Kaufman, 2002).

In addition to heat shock preconditioning, studies have demonstrated that subjecting the heart muscle to brief episodes of mild ischaemia (ischaemic preconditioning-IP) also preserve the myocardium against fatal I/R injury (Arnaud *et al.*, 2003; Brar *et al.*, 1999; Piot *et al.*, 1999; Martin *et al.*, 1997). This discovery has led to intense investigation into the subject, more so over the past decade. The aim is to develop a better understanding of the mediators and mechanisms underlying cytoprotection, which comes about as a result of preconditioning, in the hope that these may provide novel targets for therapeutic intervention against chronic and acute I/R injury. To date the cytoprotective effects of heat shock- and ischemic preconditioning have largely been ascribed to increased expression of Hsps. However, the mechanism(s) of this preservation is still not fully understood. Thus it is conceivable that there are yet-to-be-discovered mediators in these cytoprotective pathways.

This literature review summarises present knowledge about the effects of stress on cellular functions, the role of stress-mediated apoptotic signalling pathways in cardiomyocyte death, cellular response to stress, the cytoprotective roles of stress proteins, the importance of stress proteins as potential therapeutic targets against fatal I/R injury, and recent developments in *in silico* analysis of gene regulation. The last section of this chapter outlines the history behind this study and the objectives that were set.

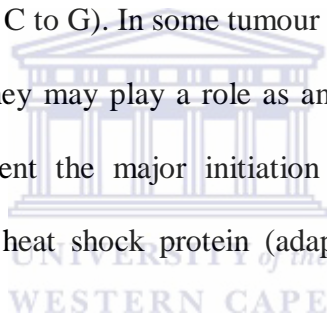
1.2 The effects of stress on cellular function

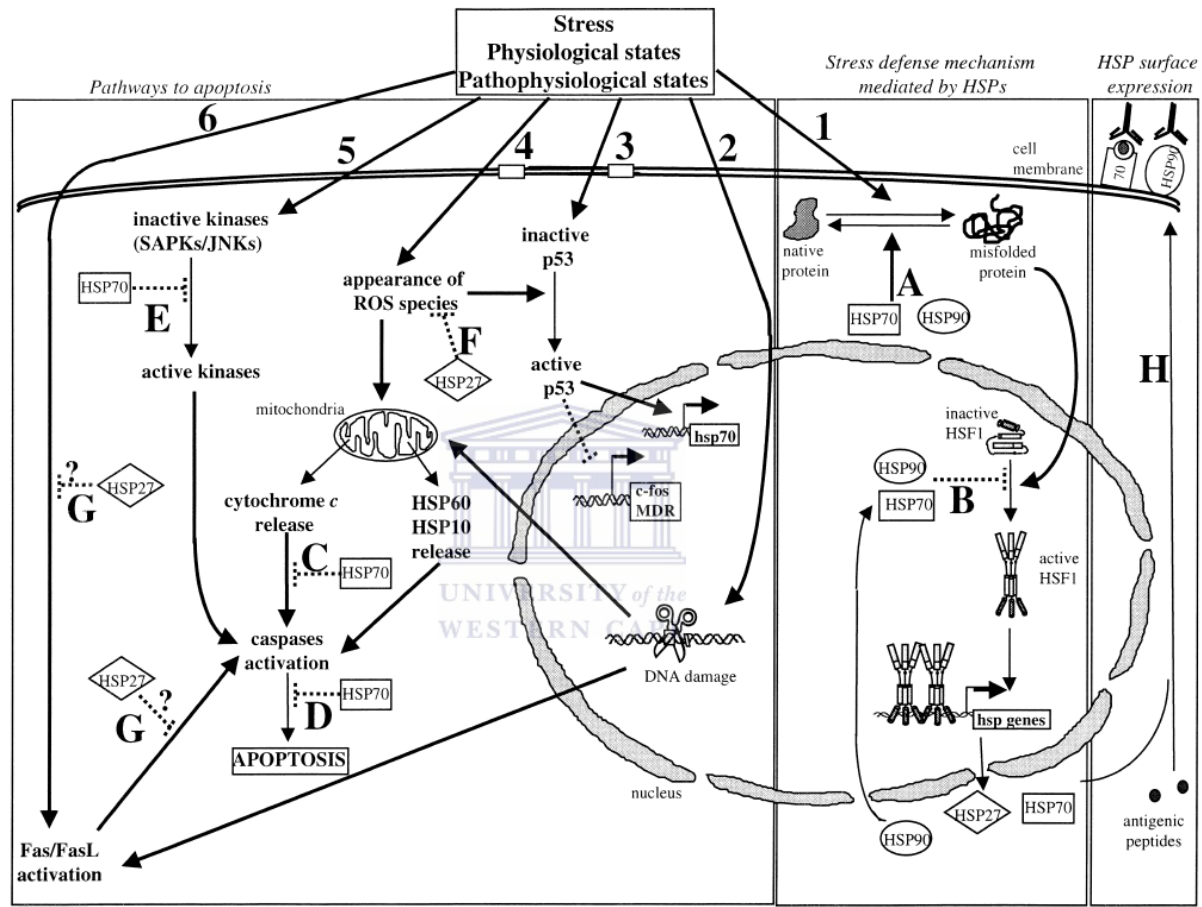
Throughout their lifespan, cells and tissues are constantly exposed to a plethora of harsh environmental (heat shock, UV irradiation, toxic chemicals), physiologic (oxygen radicals, pH fluctuations), and pathophysiological (inflammation, tissue injury, infection, proteasome inhibitors, I/R injury) stress conditions. Exposure to such stressful conditions causes severe damage to cellular proteins and promotes intracellular aggregation of damaged/misfolded proteins. These protein aggregates disrupt cellular homeostasis and induce cellular stress, which might activate apoptotic signalling pathways, leading to the death of the stressed cell (Tannous *et al.*, 2008; Demasi and Davies, 2003; Bucciantini *et al.*, 2002; Bence *et al.*, 2001; Wttenbach *et al.*, 2000).

Typically, cells respond to these potentially deleterious perturbations by inducing the expression of a set of evolutionary conserved genes that encode a very large and diverse class of proteins that are collectively known as stress proteins. Heat shock proteins (Hsps) (section 1.5) are the most common and best-studied members of stress proteins. Figure 1.2 summarises apoptotic signalling pathways (pathways 2, 3, 4, 5, and 6) that are activated by various stress conditions leading to apoptosis. However, also shown is a defence pathway (pathway 1) which protects the cell against stress-induced death. The cytoprotective effects are brought about by induced expression of stress proteins, including Hsps which, in addition to their protein folding roles (section 1.9), have also been shown to block apoptotic signalling pathways at various points (section 1.10).

Figure 1.2: A schematic illustration of major cellular pathways that are activated in response to stress.

Exposure of cells to environmental, physiologic, and pathophysiological stressors activates apoptosis signalling pathways (pathways 2 to 6) which leads to cell death. Pathway 1 is a protective pathway showing stress-induced activation of the heat shock transcription factor 1 (HSF1) which regulates transcription of Hsps. Hsps function as molecular chaperones that assist proteins to fold into native conformations (pathway A) and their synthesis exhibits autoregulation (pathway B). Several Hsps have been shown to block apoptotic signalling pathways at various points (pathways C to G). In some tumour cells, Hsps are also expressed at the cell surface where they may play a role as antigen-presenting cells (pathway H). Bold arrows represent the major initiation events; dotted lines represent inhibitory events; HSP, heat shock protein (adapted from Jolly and Morimoto, 2000).





1.3 Apoptosis

Apoptosis (Kerr *et al.*, 1972) is a distinct, genetically-controlled, energy-dependent form of cell death that occurs without inducing an inflammatory response in surrounding tissues. It plays a vital role in several physiological processes including embryonic development, maintenance of normal adult tissue homeostasis, and immune response (Fink and Cookson, 2005; Kroemer *et al.*, 1995). However, deregulation of apoptosis is implicated in the pathogenesis of several neurodegenerative disorders (Sherman and Goldberg, 2001; Mattson *et al.*, 2000; Nishimoto *et al.*, 1997), cancers (Webb *et al.*, 1997), and cardiac dysfunction (Danial and Korsmeyer, 2004; Nicholson, 1999; Umansky and Tomei, 1997).

Apoptotic signalling is induced by a wide variety of stimuli and is mediated by cysteine-dependent aspartic acid-specific cysteine proteases (caspases) (Danial and Korsmeyer, 2004; Korsmeyer, 2004; Nicholson, 1999; Zheng *et al.*, 1999; Thornberry and Lazebnik, 1998). Characteristic hallmarks of apoptosis include loss of plasma membrane symmetry (i.e., translocation of phosphatidylserine- PS, from the inner to the outer leaflet of the plasma membrane), plasma membrane blebbing, cytoplasmic shrinkage, chromatin condensation, activation of caspases, DNA fragmentation, and the collapse of the apoptotic cell into small intact membrane-bound fragments (apoptotic bodies) (Fink and Cookson, 1995; Martin *et al.*, 1995).

1.3.1 Mitochondrial stress-induced apoptotic signalling pathway

A variety of cytotoxic agents, particularly those that cause increased generation of ROS, cause mitochondrial stress. This results in the permeabilisation of the outer mitochondrial membrane and consequent release of pro-apoptotic factors, including cytochrome *c*, apoptosis inducing factor (AIF), pro-caspases, Smac/Diablo, HtrA2/Omi and endonuclease G, into the cytosol (Gill *et al.*, 2006; Donovan and Gotter, 2004). In the cytosol, cytochrome *c* interacts with apoptosis protease activating factor-1 (Apaf-1), thereby triggering the ATP-dependant oligomerisation of Apaf-1 (Cecconi, 1999). Oligomerised Apaf-1 binds to pro-caspase-9 leading to the formation of the caspase-9 activation complex (the apoptosome), which in turn triggers the proteolytic maturation of pro-caspase-3 leading to apoptotic cell death (Figure 1.3).

1.3.2 The endoplasmic reticulum (ER) stress-mediated apoptotic signalling pathway

The role of prolonged ER stress in regulation of apoptosis is relatively new and not yet fully understood. ER stress-mediated cell death (Figure 1.4) has been shown to involve elements of both the death receptor- and the mitochondrial apoptotic signalling pathways (Boyce and Yuan, 2006). Studies suggest the involvement of caspase-4, -7 and -12 (Rao *et al.*, 2001; Nakagawa *et al.*, 2000).

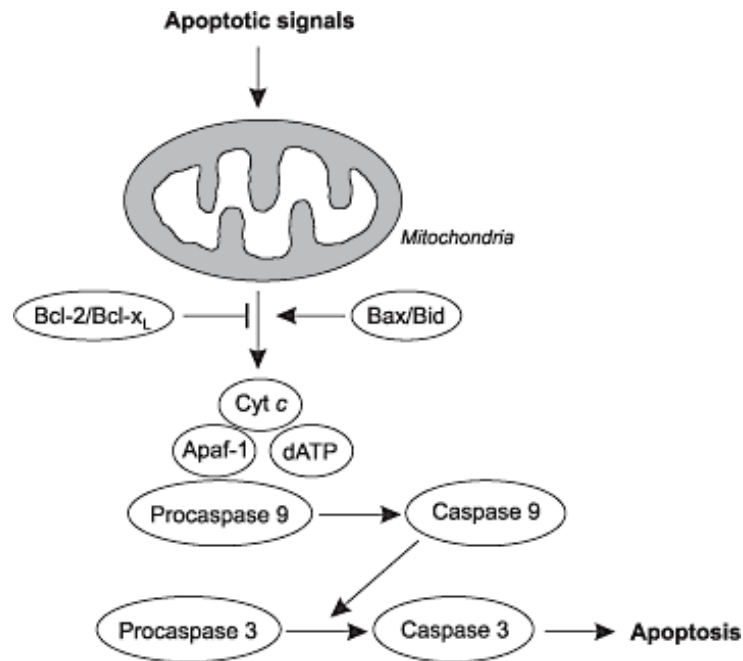


Figure 1.3: A schematic illustration of the mitochondrial stress-induced apoptotic signalling pathway.

Cellular stress (e.g., ROS) induces permeabilisation of the outer mitochondrial membrane, leading to the release of cytochrome *c* into the cytosol. Cytochrome *c* binds to Apaf-1 in the cytosol and triggers its oligomerisation. This complex binds and activates pro-caspase-9, in the presence of dATP, which leads to the downstream activation of caspase-3 and apoptosis (adapted from Ogata and Takahashi, 2003).

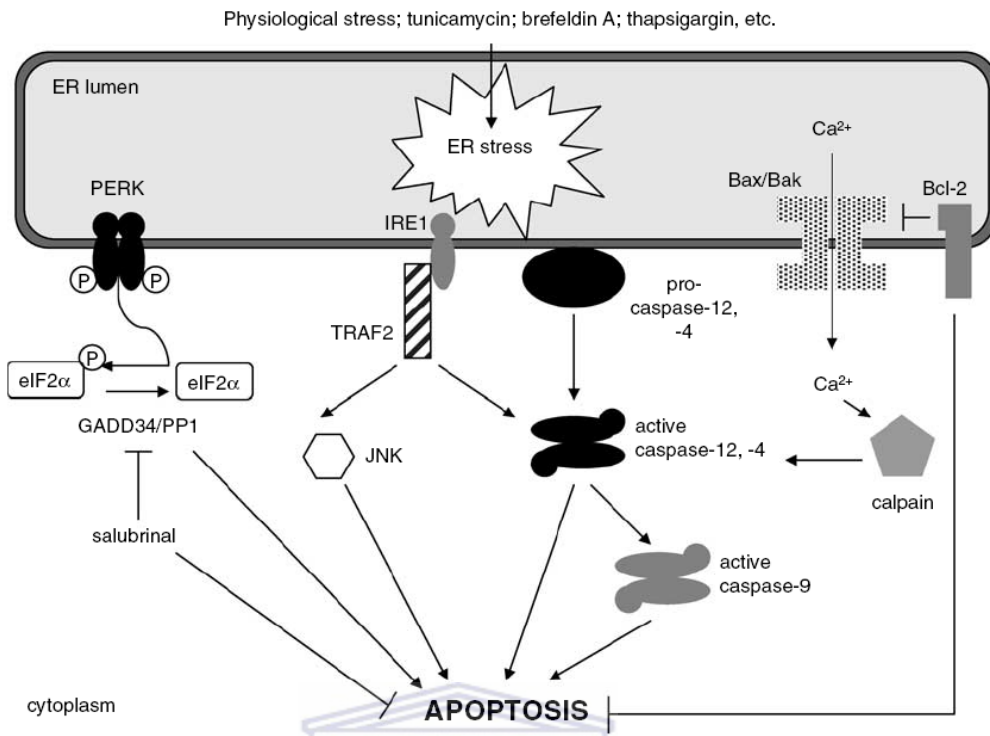


Figure 1.4: ER stress-mediated apoptotic signalling pathways.

Excessive or prolonged ER stress leads to the activation of PERK and, eventually, the GADD34/PP1 phosphatase complex, which dephosphorylates eIF2, promoting apoptosis. Caspase-12 (mice) or -4 (humans) bind to the outer ER membrane and are activated by IRE1 and TRAF2 or by cleavage by calpain, which is in turn activated by the release of calcium from ER. Bcl-2 family members also regulate apoptosis induced by ER stress, both through the regulation of calcium flux and amplification of the apoptotic signal through the mitochondrial pathway (adapted from Boyce and Yuan, 2006).

Thus the regulation of apoptosis determines the ability of a cell to survive potentially harmful cellular insults. Therefore regulatory elements that are involved in regulation of stress response and apoptosis directly influence cell longevity.

1.4 Cellular defence mechanism against stress and cell death

The ability of a cell to respond to a wide variety of physiological stresses is critical to its survival. The ER regulates several essential cellular functions including post-translational modification, folding and assembly of newly synthesised proteins destined for secretion or routing into various subcellular compartments, Ca^{2+} homeostasis, and cellular response to stress (Berridge, 1995; Rapoport, 1992; Sambrook, 1990). ER perturbations such as oxidative stress, inhibition of protein glycosylation, impairment of protein transport from the ER to the Golgi, depletion of intracellular Ca^{2+} , ER lipid and glycolipid imbalances and an excessive accumulation of unfolded/misfolded proteins causes ER stress and cellular damage, which may result in apoptosis. Mild ER stress activates a self-protective cellular mechanism known as the ER stress response (ESR) which enables cells to adapt and survive under stressful conditions (Ron and Walter, 2007; Boyce and Yuan, 2006; Kaufman, 1999; Lee, 1992). The ESR function to restore normal ER homeostasis through activation of the unfolded protein response (UPR) and the proteasome-dependent ER-associated degradation (ERAD) (Figure 1.5). The UPR increases the polypeptide folding capacity of the ER by coordinated transcriptional activation of multiple UPR-target genes (e.g., Hsps, inositol-requiring enzyme [IRE1], PKR-like ER kinase, and activating transcriptional factor 6 [ATF6]), whilst ERAD rapidly removes irreversibly damaged proteins from the ER (Boyce

and Yuan, 2006; Schröder and Kaufman, 2005a; Schröder and Kaufman, 2005b; Yoshida *et al.*, 2000). Table 1.1 shows some of the proteins that are targeted for degradation by ERAD.

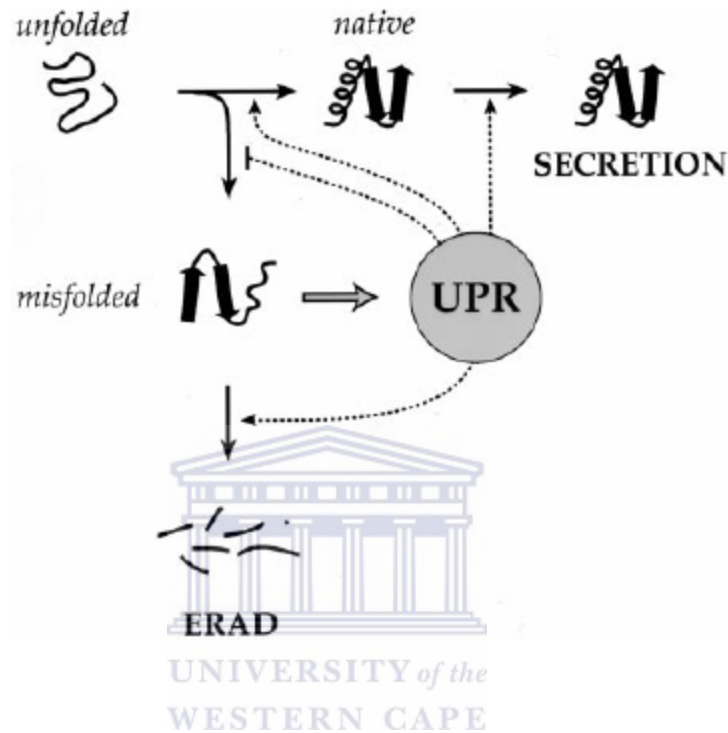
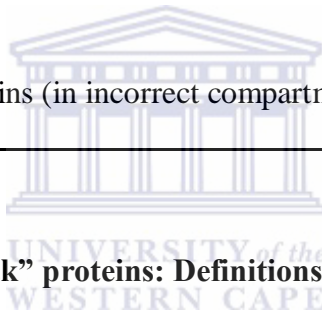


Figure 1.5: A schematic model illustrating the coordinated action of the ESR through the UPR and ERAD.

Nascent, unfolded proteins enter the ER, where they are folded and are passed on to the secretory pathway. Irreversibly misfolded or damaged proteins are removed by ERAD. Cellular stress or dysfunction of ERAD results in intracellular accumulation of misfolded proteins leading to activation of the UPR. The UPR reduces levels of misfolded proteins by regulating transcription of genes that encode molecular chaperones, promoting transit to the secretory pathway, and enhancing the rate of ERAD (adapted from Travers *et al.*, 2000).

Table 1.1: A list of abnormal proteins that are targeted for degradation by ERAD (adapted from Sherman and Goldberg, 2001).

-
- a) Incomplete proteins
 - b) Misfolded proteins (from mutations and biosynthetic errors)
 - c) Denatured proteins
 - d) Free subunits of multimeric complexes
 - e) Proteins that fail to bind cofactors
 - f) Oxidant-damaged proteins
 - g) Membrane or secretory proteins that fail to fold in the endoplasmic reticulum (ER)
 - h) Misdirected proteins (in incorrect compartments)
-



1.5 Stress or “Heat shock” proteins: Definitions and nomenclature

The term “heat shock” proteins has been maintained as a legacy of Ritossa’s ground-breaking discovery in 1962 who observed that exposure of larval salivary glands of *Drosophila* to elevated temperature result in appearance of new puffs in the giant chromosomes of these cells (Ritossa, 1962). These puffs represent transcriptional induction of Hsps in response to heat shock (Lindquist and Craig, 1988; Tissieres *et al.*, 1974). Although named “heat shock” proteins based on the original observation that they were induced in response to elevated temperature, the term is misleading since these proteins are induced by a wide variety of stress stimuli, including, oxidative stress, heavy metals, inhibitors of metabolism, fever, inflammation, and I/R injury (Benjamin and McMillan, 1998). Hence the term

“stress proteins” is preferred. However, both terms are used synonymously throughout this thesis.

Stress proteins belong to very large and diverse multigene families that constitute an ancient and essential cellular defence mechanism against a wide range of potentially harmful conditions. Genes encoding stress proteins are amongst the most evolutionary conserved in many organisms ranging from prokaryotes such as *E. coli* to more complex multicellular mammals (Ferder and Hofmann, 1999; Fink, 1999; Lindquist and Craig 1988; Lindquist, 1986). For example, among eukaryotic organisms the identity of the nucleotide sequence of the Hsp70-gene varies from 60 to 78 % (Kiang and Tsokos, 1998). Compared with the human hsp70-gene, the *Drosophila* Hsp70-gene and the *E. coli* dnaK-gene have a 72 and 50 % identities, respectively (Hunt and Calderwood, 1990). This strong evolutionary conservation of stress proteins and their ability to respond to a wide variety of stressful stimuli that is potentially damaging to the cell suggests that they are crucial for cell survival. Some of these stress proteins (e.g., Hsc70) are constitutively synthesised by cells under normal conditions for routine housekeeping purposes. Thus stress proteins are required even in unstressed cells and their functions become even more crucial under stressful conditions.

Conventionally, Hsps are classified into families according to their related function and molecular weight in kilodaltons (kDa) (Hightower and Hendershot, 1997; Lindquist and Craig 1988). Family names are conventionally written in capital letters, for example, the HSP70 family. Some proteins that were first discovered in a non-related domain carry particular names like the major structural

ocular lens protein $\alpha\beta$ -crystallin or those proteins targeting abnormal proteins for degradation, i.e., ubiquitins (Benjamin and McMillan, 1998). The name of some Hsps that are restricted to specific organelles is often preceded by an indication of their cellular localisation, for example, mitochondrial Hsp75 (mt-Hsp75). Additionally, a distinction has been made between members that are constitutively expressed (e.g., Hsc70 and Hsp90 β) and their inducible isoforms that are almost absent under normal conditions but are rapidly synthesised in response to cellular stress (Hsp70 and Hsp90 α respectively). However, this distinction is arbitrary, since emerging evidence indicates that such relationships depend on cell- and tissue-specific expression (Snoeckx *et al.*, 2001). The synthesis of some stress proteins increases in response to lowered extracellular glucose concentrations and these are called glucose-related proteins (Grps). However, other stimuli, such as depletion of intracellular calcium stores or inhibition of protein glycosylation can also lead to an increase in Grp synthesis (Snoeckx *et al.*, 2001). Grps are members of various HSP families and comprise Grp58, Grp78, Grp94, and Grp170 and they are all localised in the ER. The nomenclature and classification for related Hsps in prokaryotic and eukaryotic organisms differs.

1.6 The role of stress proteins in diseases

The expression of stress proteins has been shown to have both deleterious and beneficial effects in the cell. Deregulated expression of Hsps has been implicated in tumourigenesis where they presumably function as modifiers of protein activity, in particular, components of the cell cycle machinery, kinases, and several other proteins implicated in cancer progression. Increased levels of members of the HSP70 and HSP27 families have been detected in a number of cancers, including

breast cancer and endometrial cancer (Jolly and Morimoto, 2000), and this is consistent with the observations that Hsps interfere with apoptotic signalling pathways. On the other hand, prior induction of Hsps has been shown to have a protective effect against subsequent fatal thermal and I/R injury.

1.7 Expression of stress proteins in the cardiovascular tissues

Several stress proteins are expressed in the cardiovascular system either constitutively or in response to specific stressors (Snoeckx *et al.*, 2001; Benjamin and McMillan, 1998). In mice, for example, Hsp27, Hsc70 and Hsp84 are constitutively expressed in the heart, but at lower levels compared with other tissues (Tanguay *et al.*, 1993). In unstressed rats, the heart contains relatively high levels of $\alpha\beta$ -crystallin, whereas intermediate levels of Hsp27 have been reported (Beck *et al.*, 1995). In both human and rat heart, Hsp27 has been detected in endothelial cells, smooth muscle cells, and cardiomyocytes, whereas $\alpha\beta$ -crystallin is reportedly present only in the cardiomyocytes where it is constitutively abundant (Klemenz *et al.*, 1993; Salo *et al.*, 1991). $\alpha\beta$ -crystallin plays an essential role in cardiac development where it activates genetic programs responsible for cardiac morphogenesis (Snoeckx *et al.*, 2001). The induced expression of some of the Hsps in the heart in response to hyperthermia and I/R injury, and their protective roles against subsequent stress will be discussed in the following sections.

1.8 The protective effect of stress proteins in the myocardium

It is well-established that preconditioned cells are less susceptible to cytotoxicity induced by various stimuli including hyperthermia, heavy metals, growth factor withdrawal, radiation and anti-cancer drugs (Jäättelä, 1999; Samali and Orrenius, 1998; Samali and Cotter, 1996). The clinical implication of this cytoprotection has attracted a lot of attention, particularly of those in cardiac research. Numerous studies have been done using both cultured cardiomyocytes and intact hearts in models simulating I/R injury. Currie and co-workers (Currie, 1987; Currie *et al.*, 1988) were amongst the first researchers to demonstrate the cytoprotective effects of heat shock preconditioning by exposing rats to elevated temperatures and then removing their hearts and exposing them to ischemia on a Langendorff perfusion apparatus. They demonstrated that the hearts isolated from rats which had prior exposure to elevated temperature had improved recovery of contractile function following subsequent ischemia and reperfusion compared to hearts from control animals. Also they showed that the reperfusion damage was significantly reduced in the heat-shocked hearts. Their findings demonstrated, for the first time, that there was a positive correlation between stress-induced expression of Hsp expression in the intact heart and a protective effect against subsequent exposure to ischaemia/reperfusion. These observations raised the question of whether a similar protective effect would be observed in hearts exposed to myocardial ischaemia within the whole animal following a prior exposure to heat shock. This was confirmed by Donnelly *et al.* (1992) who reported a significant reduction of infarct size when rat hearts were exposed to 35 minutes of left coronary artery occlusion in the whole animal following exposure to heat shock. Researchers soon

realised that the induction of stress proteins was not only in response to thermal stress but to a wide variety of stressors. Marber *et al.* (1993) reported that brief episodes of cardiac ischaemia induced Hsp synthesis and also reduced infarct size when the hearts were subsequently exposed to ischaemia in the intact animal.

Thus *in vivo* induction of stress proteins in the intact heart or in cardiac cells in culture produces a protective effect against subsequent damaging thermal or I/R injury (Arnaud *et al.*, 2003; Brar *et al.*, 1999; Martin *et al.*, 1997). Some studies have gone further and demonstrated that the protective effect correlates with the amount of Hsps induced (Hutter *et al.*, 1994; Marber, *et al.*, 1994). The majority Hsps, including Hsp70 and Hsp27, have since been over-expressed in cardiac myocytes and other mammalian cell lines where they confer cytoprotective effects against thermal stress or simulated ischaemia. More recently Lusardi *et al.* (2010) showed that ischaemic pre-conditioning regulates microRNA expression in the mouse brain cortex, which in turn regulate post-transcriptional gene expression of target genes, most of which encode transcriptional regulators. They suggested that microRNAs and their target genes (e.g., methyl-CpG binding protein 2) could serve as effectors of ischemic preconditioning-induced tolerance.

Different Hsps respond differently to various stimuli and have different cytoprotective effects. The combined expression of Hsp60 and Hsp10 in cardiac myocytes has been shown to protect mitochondrial function and to protect against apoptotic cell death induced by simulated ischaemia/reoxygenation (Lin *et al.*, 2001). However, role of Hsp60 as an antiapoptotic and cytoprotective protein is not as well established as that of Hsp70. Hsp70 over-expression has been shown to protect cells against both thermal and simulated ischaemic stress (Mosser *et al.*,

2000). Martin *et al.* (1997) demonstrated that cardiac cells over-expressing Hsp27 or $\alpha\beta$ -crystallin were protected from simulated ischaemia and that decreasing levels of endogenous Hsp27 enhanced the damaging effects of a subsequent ischaemic stimulus.

These observations raised the speculation that stimulating over-expression of individual stress proteins or a combination of stress proteins *in vivo* may be of therapeutic importance. Consequently this has led to intensive research aimed at elucidating the mechanism(s) mediating these protective effects by identifying specific biological processes that are targeted by these protective proteins. These include apoptotic signalling pathways.

1.9 Hsps function as molecular chaperones

The majority of stress proteins function as molecular chaperones that facilitate the correct folding, assembly, and degradation of other proteins (Fink, 1999; Hendrick and Hartl, 1993). They include members of the HSP70, HSP90, HSP104, HSP40/DnaJ, and small HSP (e.g., Hsp27, $\alpha\beta$ -crystallins) families (Narberhaus, 2001; Morimoto *et al.*, 1994; Georgopoulos and Welch, 1993; Gething and Sambrook, 1992; Ellis and van der Vies, 1991). Molecular chaperones have critical roles in cardiac function (Snoeckx *et al.*, 2001; Benjamin and McMillan, 1998) and their functions include (i) transiently binding nascent polypeptide chains and delay their folding until translation is complete, (ii) maintaining polypeptide chains in an appropriate conformation suitable for translocation across organelle membranes, (iii) selectively binding to denatured or partially unfolded polypeptides, preventing intracellular protein aggregation, and (iv) assisting in

degrading toxic metabolites by promoting ubiquitination and proteasome lysis (Benjamin and McMillan, 1998).

1.9.1 Cytosolic and nuclear chaperones

The HSP70 family of stress proteins constitute the most conserved and best studied class of Hsps. Eukaryotic cells express several HSP70 family members including constitutively expressed Hsc70, stress-inducible Hsp70 (also referred to as Hsp70i or Hsp72) and Grp78 which is localised in the ER (Jäättelä, 1999; Tavaría *et al.*, 1996). All members of the Hsp70 chaperone class possess two distinct domains: a highly conserved N-terminal ATPase domain and a more divergent C-terminal domain, which binds short hydrophobic peptides of target substrates (Benjamin and McMillan, 1998). Under normal, unstressed conditions Hsp70 bind to and stabilise nascent polypeptides in an ATP-dependent manner and maintain them in an unfolded or partially folded state until they reach their final cellular compartment. It also assists in the assembly of multiprotein complexes and the transport of proteins across cellular membranes (Parcellier *et al.*, 2003; Fink, 1999). Figure 1.6 shows a model for the cellular chaperone function of Hsc70.

Under stressful conditions, the induced synthesis of Hsp70 enhances the ability of cells to cope with increased concentrations of unfolded or denatured proteins (Marber *et al.*, 1995). Specifically, Hsp70 has been shown to associate with cytoskeletal proteins, cell surface glycoproteins, calmodulin, and saturated long-chain fatty acids, like palmitate, stearate, and myristate (Huang *et al.*, 2009; Snoeckx *et al.*, 2001; Sun *et al.*, 2000).

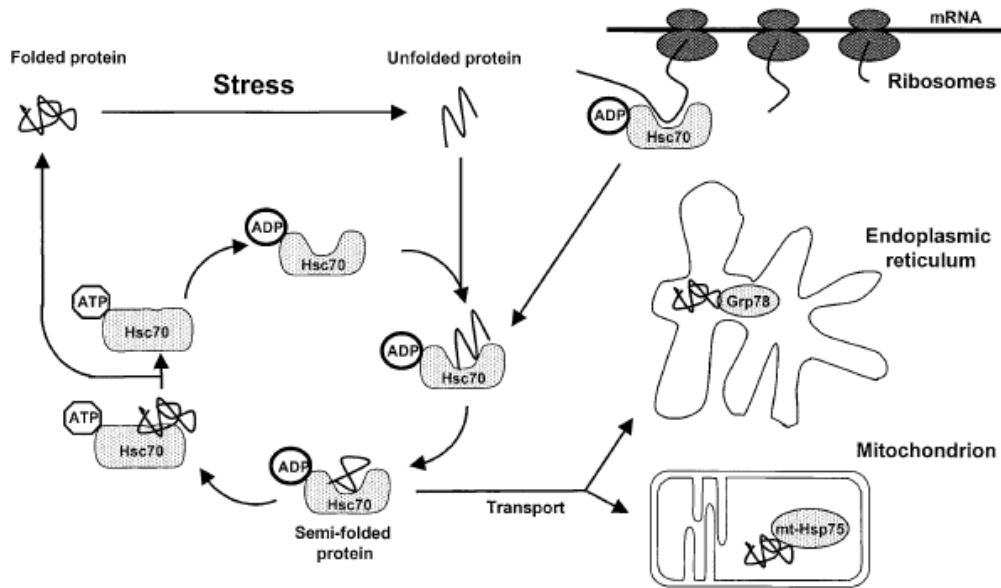


Figure 1.6: Schematic illustration of interactions between the chaperones Hsc70 and nascent peptide chains or unfolded proteins.

Hsc70 recognise and bind to domains in unfolded proteins and nascent polypeptides as they exit ribosomes. Partially folded proteins that are shuttled into the ER and mitochondria are further bound and folded by ER-resident (e.g., Grp78) and mitochondria-resident (e.g., mt-Hsp75) chaperones. Grp78, glucose-related protein 78; mt-Hsp75, mitochondrial 75-kDa heat shock protein (adapted from Snoeckx *et al.*, 2001).

HSP90 proteins are one of the most abundant cytosolic proteins, making up 1-2% of cytosolic proteins and can further accumulate in response to stress. Members of the Hsp90 family include the ATP-dependent chaperones Hsp90 α , Hsp90 β , and Grp94 (Pearl and Prondromou, 2006; Csermely *et al.*, 1998). The main chaperone role of HSP90 proteins is promoting the conformational maturation of

transcription factors and signal transducing kinases including ligand-dependent transcription factors such as MyoD, tyrosin kinases such as v-Src, and serine/threonine kinases such as Raf-1 (Parcellier *et al.*, 2003).

Mammalian Hsp60, also called chaperonin, is a constitutively expressed protein found primarily within the mitochondrial matrix, although 15 to 20 % of the protein is found in the cytosol (Gupta and Knowlton, 2005). HSP60 facilitates the folding and assembly of mitochondrial proteins and the proteolytic degradation of misfolded or denatured proteins in an ATP-dependent manner (Parcellier *et al.*, 2003). The chaperone function of Hsp60 is regulated by Hsp10, which binds to Hsp60 and regulates substrate binding and ATPase activity (Bukau and Horwich, 1998).

Unlike the ubiquitous Hsp70 and Hsp90 counterparts, members of the small Hsps (HO-1 or Hsp32, Hsp27, Hsp25, $\alpha\beta$ -crystallin, and Hsp20 chaperones) exhibit tissue specific expression and are of special interest to cardiovascular biology (Benjamin and McMillan, 1998). These proteins vary in size from 15 to 30 kDa and share sequence homologies and biochemical properties such as phosphorylation and oligomerisation.

1.9.2 *Molecular chaperones in cellular organelles*

Generally it is thought that molecular chaperones associated with specific organelles such as the ER may be of more clinical importance. ER stress and alterations in Ca^{2+} homeostasis are associated with apoptotic signalling events. Stress stimuli such as anoxia and glucose starvation are known to induce expression of members of the Ca^{2+} -binding glucose-related family of Hsps such as

Grp170, Grp194, and Grp78/BiP (Gething, *et al.*, 1992). Variable levels of expression of these Hsps have been reported after experimental ischaemia (Nishizawa *et al.*, 1996). However, there is limited information on Grp expression and their role in pathological conditions in which abnormal proteins are expressed or secreted via the ER-Golgi pathway.

1.10 Hsps associate with key apoptotic proteins

Several Hsps have been shown to enhance cell survival by blocking both caspase-dependent and caspase-independent apoptotic signalling pathways at multiple points (Arya *et al.*, 2007; Gill *et al.*, 2006; Parcellier *et al.*, 2003). A summary of these pathways is shown on Figure 1.7. Hsp27 binds to cytochrome *c*, after its release from the mitochondria following mitochondrial perturbation, and prevents it from binding to Apaf-1, thus blocking downstream cascades which lead to caspase-mediated apoptosis (Concannon *et al.*, 2003; Paul *et al.*, 2002; Bruery *et al.*, 2000). Hsp27 also binds to procaspase 3, blocking the formation of the apoptosome. Additionally Hsp 27 has been shown to bind to Daxx, preventing its recruitment to Fas which causes a blockage of this caspase-independent pathway (Charette *et al.*, 2000). Daxx is a nuclear protein that translocates to the membrane and binds on one end to Fas and at the other to Ask1, triggering caspase-independent apoptosis. Hsp27 prevents the translocation of Daxx to the membrane and its interaction with Fas and Ask1 (Concannon *et al.*, 2003).

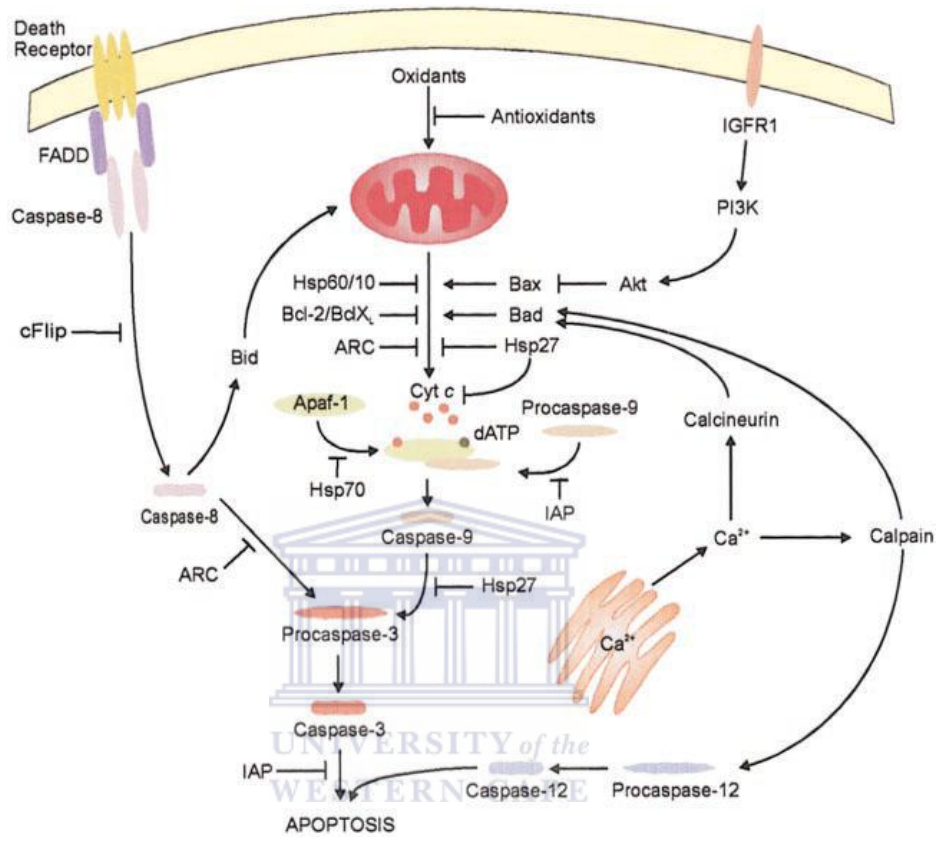
Hsp90 binds to Apaf-1 and prevent it from binding to cytochrome *c* (Parcellier *et al.*, 2003; Pandey *et al.*, 2000). Also, Hsp90 has been shown to interact with RIP-1 kinase and Akt to promote NF- κ B-mediated inhibition of apoptosis (Parcellier *et al.*, 2003). Hsp70 prevents oligomerised Apaf-1 from recruiting pro-caspase-9

(Beere *et al.*, 2000). Komarova *et al.* (2004) demonstrated that Hsp70 suppresses caspase-dependent apoptotic signalling by binding both caspase-3 and caspase-7 and preventing their proteolytic maturation. Additionally Hsp70 has been shown to suppress JNK activation, thus inhibiting the JNK pathway of apoptosis (Gabai *et al.*, 2002; Volloch *et al.*, 2000). Hsp60 and Hsp10 block the release of cytochrome *c* from the mitochondria (Lin *et al.*, 2001) and over-expression of both Hsps has been shown to inhibit caspase-3 and modulate Bcl-2 family members to attenuate doxorubicin-induced cardiac muscle death (Shan *et al.*, 2003).



Figure 1.7: Summary of regulation of apoptosis signalling pathways in cardiomyocytes.

Apoptotic signalling pathways in cardiomyocytes include those initiated by the death receptor, mitochondrial stress, and ER stress. These pathways are down-regulated at several points by antiapoptotic Bcl-2 family members, inhibitors of apoptosis (e.g., cFLIP, IAP, and ARC), and heat shock proteins. In contrast, proapoptotic Bcl-2 family members such as Bax, Bad, and Bid, which are activated by several factors including calpain and calcineurin, up-regulate apoptosis. Hsp27 binds to both cytochrome *c* and procaspase-3, which blocks the formation of the apoptosome and downstream signalling events that eventually lead to caspase-mediated apoptosis. Also, Hsp27 regulates caspase-independent apoptosis through its interaction with Daxx (not shown). Hsp70 prevents oligomerised Apaf-1 from recruiting pro-caspase-9. Hsp60 and Hsp10 block release of cytochrome *c* from the mitochondria. IAP, inhibitor of apoptosis; cFLIP, cellular FADD-like inhibitory protein; Cyt *c*, cytochrome *c* (adapted from Gill *et al.*, 2002).



1.11 Hsps as potential therapeutic targets to modulate apoptosis

The preceding sections reviewed how the expression of Hsps varies in response to exposure to various cellular stressors. Also reviewed here were the roles of Hsps as molecular chaperones and regulators of the apoptotic signalling processes to enhance cell survival. This makes the regulation of the expression and the activity of Hsps, either by pharmacological or genetic manipulation, a potential tool to modulate apoptosis in pathological conditions (Kalmar and Greensmith, 2009; Söti *et al.*, 2005). Therefore, the induction of Hsps *in vivo* may have several benefits and wide ranging clinical applications, for example, in cardio protection, cellular defence against stroke and various neurodegenerative diseases. The mechanism(s) of preconditioning-induced cytoprotection is not yet fully understood. However, preventative procedures such as heat shock- and I/R preconditioning have been shown to prevent lethal I/R injury by decreasing intracellular influx of Ca²⁺, improving endothelial function, and protecting cardiomyocyte against apoptosis (section 1.8).

1.12 Methods used to active the stress response

Heat shock is the archetype of the induction of stress proteins (Ritossa, 1962). However, whole body or partial hyperthermia is cumbersome and may not be feasible in conscious humans hence other methods of inducing expression of stress proteins have been devised.

1.12.1 Pharmacological methods

A multi-target pharmacological approach has been adopted to alleviate lethal effects of I/R injury. Several pharmacological agents that modulate Hsp expression levels by acting as Hsp inhibitors or cellular stress inducers, which transiently elevate the level of unfolded proteins inside the cell, are commercially available (Table 1.2)

Table 1.2: Pharmacological modifiers of Hsp action (Sreedhar and Csermely, 2004).

| Drug | Affected Hsp |
|---------------------------|--------------|
| <i>A. Hsp inhibitors</i> | |
| Geldanamycin and 17-AAG | Hsp90 |
| Radicicol | Hsp90 |
| Cisplatin | Hsp90 |
| Novobiocin | Hsp90 |
| Deoxyspergualine | Hsp70, Hsp90 |
| MKT-077 | Hsp70 (mot2) |
| Mizobirin | Hsp60 |
| <i>B. Hsp inducers</i> | |
| Amphetamine | all Hsp |
| Carbenoxolone | all Hsp |
| Geldanamycin and 17-AAG | all Hsp |
| Proteasome inhibitors | all Hsp |
| Stannous chloride | all Hsp |
| p38 kinase inhibitors | Hsp27 |
| Geranyl-geranyl-acetone | Hsp70 |
| <i>C. Hsp co-inducers</i> | |
| Aspirin | all Hsp |
| Bimoclomol | all Hsp |

Among the Hsp inhibitors, only geldanamycin, its less toxic derivative, 17-AAG, and radicicol are the only relatively specific inhibitors of Hsp90. Aspirin and bimoclomol do not induce Hsp themselves, but only help the induction process provoked by any by environmental stress.

Amphetamine-induced lipolysis elevates body temperature which in turn leads to up-regulated Hsp synthesis and improved post-ischemic heart recovery (Maulik *et al.*, 1995). Interleukin-6-like cytokine cardiotrophin-1 (CT-1) has been shown to induce Hsp synthesis in cultured cardiac cells and that treatment of these cells with CT-1 protects them against subsequent exposure to thermal or ischemic stress (Stephanou *et al.*, 1998). Herbimycin A, a tyrosine kinase inhibitor, produces similar effects in cultured cardiac cells (Morris *et al.*, 1996). Proteasome inhibitors up-regulate Hsp synthesis by increasing the amount of misfolded proteins in the cell, triggering the stress response (Marcu *et al.*, 2000).

Bimoclomol, a nontoxic hydroxylamine derivative, induce Hsp synthesis in the intact heart by perturbing various membrane structures and helping the release of putative lipid-signalling molecules (Víggh *et al.*, 1997). Also, it prolongs the binding of HSF1 to the heat shock element on the DNA (Hargitai *et al.*, 2003). Similarly, Meng *et al.* (1996) demonstrated that treatment of rats with norepinephrine results in Hsp induction in the heart and protection against ischemia when the heart was subsequently perfused *ex vivo*.

The identification of pharmacological compounds with the ability to induce stress proteins without producing severe side effects could make pharmacological induction of stress protein synthesis a viable therapeutic approach. Alternative methods may involve the development of small molecules and peptides that mimic the *in vivo* actions of chaperones with therapeutic benefits and their delivery to target tissues using biomarkers and nanotechnology.

1.12.2 Gene therapy methods

Unfortunately, several of the above-mentioned pharmacological inducers of Hsps are also associated with significant side effects, which limits their clinical application (Latchman, 2001). Such side effects can be avoided if hsp-genes could be efficiently delivered to the heart. Since transgenic procedures are not applicable in humans, this will require the development of procedures able to safely and effectively deliver stress protein genes to the heart of the individual patient. Previously it has been shown that the Hsp70 gene within a plasmid vector can be delivered to the heart via intra-coronary infusion of liposome particles containing it (Suzuki *et al.*, 1997). The elevated Hsp70 expression produced by this means conferred effective protection against subsequent I/R injury. However, the need to safely and efficiently deliver stress protein genes to the target tissue remains a problem in Hsp-gene delivery to the heart. The possible development of viral vector able to safely and efficiently deliver Hsp-genes to the cardiac cells gives hope towards the therapeutic application of Hsps in pathological conditions through targeted gene delivery.

1.13 Principles of transcriptional regulation

Temporal and spatial expression of functionally related genes is regulated in part at transcription level. Such genes are co-regulated by the same transcription factors. The response to specific environmental and developmental signals is mediated by distinct modular and combinatorial interactions of a set of transcription factors binding to their cognate transcription factor binding sites typically in close proximity to each other (Cartharius *et al.*, 2005; Diamond *et al.*, 1990).

1.14 Transcriptional regulation of heat shock genes (Hsp-genes)

The inducible expression of Hsps is regulated at transcriptional level by heat shock factors (HSFs) that bind to cognate *cis*-acting regulatory elements (CARE), known as heat shock elements (HSEs), that are located in promoters of heat shock responsive genes (Dai *et al.*, 2003; Morimoto, 1998; Wu, 1995; Morimoto *et al.*, 1992). HSEs are composed of multiple inverted repeats of adjacent pentanucleotide 5'-nGAAn-3' motifs (Figure 1.8).



Figure 1.8: Nucleotide sequence of the Hsp70 HSE (nt -130 to -81).

The grey boxes indicate individual HSF1 binding sites (adapted from Jolly *et al.*, 2002).

At present, four different HSFs have been identified in vertebrates and plants, HSF1, HSF2, HSF3 and HSF4, whilst only one HSF is expressed in *Saccharomyces cerevisiae*, *Caenorhabditis elegans*, and *Drosophila* (Sorger and Pelham, 1988; Jedlicka *et al.*, 1997). The four factors have been shown to respond differently to various forms of cellular stress (Pirkkala *et al.*, 2001). HSF1 is ubiquitously expressed and is the main heat shock transcription factor that is activated in response to thermal stress (Rabindran *et al.*, 1991). In non-stressed eukaryotic cells, HSF1 is maintained in a transcriptionally inactive, non-DNA binding state. Upon exposure to heat shock or other forms of cellular stress, HSF1 monomers form an activated, DNA-binding trimeric complex (Pirkkala *et al.*,

2001; Wu, 1995) which binds to the HSE and induce transcription of stress responsive genes (Figure 1.9).

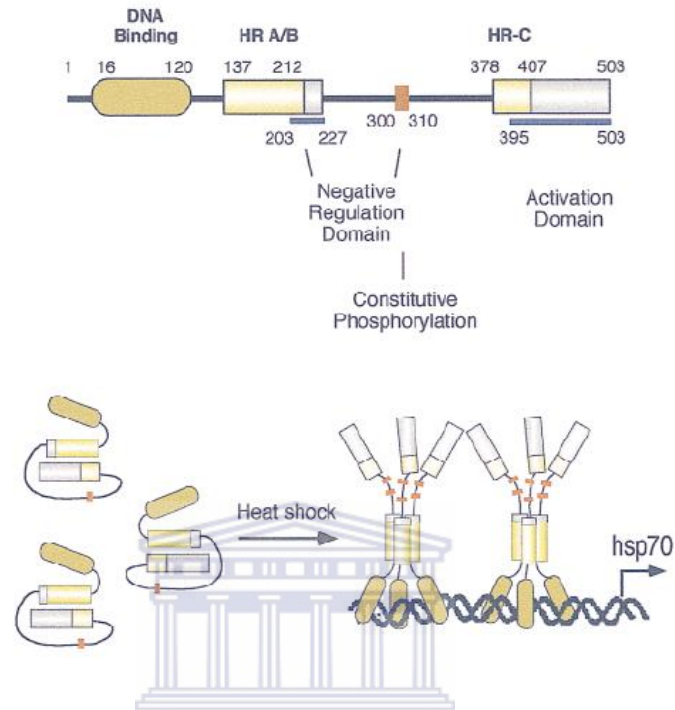


Figure 1.9: General structure and regulatory features of HSFs.

WESTERN CAPE

A schematic representation of HSF1 structural motifs showing the DNA-binding domain, hydrophobic heptad repeats (HR-A/B and HR-C), the carboxy-terminal transcription activation domain, and the negative regulatory domains that influence HSF1 activity. The amino acid residues indicate the relative positions of these domains in HSF1. The bottom section shows a schematic of the intramolecular negatively regulated monomer that is activated upon exposure to stress to form homotrimers with DNA-binding activity (adapted from Morimoto, 1998).

HSF2 is mainly involved in regulation of differential Hsp-gene expression during development (Morimoto, 1998; Schuetz *et al.*, 1991). HSF3, which, to date, has only been characterised in avian species, behaves like HSF1 (Nakai and Morimoto, 1993). HSF4 is expressed in a tissue-specific manner and displays constitutive DNA-binding activity (Morimoto, 1998; Nakai *et al.*, 1997; Wu, 1995).

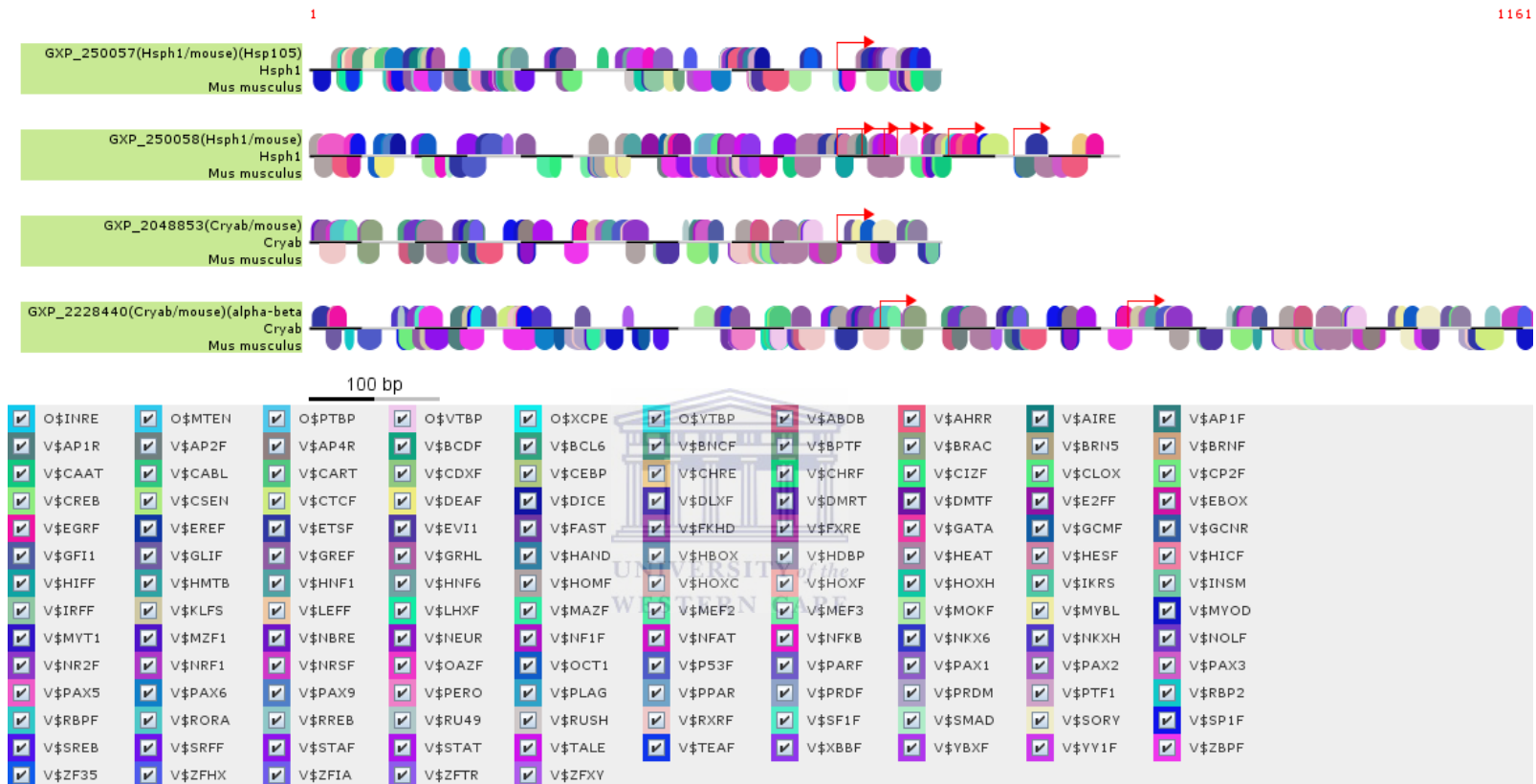
1.15 Bioinformatics tools and the principle of transcriptional co-regulation

Gene expression profiling methods such as microarrays have yielded large amounts of data linking genes, through altered RNA levels, to gene expression patterns. This offers insight into global gene expression patterns in response to a specific stimulus. However the simultaneous detection of altered RNA levels of two different genes in response to a single stimulus does not necessarily imply that the same pathway regulates both genes. Generally a single stimulus activates several pathways simultaneously, leading to coincidental alterations in levels of expression of several different genes. Such genes are co-expressed, not co-regulated. Therefore, there is often a need to distinguish between co-expressed and co-regulated genes.

The information concerning transcriptional regulatory networks responsible for the observed expression patterns is not contained within the cDNA sequences used to generate the arrays. Regulation of gene expression is determined, to a large extent, by the regulatory sequences of the individual genes (promoters and enhancers) (Fessele *et al.*, 2002; Werner, 2003). These regions are thus of special interest as they govern most aspects of developmental and functional integrity of multicellular organisms (Werner, 2001).

1.16 Progress in *in silico* promoter analysis

Until recently, it was almost impossible to reliably identify transcriptional promoters in large DNA sequences (Fickett and Hatzigeorgiou, 1997). Recent advances in bioinformatics have made it possible to locate DNA sequences corresponding to promoter, even in complex eukaryotic genomes (Scherf *et al.*, 2002). However, merely locating the promoter sequence is not very informative. Additionally, there is need to establish the functional organisation of the promoter, what is also referred to as the “anatomy” of the promoter or the “context” of the transcription factor binding sites. Typically, promoters are composed of functionally defined modular units that enable them to respond to specific signalling pathways or induction in a cell- or tissue-specific manner. However, in some cases the detailed experimental data on the functional organisation of a specific promoter are not available. Fortunately bioinformatics tools such as MatInspector and ModelInspector that enable *in silico* prediction and modelling of the functional organisation of the promoter in the absence of experimental data are now available (Figure 1.10). Such algorithms cluster co-regulated genes on the basis of shared promoter modules and provide powerful alternatives for elucidating the function of novel genes (Gailus-Durner *et al.*, 2001; Werner, 2001).



Thus, as evidenced by this literature review, there is a close link between pathways leading to apoptosis and stress response and an increasing number of reports have shown that stress proteins function at multiple points in the apoptotic signalling pathway. Currently available pharmacological regulators of Hsps against fatal ischemic/reperfusion heart injury have had limited clinical success and a multi-target pharmacological approach has been proposed (Yellon and Hausenloy, 2007).

A previous study (Gill, 2004) identified 127 genes that are differentially expressed in H9c2 cells following heat shock using suppression subtractive hybridization (SSH). This included genes that have not previously been associated with the heat shock response. However, the application of differential gene expression strategies such as SSH is limited by high false positive rate. Therefore there is need to validate data generated using these methods. The current study aimed to identify novel heat shock elements in H9c2 cells. Functionally related genes such as heat shock responsive genes are co-regulated by the same set of transcription factors which bind to conserved cognate DNA sequence motifs in the promoter region. Therefore the hypothesis was that the promoters of such genes share conserved sequence motifs and that the identification of such sequence motifs may enable the identification of novel heat shock responsive genes *in silico*. Potentially such genes could have cytoprotective roles and the identification of novel regulatory elements in stress response and cytoprotective pathways could provide new therapeutic targets against cardiovascular disease.

Specific aims were to:

- Analyse promoter sequences of putative heat shock responsive genes using *in silico* tools.
- Demonstrate the cytoprotective effect of heat shock preconditioning in H9c2 cells against apoptosis.
- Investigate the expression of putative heat shock responsive genes in H9c2 cells following heat shock treatment using real-time quantitative reverse transcription polymerase chain reaction (qRT-PCR).



CHAPTER 2.0: MATERIALS AND METHODS

2.1 General chemicals and suppliers

| | |
|---|----------------|
| Agarose | Promega |
| Ammonium persulphate (AMPS) | Promega |
| Ampicillin | Roche |
| APOPercentage™ assay dye | BD Biosciences |
| Bacteriological agar | Merck |
| Boric acid | Merck |
| Bovine serum albumin (BSA) | Roche |
| Bromophenol blue | Sigma-Aldrich |
| Buffer saturated phenol | Invitrogen |
| Cesium chloride | Roche |
| Chloroform | BDH |
| Coomassie Brilliant Blue R 250 | Sigma-Aldrich |
| Diethyl Pyrocarbonate (DEPC) | Sigma-Aldrich |
| Dimethyl sulphoxide (DMSO) | Sigma-Aldrich |
| DTT (Dithiothreitol) | Roche |
| EDTA (Ethylene diamine tetra acetic acid) | Merck |
| Ethanol | Sigma-Aldrich |
| Ethidium bromide | Promega |
| G418-sulphate | Promega |



| | |
|---|--------------------------|
| Glucose | Merck |
| Glacial acetic acid | Merck |
| Glycine | Sigma-Aldrich |
| Isoamyl alcohol | Merck |
| Metafectene™ transfection reagent | Biontex Laboratories |
| Methanol | Merck |
| Penicillin | Sigma-Aldrich |
| Potassium acetate | Merck |
| Propan-2-ol | Merck |
| SDS (Sodium dodecyl sulphate) | Promega |
| SAP (Shrimp alkaline phosphatase) | Fermentas |
| Sodium acetate | Merck |
| Sodium chloride | Merck |
| Sodium hydroxide | Merck |
| TEMED (N, N, N', N'-Tetra methylethylene-diamine) | Promega |
| Tris [hydroxymethyl] aminomethane | Merck |
| TRIzol® reagent | Invitrogen Life Sciences |
| Trypsin | Invitrogen Life Sciences |
| Tryptone | Merck |
| Xylene cyanol | BDH |
| Yeast extract | Merck |
| Zeocin | Invitrogen Life Sciences |



The chemicals used were all of A or equivalent grade.

2.2 Kits

| | |
|---|------------------------|
| Cell culture media | GIBCO |
| First strand cDNA synthesis kit | Promega |
| LightCycler [®] FastStart DNA Master SYBR Green 1 | Roche Applied Sciences |
| Wizard [®] <i>Plus</i> Minipreps DNA Purification System | Promega |
| Wizard [®] SV Gel and PCR Clean-Up System | Promega |

2.3 Enzymes

| | |
|-----------------------------|-----------|
| <i>Bam</i> HI, <i>Not</i> I | Fermentas |
| Proteinase K | Roche |
| RNase A | Roche |
| DNase | Roche |
| T4 ligase | Fermentas |

The logo of the University of the Western Cape, featuring a classical building with columns and the text 'UNIVERSITY of the WESTERN CAPE' below it.

2.4 General stock solutions and buffers

2x Sample buffer: 100 mM Tris-HCl (pH 6.8), 25 % glycerol, 0.01 % BPB, 50 mM DTT. *stored at -20 °C

5x Running buffer: 25 mM Tris-HCl, 0.95 M glycine, 1 % SDS)

6x Glycerol BPB gel loading buffer: 30 % Glycerol, 0.25 % Bromophenol blue and 0.25 % Xylene cyanol

10x MOPS: 0.2 M Na-MOPS, 50 mM Na-Acetate, 10 mM EDTA (pH 7.0) adjusted with acetic acid

10x Phosphate buffered saline (PBS): 137 mM NaCl, 2.7 mM KCl, 8 mM Na₂HPO₄ and 1.5 mM KH₂PO₄, pH 7.4

10x TAE: 0.4 M Tris-acetate and 0.01 M EDTA, pH 8

10x TBE: 0.9 M Tris-HCl, 0.89 M Boric acid, and 25 mM EDTA, pH 8.3. This stock solution was diluted 10 times for agarose gel electrophoresis

Ammonium persulphate: A 10 % stock solution was prepared in deionised water. This solution is stored at 4 °C

Ampicillin: A 100 mg/ml stock solution was prepared in deionised water. This solution was then filter-sterilised using a 0.22 micron filter and stored at -20 °C

Blocking solution: 1-5% fat free milk powder dissolved in 1X TBS or TBST

Coommassie staining solution: 0.25 g Coommassie Brilliant Blue R 250, 45 % (v/v) methanol, 5 % (v/v) acetic acid and 60 % (v/v) dH₂O

Destaining solution: 30 % (v/v) Methanol, 10 % (v/v) Acetic acid and 60 % (v/v) dH₂O

Digestion buffer (for DNA extraction from cultured mammalian cells): 100 mM NaCl, 10 mM Tris-HCl; pH 8.0, 25 mM EDTA; pH 8.0, and 0.5 % SDS. Proteinase K was added to a final concentration of 0.1 mg/ml just before use

GTE: 50 mM Glucose, 50 mM Tris-HCl, 10 mM EDTA, pH 8.0

Luria agar (L agar): 10 g/l Tryptone, 5 g/ml Yeast extract, 5 g/ml NaCl and 14 g/ml Bacteriological agar, antibiotic added as required

Luria broth (L broth): 10 g Tryptone, 5 g/ml Yeast extract and 5 g/ml NaCl

Lysis buffer: PBS containing 1 % Triton X-100

Lysis solution: 200 mM NaOH and 1 % SDS (w/v)

Neutralisation solution: 3 M Potassium acetate, pH 5.0

Phenol/Chloroform/Isoamyl alcohol: 25 parts Tris-saturated phenol, 24 parts chloroform, 1 part isoamyl alcohol

RIPA buffer: 50 mM Tris-HCl (pH 7.4), 150 mM NaCl, 1 % (v/v) Triton X-100, 1 % deoxycholate, 0.1 % SDS, 5 mM EDTA, 1 % (v/v) protease inhibitors. Protease inhibitors were added just before use

RNase A (DNase-free): A 20 mg/ml stock solution was prepared in a buffer containing 0.1 M sodium acetate and 0.3 mM EDTA (pH 4.8, adjusted using acetic acid). This solution was boiled for 15 minutes and rapidly cooled by placing it in ice water. The solution was then dispensed into aliquots and stored at -20 °C

Separating buffer: 1.5 M Tris-HCl, pH 8.8

Stacking buffer: 0.5 M Tris-HCl, pH 6.8

TE: 10 mM Tris-HCl, 1 mM EDTA, pH 7.4- autoclaved

Transfer buffer (Western blotting): 25 mM Tris-HCl, 192 mM glycine, 20% methanol. *The buffer was prepared fresh and kept ice cold

Transformation buffer 1 (Tfb1): 30 mM potassium acetate, 50 mM manganese chloride, 0.1 M potassium chloride, 6.7 mM calcium chloride and 15 % glycerol (v/v)- filter-sterilised

Transformation buffer 2 (Tfb2): 9 mM MOPS, 10 mM potassium chloride, 50 mM calcium chloride and 15 % glycerol (v/v)- filter-sterilised

TBS: 50 mM Tris-HCl, 150 mM NaCl (adjust pH with HCl and make 1x working solution in dH₂O)

TBST: 0.1% (v/v) Tween-20, 1x TBS

TYM: 20 g/l Tryptone, 5 g/l Yeast extract, 3.5 g/l NaCl and 2 g/l MgCl₂. The broth was sterilised by autoclaving before use

All solutions were made using deionised water unless otherwise stated.

2.5 Bacterial culture

2.5.1 Bacterial strain

Escherichia coli strain MC1061 (Casadaban and Cohen, 1980) was used in all transformation procedures to clone plasmid DNA.

2.5.2 Culturing MC1061

The bacterium was plated on L agar and grown in L broth with or without ampicillin as per experimental requirements. To select for *E. coli* containing ampicillin resistant plasmid, transformed cells were plated on L agar with ampicillin at 100 µg/mL final concentration. Selection was maintained during growth in liquid cultures by including the antibiotic at the same concentration. All bacterial cultures were grown at 37 °C.

2.5.3 Storage of bacterial strain and clones

Glycerol stocks were prepared directly from overnight cultures, grown under antibiotic selection pressure, by adding an equal volume of 80 % sterile glycerol and stored at -80 °C.

2.6 Cloning vector

2.6.1 pcDNA3.1(+)/zeocin

The mammalian expression vector, pcDNA3.1(+)/zeocin (Invitrogen, USA), was used to clone the full length coding sequences of *Atic*, cytoplasmic *poly(A)-binding protein (Pabpc1)* and *Hsp27*. pcDNA3.1(+) is a 5.4 kb vector derived from pcDNA3 which is designed for high level stable and transient expression in mammalian cells. It contains a cytomegalovirus immediate-early (CMV)

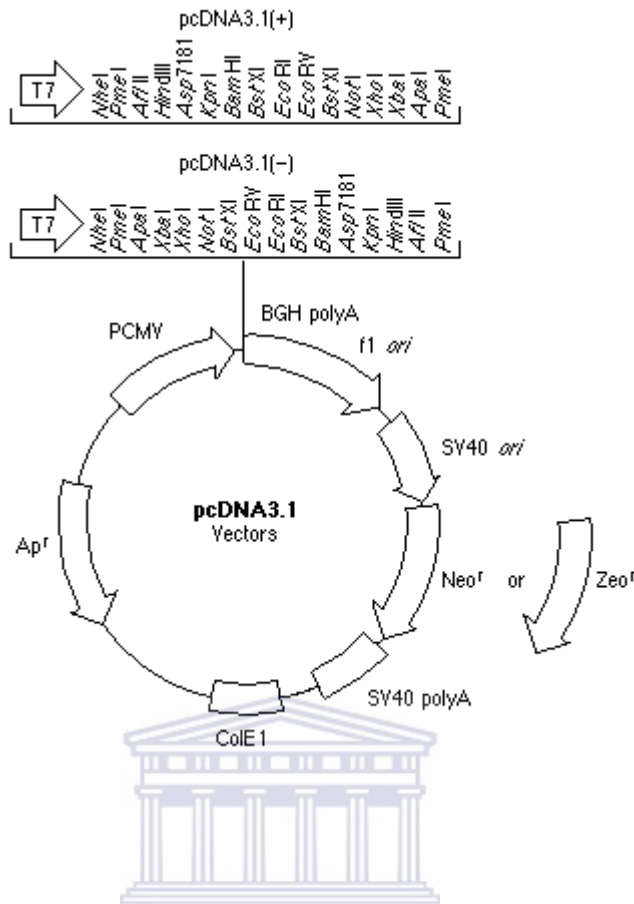
promoter, a multiple cloning site (MCS) in a forward orientation, zeocin resistance gene for selection of stable cell lines and universal T7 forward and BGH reverse primers flanking the MCS (Figure 2.1).



Figure 2.1: Restriction maps of pcDNA3.1 vectors and the MCS of pcDNA3.1(+) (adapted from www.google.com).

- (a) Restriction maps of both pcDNA3.1(+) and pcDNA3.1(-). Only pcDNA3.1(+) carrying the zeocin resistance gene was used in all cloning experiments.
- (b) The DNA sequence of the MCS of pcDNA3.1(+) showing restriction enzymes recognition sequences and the positioning of universal T7 and BGH primer sequences.





(a)

enhancer region (3' end)

```

689 CATTGACGTC AATGGGAGTT TGT TTTGGCA CAAAATCAA CGGGACTTTC CAAAATGTCG
749 TAACAAC TCC GCCCCATTGA CGCAAATGGG CGGTAGGCGT GTACGGTGGG AGGTCTATAT
      3' end of hCMV          CAAT          TATA
      |                   |                   |
      v                   v                   v
809 AAGCAGAGCT CTCTGGCTAA CTAGAGAACC CACTGCTTAC TGGCTTATCG AAATTAATAC
      T7 promoter/primer binding site          putative transcriptional start
869 GACTCACTAT AGGGAGACCC AAGCTGGCTA GCGTTTAAAC TTAAGCTTGG TACCGAGCTC
      BamH I          Nhe I          Pme I Afl II Hind III Asp718 I Kpn I
929 GGATCCACTA GTCCAGTGTG GTGGAATTCT GCAGATATCC AGCACAGTGG CGGCCGCTCG
      Xba I          BstX I* EcoR I          EcoR V          BstX I* Not I Xho I
989 AGTCTAGAGG GCCCGTTTAA ACCCGCTGAT CAGCCTCGAC TGTGCCTTCT AGTTGCCAGC
      Xba I          Apa I Pme I          pcDNA3.1/BGH reverse priming site
1049 CATCTGTTGT TTGCCCTCC CCCGTGCCTT CCTTGACCCT GGAAGGTGCC ACTCCCACTG
      BGH poly (A) site
1109 TCCTTTCCTA ATAAAATGAG GAAATGCAT
  
```

(b)

2.7 Preparation of *E. coli* competent cells for transformation

A glycerol stock of the MC1061 strain was used to streak an L agar plate containing 10 mM MgCl₂ and incubated for 16 hours at 37 °C. Following incubation, a single colony from the plate was used to inoculate 20 mL TYM broth and grown at 37 °C with vigorous shaking until an optical density (OD) of 0.2 at 550 nm was reached. The culture was then transferred to 100 mL fresh TYM broth and incubated at 37 °C until an OD of 0.2 at 550 nm was reached. The culture was transferred into a 2 L flask and 400 mL of fresh TYM broth were added to the culture followed by further growth under the same conditions until an OD between 0.4 and 0.6 at 550 nm was reached. The culture was then rapidly cooled by gently swirling the flask in ice water, transferred into a 250 mL centrifuge tube and centrifuged at 6 000 x g for 10 minutes at 4 °C in a Beckman J2-21 rotor. The supernatant was discarded and the pellet re-suspended in 250 mL of ice-cold Tfb1 buffer followed by incubation on ice water for 30 minutes. After incubation the cells were recovered by centrifugation at 6 000 x g for 10 minutes at 4 °C. The supernatant was discarded and the pellet gently re-suspended in 50 mL of ice-cold Tfb2 buffer. Re-suspended cells were then dispensed in 500 µL aliquots and rapidly frozen in liquid nitrogen. Competent cells were stored at -80 °C.

2.8 Bacterial transformation

A 300-500 µL aliquot of MC1061 competent cells were recovered from -80 °C and partially thawed on ice. 50 µL of cells were then carefully added onto 10 µL (1.0-10ng) of the plasmid DNA solution in a 1.5 ml tube, gently mixed by tapping the bottom of the tube and incubated on ice for 20 minutes. The bacterial cells were then heat-shocked by placing the tubes in a water bath equilibrated at 42 °C for 45

seconds after which they were immediately placed on ice and incubated for 5 minutes. Thereafter, 950 μL of pre-warmed sterile L broth containing no antibiotics was added and the mixture incubated on a shaker for 1 hour 30 minutes at 37 °C to allow for the expression of the antibiotic resistance marker. 50 μL of this transformed culture was then plated on nutrient L agar plates containing 100 $\mu\text{g}/\text{mL}$ ampicillin. Plates were incubated overnight at 37 °C.

2.9 Preparation of plasmid DNA

Plasmid DNA was isolated from bacterial cells based on the alkaline lysis procedure (Birnboim and Dolly, 1979).

2.9.1 Small-scale preparation of plasmid DNA

Five mL of L broth containing 100 $\mu\text{g}/\text{mL}$ ampicillin were inoculated with a single colony of transformed *E. coli* and cultured overnight at 37 °C with vigorous shaking. Glycerol stocks of the transformed *E. coli* were prepared from the overnight cultures as described in section 2.5.3. The rest of the culture was centrifuged at 10 000 x g for 10 minutes at 4°C in a Beckman J2-21centrifuge. The supernatant was discarded and the cell pellet re-suspended in 300 μL GTE containing 100 $\mu\text{g}/\text{mL}$ freshly prepared RNase A. The cell suspension was then transferred to a 1.5 mL tube and incubated on ice for 5 minutes. Cells were then lysed by adding 300 μL of lysis solution, carefully mixed by 4 inversions and incubated on ice for 5 minutes. After incubation 300 μL neutralisation solution were added to neutralise the alkali followed by gentle mixing by 4 inversions. The resultant mixture was further incubated on ice for 5 minutes and then centrifuged at 14 000 x g for 10 minutes at 4 °C. The supernatant were transferred to a sterile

1.5 ml tube and 450 μ L of propan-2-ol added, mixed gently by inversion and placed at -20°C for at least 30 minutes to precipitate the plasmid DNA. After incubation the samples were centrifuged at $10\,000 \times g$ for 20 minutes at room temperature. The supernatant was discarded and the pellet re-suspended in 500 μ L TE buffer. An equal volume of phenol:chloroform:isoamyl alcohol was added followed by centrifugation at $10\,000 \times g$ for 5 minutes at room temperature. The upper aqueous phase containing the DNA was transferred to a clean 1.5 ml tube and DNA precipitated by adding 0.1 volumes of 3M sodium acetate and 2.5 volumes of ethanol. This was incubated for 30 minutes at -20°C and the DNA was recovered by centrifugation at $10\,000 \times g$ for 10 minutes at room temperature. The supernatant was decanted and the pellet washed with 70 % ethanol. The plasmid DNA was again recovered by centrifugation at $10\,000 \times g$ for 5 minutes at room temperature. The pellet was air-dried and re-suspended in 50 μ L TE buffer, increasing the volume to 100 μ L if the pellet was too viscous. The DNA was quantified by measuring OD at 260 nm using a ND 1 000 spectrophotometer (one OD_{260} unit of double stranded DNA is equivalent to 50 ng/ μ L).

2.9.2 Large-scale recovery of plasmid DNA from transformed MC1061 E. coli bacterial cells by double cesium chloride/ethidium bromide fractionation

This method was used to produce high quality plasmid DNA for transfection of eukaryotic cells. 500 mL of L broth were inoculated with 10 μ L of the plasmid-containing bacterial glycerol stock and grown overnight at 37°C . Bacterial cells were harvested by centrifugation at $4\,500 \times g$ for 10 minutes at 4°C . The supernatant was discarded and the pellet was re-suspended in 4 mL GTE buffer containing 100 $\mu\text{g}/\text{mL}$ RNase A followed by incubation at 37°C for 2 hours. The

cells were then lysed by adding 8 mL of lysis solution, mixed carefully by inverting the tube six times and incubation on ice for 10 minutes. After incubation 6 ml of 3.5 M potassium acetate (pH 5.5) were added to neutralise the alkali, mixed gently by inversion and incubated on ice for 10 minutes. The precipitate of cell debris, chromosomal DNA and SDS was removed by centrifugation at 10 000 x g for 15 minutes at 4 °C. The resulting supernatant was filtered through glass wool to remove particulate material and nucleic acids were precipitated by adding 0.8 volumes of propan-2-ol followed by incubation at -20 °C for 20 minutes. Nucleic acids were then recovered by centrifugation at 10 000 x g for 10 minutes at 4 °C and re-suspended in 5 ml TE. Plasmid DNA was separated from RNA by double CsCl/ethidium bromide fractionation.

Thereafter, 500 µL ethidium bromide and 5.75g cesium chloride were added to the 5 mL solution containing resuspended nucleic acids and thoroughly mixed to give a final density of 1.61 g/mL. If necessary the density was adjusted using TE and cesium chloride-saturated TE. The mixture was centrifuged at 10 000 x g for 10 minutes at -20 °C. The resulting pellet was mainly RNA and the DNA remained in the supernatant which was recovered using a syringe, filtered through glass wool, and the density re-adjusted using TE and cesium chloride-saturated TE to give a final density of 1.61 g/mL. 5 mL of the supernatant were transferred to a Quickseal tube and centrifuged at 55 000 x g for 18 hours at 20 °C in a Beckman Coulter Optima™ L-80 XP ultracentrifuge (Beckman Coulter, USA) using an NV65.2 rotor. After centrifugation the plasmid DNA band was visualised using a 360 nm UV illuminator and recovered using a syringe.

An equal volume of sodium chloride-saturated isopropanol was added followed by centrifugation at $4\ 500 \times g$ for 5 minutes at room temperature to remove the ethidium bromide from the DNA. The top ethidium bromide layer was aspirated and the extraction repeated at least four times, discarding the coloured top layer each time. Two volumes of water and one volume of propan-2-ol were added, mixed by vortexing and incubated for 30 minutes at $-20\ ^\circ\text{C}$. The DNA was then recovered by centrifugation at $10\ 000 \times g$ for 15 minutes at room temperature and the resulting pellet was air-dried and re-suspended in TE. The concentration was determined by measuring absorbance at λ_{260} nm and the DNA stored at $-20\ ^\circ\text{C}$.

2.10 Restriction enzyme digestion of plasmid DNA

To enable ligation of a DNA fragment into the MCS of pcDNA3.1(+), double restriction enzyme digestion of the vector was carried out using *NotI* and *BamHI* FastDigest[®] restriction enzyme in a compatible 1x FastDigest[®] buffer (Fermentas Life Sciences, USA) according to the manufacturer's instructions. Approximately 1 μg of plasmid DNA was digested with 10 units of each restriction enzyme in a 50 μl reaction (Table 2.1).

Table 2.1: Restriction enzyme digestion mix.

One μg of DNA was double-digested using *NotI* and *BamHI* FastDigest[®] restriction enzyme in 1x FastDigest[®] buffer.

| REAGENT | VOLUME (μL) |
|--|--------------------------|
| Nuclease-free water | - |
| 10x FastDigest [®] buffer | 5 |
| FastDigest [®] enzymes (10 U) | 2 |
| DNA (1 μg) | - |
| TOTAL VOLUME | 50 |

The digest mixture was incubated for 30 minutes on a heating block at 37 °C. After incubation restriction enzymes were inactivated by incubating for 5 minutes at 80 °C. The digested plasmid DNA and PCR products were extracted by electrophoresis on a 1 % agarose gel.

2.11 Dephosphorylation of digested plasmid DNA

To prevent re-circularisation of a partially digested, empty vector during ligation, the digested vector was dephosphorylated using shrimp alkaline phosphatase (SAP) (Fermentas Life Sciences, USA). SAP catalyses the release of 5' and 3' phosphate groups from DNA and RNA. The dephosphorylation reaction was set up as shown on Table 2.2 and incubated for 1 hour on a heating block at 37 °C. After incubation the SAP was inactivated by incubating for 15 minutes at 65 °C.

Table 2.2: Dephosphorylation reaction set-up using shrimp alkaline phosphatase (SAP).

| REAGENT | VOLUME (μL) |
|-------------------------|-----------------------------------|
| Nuclease-free water | - |
| 10x SAP reaction buffer | 5 |
| DNA (100 ng) | - |
| SAP (10 U) | 1 |
| TOTAL VOLUME | 50 |

2.12 Design of cloning primers

Primers were designed to amplify the full-length coding sequence (CDS) of three genes from the *Rattus norvegicus* genome; *Atic* (Accession number: NM_031014), cytoplasmic *Poly(A)-binding protein (Pabpc1)* (accession number: NM_008774) and *Hsp27* (accession number NM_031970.3) (<http://www.ncbi.nlm.nih.gov/>). To enable digestion of the PCR product with restriction enzymes, the recognition sequence for *Bam*HI was designed into the 5' end of the forward primers and that of *Not*I was designed into the 5' end of the reverse primers (Table 2.3). Additionally, a Kozak translation initiation sequence and an ATG start codon, (**G/ANNATGG**) were designed into the 5' end of the forward primer where possible for proper initiation of translation (Kozak, 1991; Kazak, 1990). Figures 22, 23 and 24 show the full coding sequences for *Atic*, *Pabpc1* and *Hsp27* respectively, and the positioning of the forward and reverse primers.

Table 2.3: Primers that were designed to amplify full-length coding sequences of *Atic* (1 779 bp), *Pabpc1* (1 911 bp) and *Hsp27* (618 bp) by PCR.

Underlined sequences represent restriction recognition sequences for *Bam*HI and *Not*I in the forward and reverse primers respectively. Bold letters represent the Kozak sequence inserted at the 5' end of the forward primers to enable proper initiation of translation.

| Gene | Forward primer (5'-3') | Reverse primer (5'-3') | Expected size (bp) |
|---------------|--|-----------------------------------|--------------------|
| <i>Atic</i> | GTG <u>GAGGATCCGACATGG</u> CTTCCTCCCAGCTTG | ATAAGCGGCCGCTCAGTGGTGGTGAAGAGACGC | 1 779 |
| <i>Pabpc1</i> | CTAAGGATCCGACATGAACCCCAGCGCCCC | CAGAGCGGCCGCTTAGACAGTTGGAACACCAGT | 1 911 |
| <i>Hsp27</i> | CTGAGGATCCGACATGACCGAGCGCCGCGTGC | ACTAGCGGCCGCTACTTGGCTCCAGACTGTTC | 618 |

ATGGCTTCCTCCCAGCTTGCCCTGTTTCAGTGTGTCTGACAAAACCTGGCCTCGTGGAAATTTGCCAGA
AACCTCGCGTCTCTTGGTTTGGAGTTTGGTCGCTTCTGGAGGCACGGCAAAAGCGATCAGGGATGCT
GGCCTGGCAGTGAGAGATGTGTCTGAGCTAACTGGGTTCCCTGAAATGTTAGGGGGGCGTGTGAAA
ACCTTGCATCCTGCAGTCCATGCTGGAATCTTAGCACGCAATATTCCAGAAGATGCTGCTGACATG
GCCAGGCTTGATTTCAACCTCATAAGAGTTGTTGTCTGTAACCTGTACCCGTTCTGTGAGACTGTG
GCTTCTCCAGATGTAACCGTTGAGGCAGCTGTTGAGCAAATTGACATTGGTGGCGTGACCTTACTG
AGAGCTGCAGCCAAAAACCATGCTCGAGTGACAGTTGTGTGTGAGCCAGAGGACTATGGTGCGGTG
GCTGCAGAGATGCAGGGCTCTGGTAATAAGGACACCTCCCTGGAGACCAGGCGCCACTTGGCATTG
AAGGCATTACGCATAACCGCTCAATATGATGAAGCGATTTCCGATTACTTCAGGAGACAGTACAGT
AAAGGAATTTCTCAGATGCCCTTGAGGTATGGGATGAACCCCATCAGACTCCTGCCAGCTGTAT
ACACTGAAGCCCAAGCTTCCCATCACAGTTCTCAACGGAGCCCCAGGATTCATAAACCTCTGCGAT
GCTTTGAATGCCTGGCAGCTGGTGACAGACTGAGAGGAGCAGTAGACATTCAGCTGCGGCGTCT
TTCAAGCACGTGAGCCAGAGGTGCTGCTGTTGGGGTTCCACTCAGTGAGGACGAAGCCAGAGTC
TGCATGGTCTATGACCTCTATCCGACCCTCACGCCCCCTGGCCATTGCATATGCAAGAGCAAGAGGA
GCTGATAGGATGTCTTCATTTGGTGATTTTGTGCTTATCTGATGTTTGTGATGTCCCAACTGCA
AAAATTATCTCCAGAGAAGTGTGAGATGGTATTGTTGCCCCAGGATATGAGGAAGAGGCCTTGAAA
ATACTTTCTAAAAAGAAAAATGGAAGCTACTGTGTTCTTCAGATGGACCAGTCTACAAACCGGAT
GAAAATGAAGTTTCGAACGCTCTTTGGTCTTCGTTTAAAGCCAGAAGAGAAAATAATGGTGTGTTGAC
AAGTCGTTGTTTAGCAATATTGTCACCAAGAATAAAGATCTGCCGGAATCTGCTCTCCGAGACCTC
ATTGTCGCCACCATCGCTGTCAAGTATACTCAGTCTAATTCGGTGTGCTATGCCAAGGACGGGCAG
GTTATTGGCCTCGGAGCAGGACAGCAGTCTCGGATACACTGTACACGCTTGCAGGTGATAAGGCA
AACTCTTGGTGGCTTCGGCACCATCCACGAGTGCTTTCCATGAAGTTTAAAGCTGGGGTGAAGAGA
GCAGAAGTCTCCAATGCCATCGATCAGTATGTGACCGGCACCATTGGTGAGGGTGAAGACCTGGTG
AAATGGAAAGCACTGTTTGAAGAGGTTCTGAGTTACTCACTGAGGCGGAGAAGAAGGAATGGGTG
GACAAGCTGAGTGGCGTGTCTGTGAGTTCCGATGCTTTCTTTTCTTTTCCAGGGATAATGTAGACCGA
GCGAAAAGGAGTGGTGTGGCCTACATTGTTGCTCCATCCGGATCTACTGCTGACAAGGTTGTGATC
GAGGCGTGTGACGAGCTGGGGATCGTGTGGCTCATAACAGATCT**GCGTCTCTTCCACCACTGA**

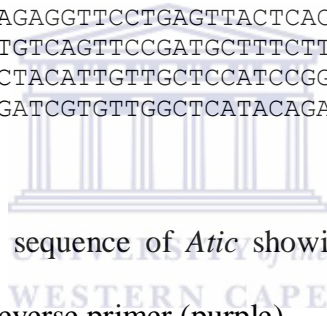


Figure 2.2: Full coding sequence of *Atic* showing the position of the forward primer (yellow) and the reverse primer (purple).

ATGAACCCCAGCGCCCCCAGCTACCCCATGGCCTCTCTGTACGTGGGGGACCTGCACCCCGACGTG
 ACCGAGGCGATGCTCTACGAGAAGTTTCAGCCCGCCGGGCCATCCTCTCCATCCGGGTCTGCAGG
 GACATGATCACCCGCGCTCCTTGGGCTACGCGTACGTGAACTTCCAGCAGCCGGCGGACGCGGAA
 CGTGCTTTGGACACCATGAATTTTGTATGTTATAAAGGGCAAGCCAGTACGCATCATGTGGTCTCAG
 CGTGATCCATCACTTCGCAAAAGTGGAGTAGGCAACATATTCATTAAAAATTTGGACAAATCCATC
 GACAATAAAGCACTATATGATACGTTTTTCTGCGTTTTGGTAACATCCTTTTCATGTAAGGTGGTTTGT
 GATGAAAATGGCTCCAAGGGCTATGGATTTGTACACTTTGAAAACACAGGAAGCAGCTGAAAAGAGCT
 ATTGAAAAAATGAATGGGATGCTTCTAAATGATCGTAAAAGTGTGTGGTGGACGATTTAAATCTCGG
 AAGGAACGAGAAGCAGAGCTTGGAGCCAGGGCAAAGGAGTTCACCAATGTTTACATCAAGAACTTT
 GGAGAAGACATGGATGATGAGCGCCTTAAGGAACTCTTTGGCAAGTTTGGGCTGCCTTAAGTGTG
 AAAGTAATGACAGATGAAAGTGGAAAATCCAAAGGATTTGGATTTGTAAGCTTTGAAAGGCATGAA
 GATGCGCAGAAAGCTGTGGATGAGATGAATGGGAAGGAGCTCAATGAAAACAGATTTATGTTGGA
 CGAGCTCAGAAAAAAGTGGAACGGCAGACGGAATTAAGCGCAAATTTGACGAGATGAAGCAAGAT
 AGGATCACCAGATATCAGGGTGTGAACCTTTATGTGAAAAATCTTGATGACGGGATGATGATGAG
 CGTCTCCGGAAGGAGTTTTCTCCGTTTTGGTACAATCACCAGTGCAAAAAGTAATGATGGAGGGTGGG
 CGCAGCAAAGGGTTTTGGTTTTGTATGTTTTCTCATCCCCTGAAGAAGCCACTAAAGCAGTTACAGAG
 ATGAATGGTAGAATTGTGGCCACGAAGCCACTGTATGTAGCTTTAGCTCAGCGCAAAGAAGAGCGC
 CAGGCTCACCTCACTAACCAGTATATGCAGAGGATGGCAAGTGTACGAGCTGTGCCAACCCCGTG
 ATCAACCCCTACCAGCCAGCACCTCCTTCAGGTTACTTTCATGGCAGCTATCCCACAGACTCAGAAC
 CGTGCTGCATACTATCCTCCTAGCCAAATTGCTCAACTAAGACCAAGTCTCGCTGGACTGCTCAG
 GGTGCCAGACCTCATCCATTCCAGAATATGCCCGGTGCTATCCGCCAGCTGCTCCTAGACCACCA
 TTTAGTACGATGAGACCAGCTTCCCTCACAGGTTCCACGAGTCATGTCAACACAGCGTGTGCTAAC
 ACATCAACACAGACAATGGGTCCACGTCTGCAGCTGCTGCTGCTGCAGCCACTCCTGCTGTCCGC
 ACCGTTCCCCAGTATAAATATGCTGCGGGAGTCCGCAATCCCCAGCAACATCTTAATGCACAGCCA
 CAAGTTACCATGCAACAGCCTGCTGTTTCATGTGCAAGGTCAAGAACCTTTAACTGCTTCCATGTTG
 GCATCTGCGCCCCCGCAAGAGCAGAAGCAAATGTTGGGTGAACGGCTGTTTCTCTTATCCAAGCC
 ATGCACCCTTCTCTTGTGGTAAAATCACTGGCATGCTGTTGGAGATTGATAACTCAGAATTACTT
 CACATGCTCGAGTCTCCAGAGTCTCTCCGCTCAAAGGTTGATGAAGCTGTAGCTGTACTACAAGCC
 CACCAAGCGAAAGAGGCTGCCAGAAAAGCAGTGAACAGTGCC**ACTGGTGTCCAAGTGTCTAA**



Figure 2.3: Full coding sequence of *Pabpc1* showing the position of the forward primer (yellow) and the reverse primer (purple).

ATGACCGAGCGCCCGCTGCCCTTCTCGCTACTGCGGAGCCCCAGCTGGGAGCCGTTCCGGGACTGG
 TACCCTGCCCACAGCCGCTCTTCGATCAAGCTTTCGGGGTGCCTCGGTTTCCCGATGAGTGGTCT
 CAGTGGTTCAGCTCCGCTGGTTGGCCCCGGCTATGTGCGCCCTCTGCCCGCCGACCCGCCAGGGC
 CCCGCAGCAGTGACCCTGGCCCCGGCCTTCAGCCGGGCGCTCAACCGGCAACTCAGCAGCGGTGTG
 TCAGAGATCCGACAGACGGCCGATCGCTGGCGCGTGTCCCTGGACGTCAACCACTTCGCTCCTGAG
 GAGCTCACAGTGAAGACCAAGGAAGGCGTGGTGGAGATCACTGGCAAGCACGAAGAAAGGCAGGAT
 GAACATGGCTACATCTCTCGGTGCTTACCCGGAAATACACGCTCCCTCCAGGTGTGGACCCACC
 TTGGTGTCTCTTCCCTGTCCCTGAGGGCACACTCACGGTGGAGGCTCCGCTGCCCAAAGCAGTC
 ACACAATCAGCGGAGATCACCATTCCGGTCACTTTCGAGGCCCGTGCCCAAATTTGGAGGGCCAGAG
 TCG**GAACAGTCTGGAGCCAAGTAG**

Figure 2.4: Full coding sequence of *Hsp27* showing the position of the forward primer (yellow) and the reverse primer (purple).

2.13 Amplification of target fragments by PCR

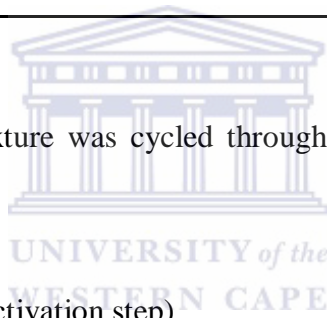
Atic, *Pabpc1* and *Hsp27* full-length coding sequences were amplified by PCR under optimum conditions from first-strand cDNA synthesised from RNA extracted from H9c2 cells. PCR reactions were carried out in 1x reaction buffer using 100 ng of cDNA, 0.5 μ M of each dNTP, 0.5 μ M of the forward and reverse gene-specific primers, 2.5 mM MgCl₂ and 0.2 U ExSel *Taq* DNA polymerase (Invitrogen, USA), in a final reaction volume of 50 μ L (Table 2.4).



Table 2.4: PCR components.

| REACTION COMPONENT | VOLUME (μL) |
|--|--|
| Nuclease-free water | 28.1 |
| 10x reaction buffer | 5.0 |
| MgCl ₂ (50 mM stock) | 2.5 |
| dNTPs (5 μM stock) | 2.0 |
| Forward primer (5 μM stock) | 5.0 |
| Reverse primer (5 μM stock) | 5.0 |
| ExSel <i>Taq</i> polymerase (0.2 U) | 0.4 |
| cDNA (100 ng/ μl) | 2.0 |
| TOTAL VOLUME | 50.0 |

The PCR reaction mixture was cycled through a pre-optimised PCR program shown below:



94 °C for 2 min (Initial activation step)

94 °C for 1 min (Denaturation step)

*(T_m) for 0.5 min (Annealing step)

72 °C for 1 min (Extension step)

} 40 cycles

72 °C for 10 min (Final extension step)

*T_m for *Atic* = 63.8 °C, *Pabp* = 64 °C and *Hsp27* = 66 °C.

2.14 Agarose gel electrophoresis of DNA

DNA was size fractionated by agarose gel electrophoresis on 1 or 2 % agarose gels containing 0.5 µg/mL ethidium bromide. Each DNA sample was mixed with 6x glycerol BPB gel-loading buffer before loading onto the gel. Appropriate DNA size markers were loaded alongside the samples to enable estimation of the size of the DNA fragments. Electrophoresis was carried out at 100 V in 1x TBE or TAE electrophoresis buffer and the DNA was visualised with shortwave UV light on a trans-illuminator and gel images captured using the Sony UVP image Store 5000 photographic system.

2.14.1 DNA molecular weight markers

Two DNA molecular weight markers were used; MassRuler™ DNA ladder mix, ready to use and GenRuler™ 1kb plus DNA ladder (Fermentas Life Sciences, USA). These markers were used to estimate DNA sizes between 0.6 to 6.0 kb (Figure 2.5).

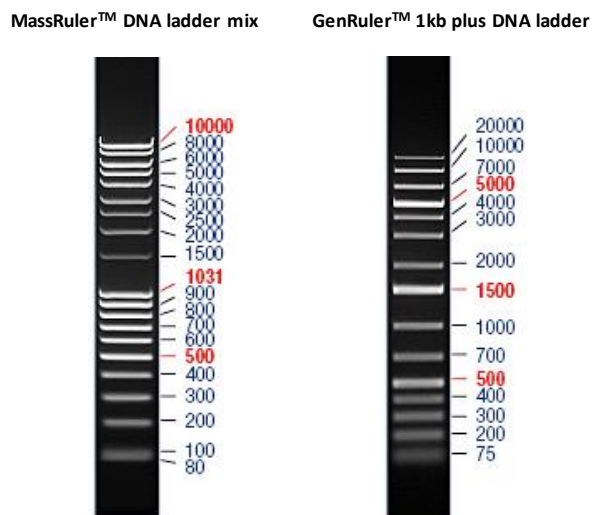


Figure 2.5: DNA molecular weight markers that were used to estimate the size of DNA fragments.

2.14.2 Agarose gel purification of DNA

This method was used to purify both PCR fragments and the digested vector for use in a ligation reaction. A small volume of the sample to be purified was loaded onto a “marker lane” and the rest of the sample loaded onto “purification lanes” on the same 1 % agarose gel. A size marker was loaded alongside the “marker lane” and electrophoresis carried out as described in section 2.14. A piece of the gel containing the DNA size marker and the “marker lane” was then separated from the rest of the gel and visualised using a hand-held UV lamp (365 nm). The position of the band of interest was excised using a blade and the gel aligned with the other piece containing the “purification lanes” without exposing the latter to UV. The fragment of interest was then excised from the “purification lanes” using a sterile blade and placed into a 1.5 mL tube and weighed. DNA was purified from the agarose using the Wizard® SV Gel and PCR Clean-up system (Promega, USA) according to the manufacturer’s instructions. The DNA was eluted from the spin column using 50 µL DNase-free water and quantified on a ND 1 000 spectrophotometer.

2.14.3 Restriction enzyme digestion of PCR fragments

500 ng of PCR product were digested with appropriate restriction enzymes as described in section 2.10. DNA was then purified on a 1 % agarose gel as described in section 2.14.2 and used in a ligation reaction.

2.15 Construction of expression vectors

The digested PCR product was ligated into pcDNA3.1(+) using T4 ligase (Fermentas, USA) to generate *Atic*, *Pabpc1* and *Hsp27* expressing constructs (Table 2.5). The amount of insert required for each ligation reaction was calculated according to the equation:

$$\text{ng vector} \times \text{kb size of insert} / \text{kb size of vector} \times \text{insert:vector molar ratio} = \text{ng of insert}$$

(Promega, USA)

Table 2.5: Components of the ligation reaction.

| LIGATION COMPONENT | VOLUME (μL) |
|------------------------------|-------------|
| Nuclease-free water | - |
| 10x ligation buffer | 5 |
| Vector (50 ng) | - |
| Insert (30 ng) | - |
| T ₄ ligase (10 U) | 1 |
| TOTAL VOLUME | 50 |

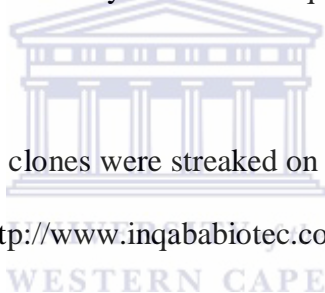
The ligation mixtures were then placed at 4 °C for 24 hours. The ligated recombinant plasmid DNA was used to transform competent MC1061 bacterial cells as described in section 2.8. Transformed bacterial cells were grown on L agar at 37 °C overnight and positive clones screened by colony PCR as described in section 2.16.

2.16 Colony PCR

To screen bacterial colonies for positive clones, part of the colony was suspended in 10 μ L of sterile water and 2 μ L of this suspension was used as template in a PCR reaction as described in section 2.13 using gene-specific primers. The PCR products were size fractionated by electrophoresis on a 1 % agarose gel and visualised under UV. The remainder of the colonies of positive clones left on L agar plates was used to inoculate 10 mL L broth containing 100 μ g/mL ampicillin and incubated on a shaker overnight at 37 °C. Glycerol stocks of each clone were prepared as described in section 2.5.3. The identity of each inserted DNA sequence was further confirmed by automated sequencing.

2.17 DNA Sequencing

Cultures of three positive clones were streaked on L agar plates and sent to Inqaba Biotech, South Africa (<http://www.inqababiotec.co.za/>) for sequencing.



2.18 Cell culture

2.18.1 Cell line

The H9c2 cell line that was used as an *in vitro* model in this study (Figure 2.6) is a sub-clone of the original clonal cell line derived from embryonic BDIX rat heart tissue (Kimes and Brandt, 1976). It exhibits many of the properties of skeletal muscles (Hescheler *et al.*, 1991). The cell line was kindly donated by the MRC/SU centre for molecular and cellular Biology, University of Stellenbosch, South Africa.

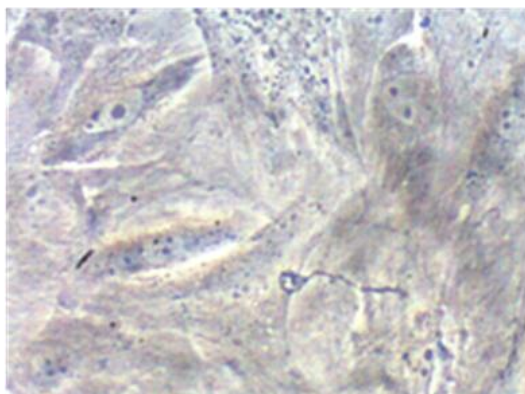


Figure 2.6: H9c2 cells viewed using a Nikon inverted light microscope (Magnification: 20x).

H9c2 cells are multinucleated myotubes formed by fusion of mononucleated myoblasts (Kimes and Brandt, 1976).

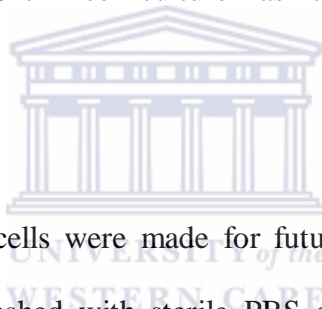
2.18.2 *Culturing of cells*

Cells were grown in Dulbecco's modified Eagle's medium (DMEM) (GIBCO, USA) supplemented with 10 % foetal bovine serum (FBS), 2 mM glutamine and antibiotics (2 % penicillin and streptomycin) under standard cell culture conditions (humidified incubator maintained at 37 °C and 0.5 % carbon dioxide). Growing cells were observed daily under a Nikon inverted light microscope to monitor confluency and contamination.

2.18.3 *Trypsinisation of cultured cells*

To maintain morphological and biochemical properties of the cell line, cultures were passaged when they reached 80 to 90 % confluency and were passaged up to 20 times. Over-confluency and increased passage numbers have been shown to cause loss of differentiation in cardiomyocytes (Hescheler *et al.*, 1991; Kimes and Brandt, 1976). Adherent cells were detached from the culture flask by decanting culture medium and washing the cells with 5 mL sterile PBS (GIBCO Life Technologies, USA). Three mL of pre-warmed sterile 2x trypsin (Invitrogen,

USA) was added and the cells placed in the incubator at 37 °C until completely detached from the bottom of the flask (usually within 10 minutes). Three mL of complete growth media was then added to inactivate the trypsin and the mixture transferred into a sterile 15 mL tube using a sterile pipette. Cells were recovered by centrifugation at 3 000 x g for 3 minutes at room temperature. After centrifugation the supernatant was decanted and the cells re-suspended in 5 mL DPBS (Invitrogen Life Sciences, USA) followed by centrifugation at 3 000 x g for 3 minutes at room temperature. The supernatant was again decanted and the cell pellet re-suspended in complete DMEM. Five mL of cell suspension were then added into each sterile 25 cm³ cell culture flask and placed in an incubator at 37 °C.



2.18.4 Freezing cells

Frozen stocks of H9c2 cells were made for future propagation of the cell line. Confluent cells were washed with sterile PBS and trypsinized as described in section 2.18.4 and cells recovered by centrifuging at 300 x g for 3 minutes at room temperature. The cell pellet was washed with 5 ml of sterile PBS and again cells recovered by centrifugation at 300 x g for 3 minutes at room temperature. The cell pellet was then re-suspended in FBS containing 10 % DMSO and dispensed into 2 ml aliquots in cryo-vials. Aliquots were immediately placed at -150 °C.

2.18.5 Transfection of cells

Only actively growing and regularly passaged cells were transfected with high quality plasmid DNA prepared by double CsCl/ethidium bromide fractionation. MetafecteneTM (Biontex, Germany) tranfection reagent was used according to the

manufacturer's instructions. The following mixtures were prepared in sterile 1.5 mL tubes:

Solution A: 1 μg of DNA in 50 μL of serum-free DMEM

Solution B: 6 μL of metafecteneTM transfection reagent in 50 μL of serum-free DMEM.

Both solutions were mixed gently by carefully pipetting up and down several times. Solution A was combined with Solution B and mixed gently by slowly pipetting up and down several times and incubated at room temperature for 20 minutes to allow lipid/DNA complexes to form. The transfection mixture was added to pre-washed cells in a 6 well plate in a drop-wise manner. 500 μL of serum-free media was then added to each well and the lipid/DNA complexes distributed evenly by gently swirling the plate. Cells were incubated at 37 °C for 4 hours and constantly monitored for bacterial and/or fungal contamination. After incubation 2 mL of complete DMEM were added to each well and cells further incubated at 37 °C for 48 hours before selection for positively transfected cells. Non-transfected controls were included in all transfection experiments to test the efficacy of the selection agent.

2.19 Isolation of total cellular proteins from cell cultures

Total proteins were extracted from confluent H9C2 cells using RIPA buffer. Cells were firstly washed in cold PBS and then 5 mL of cold PBS containing 1 % protease inhibitors was added. Cells were gently scrapped off (20-30 strokes) using a sterile cell scraper and recovered by centrifugation at 3 000 x g for 3 minutes at 4 °C. The cell pellet was then resuspended in 300 μL RIPA buffer

containing 1 % protease inhibitors and then placed on ice for 15 minutes. This was followed by centrifugation at 14 000 x g for 20 minutes at 4 °C. The supernatant containing proteins was transferred to a fresh 1.5 ml tube and stored at -80 °C until further use.

2.20 Sodium dodecylsulphate polyacrylamide gel electrophoresis (SDS-PAGE) and protein transfer

Proteins were separated by sodium dodecyl sulphate polyacrylamide gel electrophoresis (SDS-PAGE). To make a 12 % gel, 4.0 mL deionised water were mixed with 2.5 mL of 1.5 M Tris-HCl (pH 8.8), 3.5 mL of Acrylamide/Bis (37 %), 0.1 mL of 10 % sodium dodecyl sulphate (SDS) and 0.08 ml of 10 % freshly prepared ammonium persulphate (APS). 0.006 ml of TEMED was added to polymerise the gel. The mixture was then poured into a gel casting apparatus and overlaid with isopropanol. After solidifying the isopropanol was poured out and a stacking gel prepared by mixing 6.2 mL of water with 2.5 mL of 0.5 M Tris-HCl (pH 6.7), 1.3 mL of Acrylamide/Bis (37 %), 0.1 mL of 10 % SDS, 0.08 mL of 10 % APS and 0.006 mL of TEMED was poured on top of the separating gel and allowed to polymerise. One volume of protein sample was then mixed with an equal volume of sample loading buffer followed by three cycles of boiling for 5 minutes and vortexing. Samples were then centrifuged at 14 000 x g for 5 minutes and immediately 20 µL of supernatant was loaded onto the pre-run gel and electrophoresis carried out at 100 V. After electrophoresis, proteins were transferred onto an activated (by immersion into methanol) polyvinylidene fluoride membrane by applying 100 V of current in transfer buffer for 1 hour at 4 °C. After 1 hour, the transfer apparatus disassembled and the membrane carefully

stripped off. To confirm successful transfer of proteins, the membrane was stained with Ponceau's stain. After confirmation the stain was washed off the membrane by using deionised water.

2.21 Probing the blot with antibodies

The membrane was washed in TBS for 10 minutes and placed in 5 % blocking solution (low-fat powdered milk prepared in TBS Tween- TBST) and placed on a shaker for 1 hour at room temperature. A mouse Hsc/Hsp70 polyclonal primary antibody (1^o Ab) (Assay designs, USA) was diluted at 1:2 500 in 0.5 % blocking solution and added onto the membrane which was then placed on a shaker for 1 hour at room temperature. This was followed by three washes, each for 10 minutes, with TBST after which the blot was incubated in 1 % blocking solution for 10 minutes. A horse raddish peroxidase (HRP)-conjugated goat anti-mouse secondary antibody (2^o Ab) (Assay designs, USA) was diluted at 1:5 000 in 1 % blocking solution and added to the membrane followed by incubation on a shaker for 1 hour at room temperature. The membrane was then washed three times in TBST, for 15 minutes each wash.

2.22 Detection and exposure

The SuperSignal West Pico (Thermo Fisher Scientific, USA) chemiluminescence detection substrate was prepared and added onto the surface of the blot containing proteins followed by incubation in a dark place for 5 minutes. After incubation excess detection solution was drained off and detection was done using autoradiography. The blot was exposed to X-ray film for 20 minutes in a dark room. After exposure the film was developed using an x-ray processor.

2.23 Isolation of total ribonucleic acid (total RNA) from cells

Total RNA was isolated from cultured cells using TRIzol reagent (Invitrogen Life Sciences, USA) according to the manufacturer's instructions. Prior to RNA isolation, all pipettes to be used and the work area were thoroughly sanitised with 75 % ethanol diluted with DEPC-treated water. Micro tubes were washed with DEPC-treated water and further sterilised by autoclaving. Sterile gloves were worn and aseptic techniques practised throughout the procedure to prevent RNase contamination.

2.23.1 Homogenisation

Cells were lysed directly by adding 1 mL TRIzol[®] reagent to the 25 cm³ culture flask and passing the cell lysate through a pipette several times. Insoluble material was removed from the homogenate by centrifugation at 10 000 x g for 10 minutes at 4 °C. The resulting pellet contained extracellular membranes, polysaccharides, and high molecular weight DNA, whilst the supernatant contained RNA. The cleared homogenate solution was then transferred to a fresh 2 ml tube.

2.23.2 Phase separation

The homogenate solution was incubated for 5 minutes at room temperature to permit the complete dissociation of nucleoprotein complexes. Chloroform (0.2 mL per mL of TRIzol[®] reagent used in the initial homogenisation step) was then added and the solution vigorously shaken by hand for 15 seconds. This was incubated at for 3 minutes room temperature and then by centrifugation at 10 000 x g for 15 minutes at 4 °C. After centrifugation, the mixture separated into a lower red, phenol-chloroform organic phase, and a colourless upper aqueous phase containing RNA.

2.23.3 RNA precipitation

The upper aqueous phase was transferred into a fresh 2 mL tube, taking care not to disturb the interphase. RNA was then precipitated by adding 0.5 mL of ice-cold propan-2-ol per mL of TRIzol[®] reagent used in the initial homogenisation step. Samples were incubated for 1 hour at -20 °C and the RNA recovered by centrifugation at 10 000 x g for 10 minutes at 4 °C.

2.23.4 RNA wash

The supernatant was decanted and the RNA pellet washed once with 75 % ethanol in DEPC-treated water, adding at least 1 mL of 75 % ethanol per mL of TRIzol[®] reagent used for the initial homogenisation. Samples were mixed by vortexing briefly and then centrifuged at 6 000 x g for 5 minutes at 4 °C.

2.23.5 Re-dissolving the RNA

After centrifugation, the supernatant was decanted and the RNA was briefly air-dried at room temperature, taking care not to allow the pellet to dry completely as this greatly decreases its solubility. The RNA pellet was then dissolved in DEPC-treated, RNase-free water and the quality and concentration of the RNA determined by measuring OD at 260 nm using a ND 1 000 spectrophotometer (NanoDrop technologies, USA). RNA samples were stored at -80 °C until required.

2.23.6 Assessing RNA quality

2.23.6.1 RNA integrity

RNA quality and concentration were determined using the Agilent 2100 Bioanalyser (Agilent Technologies, USA). This technology is based on a

combination of microfluidics, voltage-induced sizing fractionation in gel-filled channels, and laser-induced fluorescence detection (Schroeder *et al.*, 2006). Analysis is automated and generates electropherograms and gel-like images showing separation of the 18S and 28S rRNA subunits. An RNA sample is assigned an RNA integrity number (RIN) on a scale of 1.0 to 10.0 (Figure 2.7).



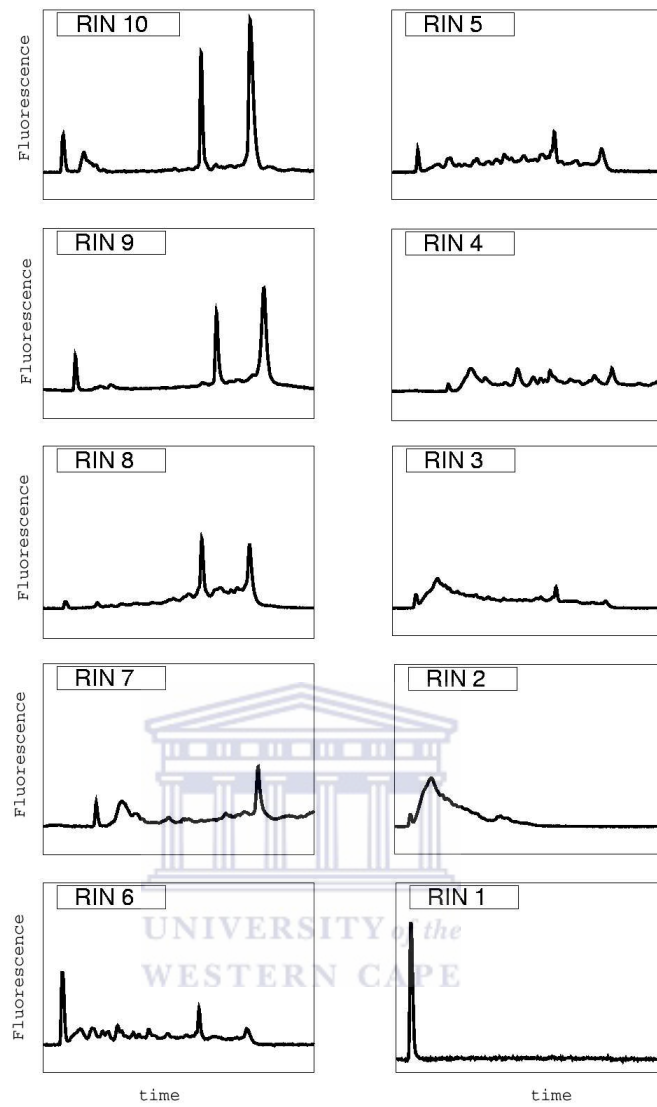


Figure 2.7: An example of electropherograms of different RNA samples with varying RIN (adapted from <http://openwetware.org>).

A RIN of 10 indicates RNA of highest integrity whilst a RIN of 1 indicates a completely degraded RNA sample.

2.23.6.2 Agarose gel electrophoresis of RNA

Total RNA was size fractionated by electrophoresis in a 1.2 % agarose gel containing 1.27 % formamide and 0.5 µg/ml ethidium bromide and electrophoresed with 1x MOPS. The RNA sample was mixed with formamide buffer before loading onto the gel. RNA was visualised with short wave UV light on a transilluminator and photographed using the Sony UVP Image Store 5000 photographic system (Sony, USA).

2.24 Reverse transcription (RT)

First strand complementary deoxyribonucleic acid (cDNA) was synthesised from tRNA using the ImProm-II™ Reverse Transcription System (Promega, USA).

2.24.1 Target RNA and oligo(dT) primer combination and denaturation

Total RNA and components of the ImProm-II reverse transcription (RT) kit were thawed on ice. One µg of RNA was then combined with 1 µL oligo(dT) in nuclease-free water to give a final volume of 5 µL (Table 2.6).

Table 2.6: Experimental reaction mix.

| REACTION COMPONENT | VOLUME (µL) |
|--------------------------------------|--------------------|
| Nuclease-free water | - |
| RNA (1 µg/reaction) | - |
| Oligo (dT) primers (0.5 µM/reaction) | 1.0 |
| FINAL VOLUME | 5.0 |

Tubes were then sealed tightly with parafilm and placed into a heating block equilibrated for 5 minutes at 70 °C. After incubation the samples were immediately place on ice and incubated for at least 5 minutes followed by

centrifugation at 10 000 x g for 10 seconds at 4 °C in a benchtop microcentrifuge to collect the condensate and maintain the original volume. Samples were then placed on ice until the reverse transcription (RT) reaction mix was ready.

2.24.2 Reverse transcription reaction

The reverse transcription (RT) reaction was prepared by mixing the following components of the ImProm-II™ Reverse Transcription System in a sterile 1.5 mL tube on ice (Table 2.7).

Table 2.7: Reverse transcription reaction mix.

| REACTION COMPONENT | VOLUME (µL) |
|---|-------------|
| Nuclease-free water | 4.5 |
| ImProm-II™ 5x reaction buffer | 3.0 |
| MgCl ₂ (final concentration 6.25 mM) | 5.0 |
| dNTP mix (final concentration 0.5 mM each dNTP) | 1.0 |
| Recombinant RNasin® Ribonuclease Inhibitor | 0.5 |
| ImProm-II™ Reverse transcriptase | 1.0 |
| FINAL VOLUME | 15.0 |

15 µL aliquots of the RT mix were then added to each reaction tube on ice to give a final RT reaction volume of 20 µL. Tubes were sealed off with parafilm and placed on a heat block for 5 minutes at 25 °C to allow the primers to anneal. After incubation tubes were then transferred onto a heat block at 45 °C and incubated for 1 hour after which reverse transcriptase was thermally inactivated by incubation for 15 minutes at 70 °C. Stock cDNA samples were stored at -20 °C.

2.25 Real-time quantitative reverse transcription polymerase chain reaction

Quantitative reverse transcription polymerase chain reaction (qRT-PCR) was optimised on the LightCycler[®] (version 4.1) (Roche, Germany) using gene-specific primers, cDNA and the LightCycler[®] FastStart DNA Master SYBR Green I kit (Roche, Germany) at the Biotechnology Department, University of the Western Cape. Annealing temperature, magnesium chloride (MgCl₂) concentration, primer concentration, template concentration and the cycling programme were optimised for the hypoxanthine phosphoribosyltransferase 1 gene (*HPRT1*), which was used as the endogenous reference gene, and each of the target genes (Table 2.8). A melting curve analysis was carried out after amplification in order to distinguish between specific and non-specific PCR products and primer dimers.

2.25.1 Primer design for qRT-PCR

Primers were designed to amplify part (from 120 to 200 bp) of the coding sequence of each target gene (<http://www.ncbi.nlm.nih.gov/>) using the Primer3 software (<http://frodo.wi.mit.edu/primer3/>) (Table 2.8).

Table 2.8: Forward and reverse primer sequences designed to amplify each of the 16 target genes and the endogenous reference gene *HPRT 1* using qRT-PCR.

| Gene | Forward primer (5'-3') | Reverse primer (5'-3') | Expected size (bp) |
|--|------------------------|------------------------|--------------------|
| <i>HPRT 1</i> | TGACACTGGCAAAACAATGCA | GGTCCTTTTCACCAGCAAGCT | 185 |
| <i>Atic</i> | TGTCTGTCAGTTCCGATGCT | TGTATGAGCCAACACGATCC | 148 |
| <i>Calcyclin-binding protein</i> | GCCTTCCTACGACTGAGG | GTCTTCCCTGGCTTGCTTCT | 142 |
| <i>Hsp27</i> | TTGGTGTCTCTTCCCTGTC | GCTCCAGACTGTTCCGACTC | 149 |
| <i>Hsp70i</i> | TCATCTCCTGGCTGGACTCT | TAATCCACCTCCTCGATGGT | 196 |
| <i>Hsp90</i> | CTGTCTTCCGGCTTCAGTCT | CTTCTTCCATGCGTGATGTG | 163 |
| <i>Moesin</i> | GCGTGTGCAGAAGCATCTTA | CAAATTCATCAATGCGCTGT | 167 |
| <i>Poly(A)-binding protein</i> | CTGGCATGCTGTTGGAGAT | TGGCACTGTTCACTGCTTTC | 153 |
| <i>RhoE</i> | ACTGGAGCAGCCACTTACAT | TCTGGTCTGCTAGGCATGTG | 170 |
| <i>Karyopherin α-3</i> | TGCAGCAACATGAAAATGAAG | GTTGGCTGTTGGGTCAAAAT | 128 |
| <i>α-β crystallin</i> | GACGTGGATCCTCTCACCAT | ACTTCTTAGGGGCTGCAGTG | 144 |
| <i>α-spectin</i> | GAGGGCAAGCCTTATGTGAC | GAGAGAACGGGTGAACTCCA | 174 |
| <i>Clathrin (heavy chain)</i> | GAGAGAACGGGTGAACTCCA | GGGGCTGACCATAAACAATG | 169 |
| <i>Prolin-4 hydroxylase</i> | AGGGCACAGATGTATTCTGG | CTTCCGTTGTTCCACAAGGT | 146 |
| <i>Filamin-α</i> | AGGCCAGAAGAGCAACTTCA | ACTCCCCTTTGTCCTTGAGC | 172 |
| <i>Formin-binding protein</i> | TCGGGACAGTGAAAAAGACA | TCATCATCCAGTTGCTCCAA | 165 |
| <i>Adrenegic- α-ID</i> | TCCATAAGATTTCGCTCTGG | GTCAGTCTCTCGGAGGTTGC | 176 |

All kit reagents were thawed on ice for 15 minutes before use and the LightCycler® FastStart DNA Master SYBR Green I vial was placed in an aluminium foil to shield the SYBR Green I fluorescence dye from sunlight. LightCycler® capillaries were placed in pre-chilled centrifuge adapters, taking care not to touch the surface of the capillaries. After thawing, the LightCycler® FastStart DNA Master mix vial and the LightCycler® FastStart Enzyme vial were briefly centrifuged and 10µl of the enzyme were added to each master mix vial and mixed gently by pipetting up and down several times. The qRT-PCR cocktail was then prepared in a 1.5 ml tube on ice as shown on Table 2.9.

Table 2.9: Real-time qRT-PCR cocktail using the LightCycler® FastStart DNA Master SYBR Green I kit.

For multiple reactions, the amount in the “volume” column was multiplied by z , where z = the number of reactions to be run plus one additional reaction.

| REACTION COMPONENT | VOLUME (µL) |
|--|--------------------|
| ddH ₂ O | 12.4 |
| MgCl ₂ (25 mM stock solution) | 1.6 |
| F-primer (10x) | 1.0 |
| R-primer (10x) | 1.0 |
| 10x LightCycler® FastStart DNA Master SYBR Green I | 2.0 |
| cDNA | 2.0 |
| FINAL VOLUME | 20.0 |


The mixture was mixed gently by pipetting up and down several times and 18 µL were pipetted into each capillary. 2 µL of water was added into non-template control (NTC) capillaries and 2 µL (~50 ng) of template cDNA was added to

reaction capillaries which were then sealed with a supplied stoppers. The LightCycler® adapters containing capillaries were centrifuged at 3000 x *g* for 30 seconds at room temperature. After centrifugation, the capillaries were transferred into the sample carousel of the LightCycler® instrument and amplified according to the optimised program. Each reaction was run in duplicate and a NTC was included for each target template. The general cycling program is shown on table Table 2.10.



Table 2.10: General qRT-PCR cycling program.

| Program | Step | Temperature | Time | Temperature transition rate | Fluorescence acquisition mode |
|----------------|--------------|------------------|--------|-----------------------------|-------------------------------|
| Pre-incubation | | 95 °C | 10 min | 20 °C /sec | None |
| Amplification | Denaturation | 95 °C | 10 sec | 20 °C /sec | None |
| Amplification | Annealing | Primer-dependent | 10 sec | 20 °C /sec | None |
| Amplification | Extension | 72 °C | 8 sec | 20 °C /sec | Single |
| Melting curve | Denaturation | 95 °C | 0 | 20 °C /sec | None |
| Melting curve | Annealing | 65 °C | 15 sec | 20 °C /sec | None |
| Melting curve | Melting | 95 °C | 0 | 0.1 °C/sec | Continuous |
| Cooling | Cooling | 40 °C | 30 sec | 20 °C/sec | None |


 UNIVERSITY of the
 WESTERN CAPE

} x40

2.25.2 Generation of standard curves

Standard curves were generated for the reference gene and some of the target genes by using four serial dilutions of the control cDNA (i.e., NHS H9c2). The template concentrations were given arbitrary values of 1 (for the undiluted cDNA), 0.1 (for the 10-fold dilution), 0.01 (for the 100-fold dilution) and 0.001 (for the 100-fold dilution). Each cDNA dilution was amplified in duplicate as shown on Table 2.10. Threshold cycles ($C_{t,s}$) were determined using ‘fit-points’ under the ‘arithmetic’ function on the LightCycler[®] software 4.1 (www.roche-applied-science.com). The software was then used to plot average C_t values against log cDNA concentration to generate standard curves.

2.25.3 Amplification efficiency (E)

The amplification efficiency (E) of each gene was calculated according to the equation below:

$$E = 10^{(-1/S)} \quad (\text{Pfaffl } et al., 2002)$$

Where E : amplification efficiency, S ; slope of the respective standard curve.

2.25.4 Relative gene expression

The expression levels of target genes were calculated relative to an endogenous reference gene ($HPRT1$) using both the ΔC_t and the $\Delta\Delta C_t$ methods.

2.25.4.1 The Δ_{ct} method

Using this method gene expression was calculated and expressed as a normalised ratio relative to the expression of $HPRT1$ in the same sample as shown in the equation below:

$$R = \frac{(E_{\text{target}})^{\Delta C_t \text{ target (control - sample)}}}{(E_{\text{ref}})^{\Delta C_t \text{ ref (control - sample)}}} \quad (\text{Pfaffl, 2001; Pfaffl et al., 2002})$$

Where R: relative expression, E_{target} : amplification efficiency of the target gene, E_{ref} : amplification efficiency of the reference gene, ΔC_t , average difference between the C_t s of the control and experimental samples).

This was the preferred method of calculation as it takes into consideration the specific E values of each target gene and reference gene.

2.25.4.2 The $\Delta\Delta C_t$ method

The $\Delta\Delta C_t$ method was used to quantify relative expression levels of genes with comparable amplification gradients in the absence of E values. The $\Delta\Delta C_t$ method differs from the ΔC_t method in that it assumes that the E value is constant and maximal amongst the various target genes.

The following steps were taken to normalise and calculate gene expression:

Step 1: calculating ΔC_t for both the target gene and the reference gene

$$C_t \text{ (treatment)} - C_t \text{ (control)} = \Delta C_t$$

Step 2: normalisation to the endogenous reference gene

$$\Delta C_t \text{ (target gene)} - \Delta C_t \text{ (reference)} = \Delta\Delta C_t$$

Step 3: calculate fold change in gene expression using the formula:

$$R = 2^{-\Delta\Delta C_t} \quad (\text{Livak and Schmittgen, 2001})$$

2.25.5 Quantification of relative gene expression in H9c2 cells by qRT-PCR

2.25.5.1 Heat shock assays

H9c2 cells were heat shocked at 42 °C for 1 hour and allowed to recover in fresh medium at 37 °C for 2 hours. Total RNA was then extracted from both heat shocked and non-heat shocked (control) cells as described previously in section 2.23. First strand cDNA was reverse transcribed from 1 µg of total RNA as described in section 2.24 and used as a template in qRT-PCR. Relative expression of the 16 genes (**Error! Reference source not found.**) in heat shocked samples as calculated using average C_t values as described in section 2.25.4.1.

2.26 Cytoprotection Assays

H9c2 cells were seeded in sterile 6-well cell culture plates at a density of 2.0×10^5 cells/mL and incubated for 24 hours at 37 °C. To induce heat shock, seeded culture plates were sealed with parafilm and submerged into a pre-heated water bath at 42 °C for 1 hour. After the heat shock treatment culture media was immediately replaced with fresh medium and the cells placed at 37 °C and allowed to recover for 0, 1, 2, 4 and 6 hours before being treated with 10 % ethanol for 4 hours. A non-heat shocked control was included for comparison in each heat shock-induced cytoprotection experiment. Percentage apoptosis was then quantified by APOPercentage™ apoptosis assay (Section 2.27).

2.27 The APOPercentage™ apoptosis Assay

Percentage cell death was detected and quantified by measuring fluorescence using the APOPercentage™ apoptosis assay (Biocolor, UK). H9c2 cells were seeded in 6-well culture plates at a density of 2.0×10^5 cells/ml and placed in a humidified incubator for 24 hours at 37 °C. The culture media was then removed and replaced with media containing 10 % ethanol. Non-treated controls were included in each treatment to ascertain that healthy cells were used for the assay. Cells were then incubated for 4 hours at 37 °C. These conditions had been established as optimal under our experimental conditions. After incubation, all the media from each well, including floating cells, was transferred to corresponding 15 ml tubes using a sterile transfer pipette for each transfer. All the wells were then washed with 1 ml PBS and the wash also transferred into the corresponding 15 ml tube containing media and floating cells. Adherent cells were trypsinised using 2x trypsin (Invitrogen, USA) and also transferred to their corresponding 15 ml tubes. Cells were recovered by centrifugation at $300 \times g$ for 5 minutes at room temperature. The supernatant was decanted and the residual supernatant aspirated, taking care not to disturb the cell pellet. The pellet was then gently re-suspended in 250 μ L of a 1:320 ($\sim 20 \mu\text{g/mL}$) dilution of APOPercentage™ dye diluted with complete DMEM. Cells were then incubated for 30 minutes at 37 °C and thereafter 4 ml of PBS were added to each tube and centrifuged at $300 \times g$ for 5 minutes at room temperature. The supernatant was discarded and the cell pellet re-suspended in 300 μ l of PBS. Cell staining was measured by flow cytometry at 670 nm using filter 3 (FL3) on a Becton Dickinson FACScan instrument (BD Biosciences, USA) fitted with a 488 nm argon laser. Acquisition was done in log mode and a

maximum of 10 000 cells per sample were acquired and analysed using CELLQuest PRO software (BD Biosciences, USA).

2.28 *In silico* analysis of gene regulation

An *in silico* strategy of analysing regulation of gene expression was developed to complement SSH data (Figure 2.8). The strategy was devised to take advantage of known transcription mechanisms regulating the expression of HS responsive genes. Only the 91 genes identified as up-regulated by SSH were considered for the *in silico* analysis which was done using the Genomatix software suite.



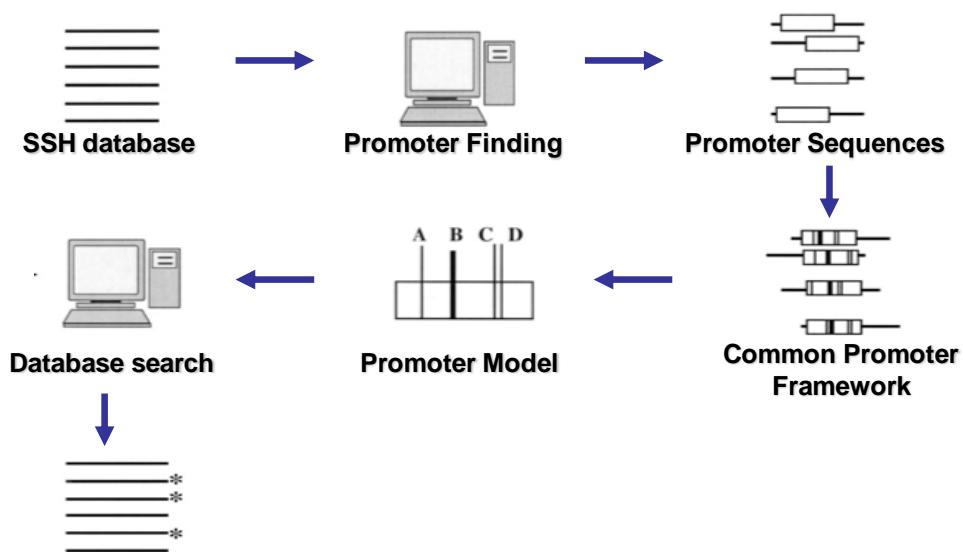


Figure 2.8: A schematic illustration of the strategy devised for *in silico* promoter analysis.

The data generated from SSH analysis was analysed *in silico* using the Genomatix software suite (Genomatix, Germany). Promoter sequences were identified using Gene2Promoter and common transcription factor binding sites were predicted using MatInspector. Conserved promoter modules were identified using ModelInspector and used to construct a promoter model which could then be applied to a DNA data base to identify co-regulated genes.

2.28.1 Identifying promoter sequences

Gene2Promoter software was used to predict promoter sequences and only experimentally verified sequences or sequences which were supported by PromoterInspector predictions were considered in the analysis. Based on these criteria the number of putative heat shock inducible genes was reduced to 60.

2.28.2 Screening promoter sequences for the HSE (V\$HEAT)

MatInspector was used to scan the 60 predicted promoter sequences for the presence of the HSE. This represents a potential binding site for HSF1 and comprise of inverted repeats of the 5'-nGAAn-3' pentanucleotide sequence. The Genomatix sequence matrix for the HSE (V\$HEAT) is 5'RGAAnttcnn3' with the random expectation value of 9.96.

2.28.3 Screening HSR genes for the presence of common promoter modules

The assumption that was made here was that the expression of HSR genes is regulated by the same set of transcription factors. As such the hypothesis was that the promoter sequences of HSR genes share conserved sequence motifs that represent binding sites for these factors. Promoter regions of three known Hsp-genes (*Hsp90*, *Hsp105 β* and *$\alpha\beta$ -crystallin*) were used as a basis to identify such common promoter modules using the ModelInspector software. The identified motifs were then used to screen the 60 genes for their presence. The expression of genes that contained these modules was further investigated in H9c2 cells following heat shock treatment using qRT-PCR.

CHAPTER 3.0: RESULTS

3.1 Establishing heat shock response in H9c2 cells

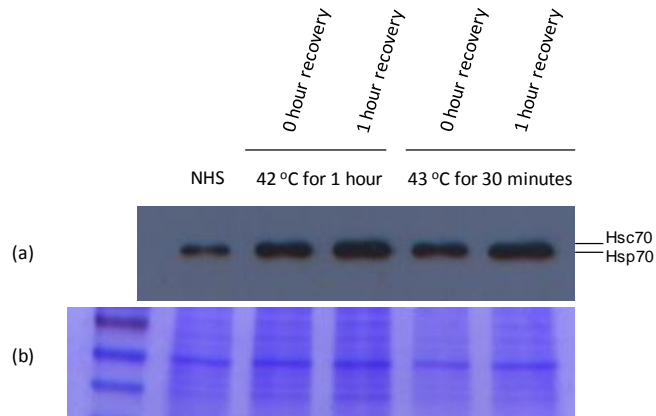


Figure 3.1: Western immunoblot of Hsc70/Hsp70 in H9c2 cells (a) and a polyacrylamide gel that was used as a sample loading control (b).

The aim of this experiment was to demonstrate the induction of Hsp70 in H9c2 cells in response to a mild heat shock treatment under experimental conditions. Cells were heat stressed as described in section 2.25.5.1. After recovery, cells were harvested and total cellular proteins extracted by using RIPA buffer (section 2.19). Proteins were separated by SDS-PAGE as described in section 2.20. The blotted membrane was then probed with a polyclonal Hsc70/Hsp70 antibody. NHS- non-heat shocked.

3.2 Characterisation of heat shock induced cytoprotection

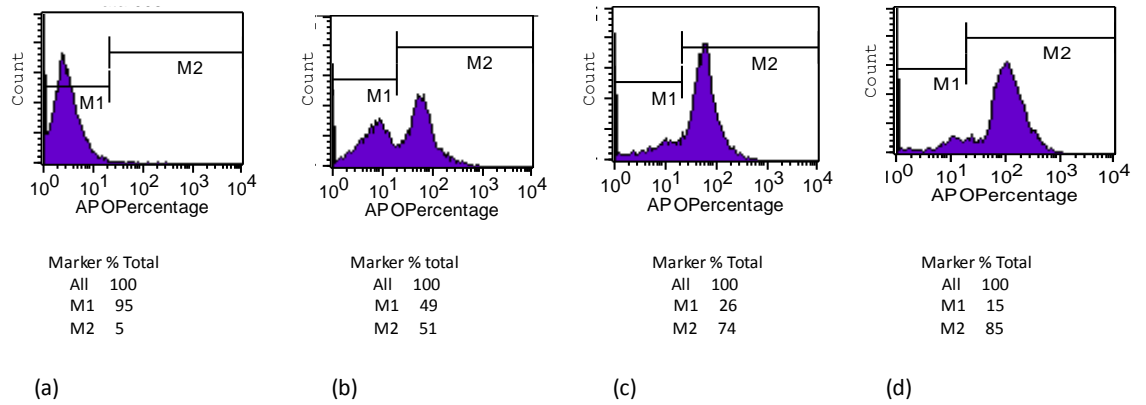


Figure 3.2: Histograms showing the shift in the position of the absorbance peak and percentage cell distribution as measured by the APOPercentage™ apoptosis assay.

In an effort to optimise the APOPercentage™ apoptosis assay, H9c2 cells were treated with 10 % ethanol for various times (section 2.26) and percentage apoptosis measured by the APOPercentage™ apoptosis assay on a FACScan machine as described in section 2.27. (a) Untreated cells; (b) Cells treated for 2 hours; (c) Cells treated for 4 hours; (d) Cells treated for 6 hours. Marker M1 represents the non-apoptotic cell population whilst Marker M2 represents the apoptotic cell population.

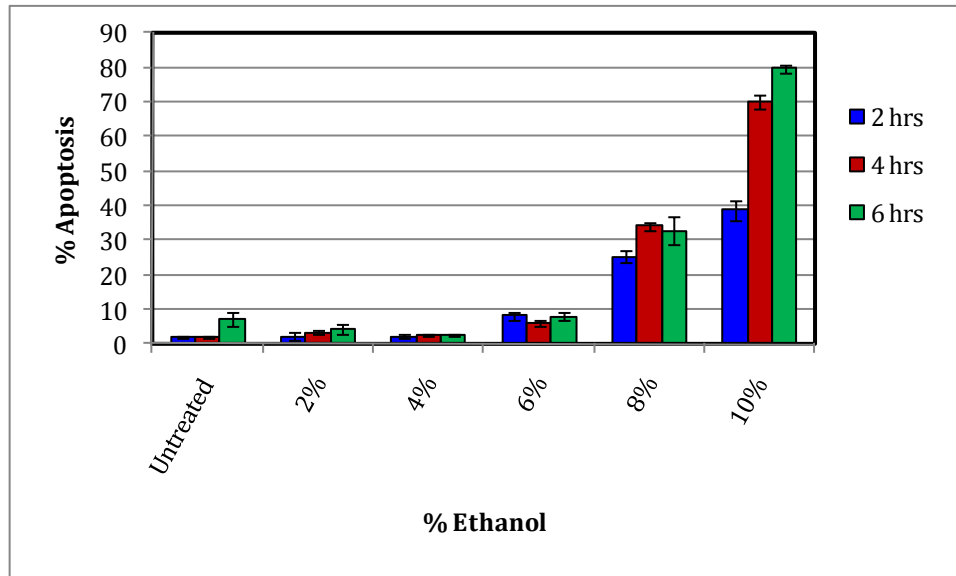


Figure 3.3: The effects of ethanol concentration and time of exposure on H9c2 cells.

The aim of this experiment was to establish a concentration of ethanol and time of treatment that would induce between 60 to 70 % cell death. H9c2 cells were exposed to varying concentrations of ethanol for 2, 4 and 6 hours. Percentage apoptosis was measured by using the APOPercentage™ apoptosis assay. Error bars represent mean \pm standard error of three independent experiments. Untr cont, untreated control.

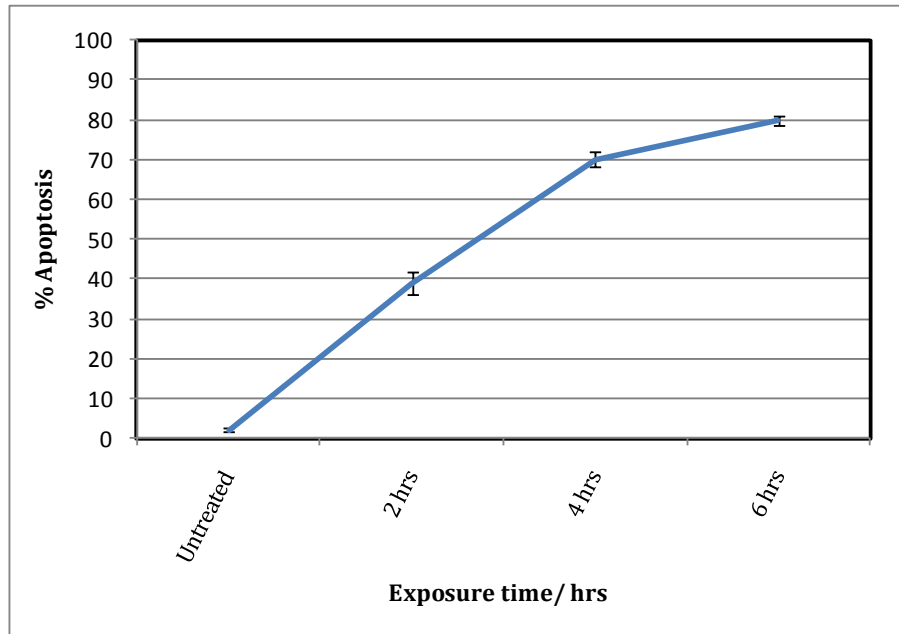


Figure 3.4: The APOPercentage™ apoptosis assay showing the exposure time-dependent effect of 10 % ethanol on H9c2 cells.

Error bars represent mean \pm standard error of three independent experiments.

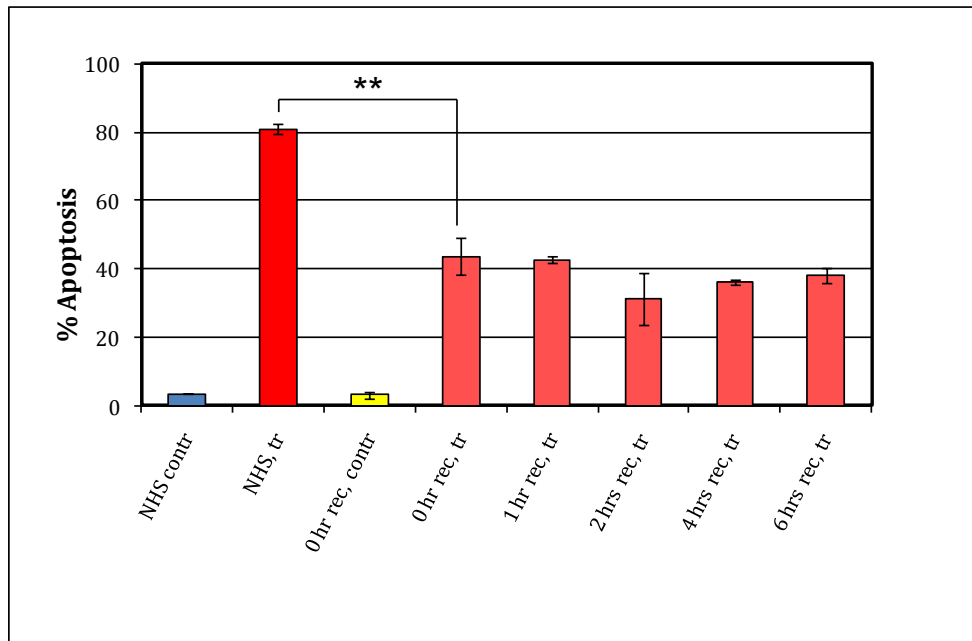


Figure 3.5: The cytoprotective effect of heat shock treatment against subsequent pro-apoptotic effects of ethanol in H9c2 cells.

The objective of this experiment was to demonstrate that prior exposure of H9c2 cells to a mild shock confers resistance to subsequent treatment with an apoptosis-inducing agent (ethanol). Cytoprotection assays were carried out as described in section 2.26 and percentage apoptosis measured by using the APOPercentage™ apoptosis assay (section 2.27). Error bars represent mean \pm standard error of three independent experiments. NHS contr, non-heat shocked, untreated control; NHS, tr, non heat shocked, treated with 10 % ethanol for 4 hours; 0 hr rec, contr, heat shocked, not treated with ethanol and processed at 0 hour recovery after heat shock; 0 hr rec, tr to 6 hrs rec, tr, heat shocked samples treated with 10 % ethanol for 4 hour after 0 to 6 hours recovery from heat shock at 37 °C, respectively.

3.4 *In silico* analysis of promoter sequences

Table 3.1: Functional classification of up- and down-regulated genes identified by SSH.

The table lists 127 genes that were identified as differentially expressed in H9c2 cells following heat shock (Gill, 2004).

| Functional Classification | Up regulated Genes | Down-regulated Genes |
|--|--|--|
| Heat shock proteins/ Chaperones | <i>α</i> B-Crystallin, Hsp90, Hsp105 β , Chaperonin subunit 80 | Cyclophilin A |
| Cytoskeleton | Moesin, Tropomyosin, Filamin, Syndecan2, Destrin, RhoE, α -spectrin, α -Parvin, Sarcolemmal associated protein | Thymosin B4, Vimentin, α -Tubulin |
| Transcription | Transcription termination factor interacting protein 5, Transcription factor IIA, Histone deacetylase 1 | Amphoterin, STAT-1 |
| Protein synthesis | PAF67, Eif4g2, Eukaryotic elongation factor 1, Ribophorin I, Ribosomal L34 | Phosphoprotein P2 and Ribosomals L31, L41, S17, S8, S27a, S20 |
| Calcium | Calcyclin binding protein, Annexin IV | Calgizzarin |
| Signal transduction | Thrombospondin 1, Syntenin, Evecitin 2, PAK 2 | Serum/glucocorticoid regulated kinase (sgk), Integrin linked kinase |
| Transport | GosR1, Connexin 43, Transportin-SR, Mss4 | MUM2 |
| Others | Damage specific DNA binding protein, Arsenite association protein, Silica induced gene 81, Desmoyokin, Gpi1, Aldose reductase like protein, Synaptogyrin 2 | Cytochrome oxidase subunit 1, Gluthathione-S-transferase alpha, Formin Binding Protein, Ubiquitin-conjugating enzyme, Succinyl-CoA synthethase B |
| EST's/Clones | 6 EST's and 9 cDNA clones of unknown function | 2 EST's and 5 cDNA's of unknown function |

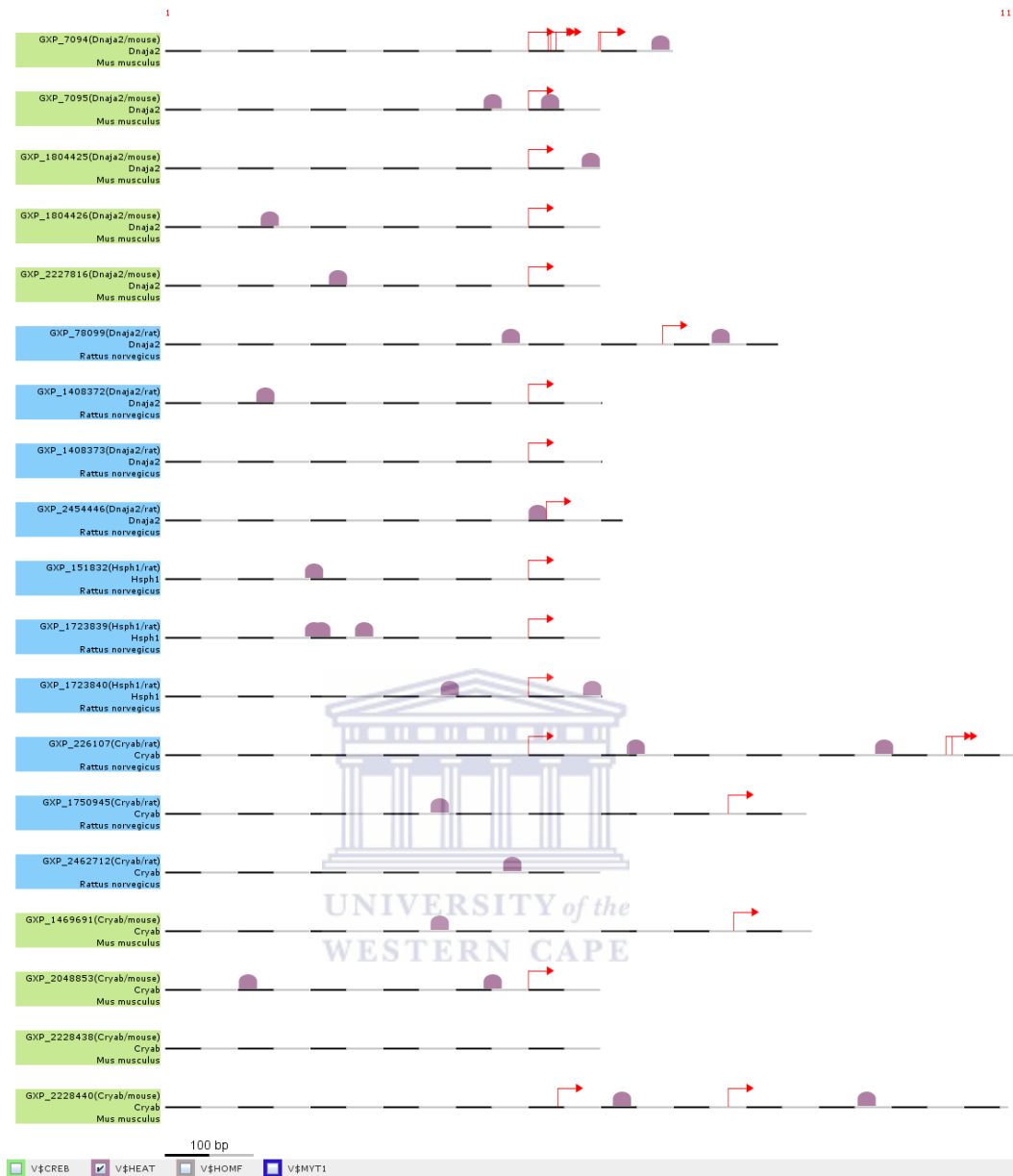


Figure 3.6: Graphic output from MatInspector showing the location of V\$HEAT in the promoters of known Hsps.

Table 3.2: Presence of the heat shock response element (V\$HEAT) in the promoter regions of genes identified by SSH.

MatInspector was used to screen the promoter sequences for the presence of the heat shock response element (V\$HEAT) sequence as described in section 2.28.2). Shown in this table is the position of the sequence in the promoter, the strand orientation, the actual sequence present in the promoter and the core similarity. The nucleotides that conform to the inverted repeat sequence are in bold.

| Gene Name | Position | Strand | Sequence | Core Similarity |
|------------------------------------|-----------|--------|----------------------|-----------------|
| Moesin | 90 - 100 | + | AGAA ag ttct | 0.975 |
| | 91 - 101 | - | GGAA ctt teta | 0.950 |
| Fms interacting protein | 525 - 535 | - | AGAA tgc tct | 0.932 |
| Cytochrome C oxidase | 186 - 196 | + | AGAA cg ctctg | 0.936 |
| X-ray radiation resistance protein | 35 - 45 | + | AGAA ta atcga | 0.943 |
| Eukaryotic translation factor 1 | 80 - 90 | + | AGAA gg atccg | 0.930 |
| | 302 - 312 | - | TGAA ta ttcat | 0.940 |
| | 303 - 313 | + | TGAA ta ttcac | 0.940 |
| Matrin 3 | 398 - 408 | - | GGAA cg ttccc | 0.962 |
| | 399 - 409 | + | GGAA cg ttct | 0.962 |
| Proline-4 hydroxylase | 545 - 555 | - | AGAA tgc teta | 0.937 |
| Syndecan 2 | 126 - 136 | - | AGAA aa atcgg | 0.935 |
| α B-Crystallin | 606 - 616 | - | GGAA tct tct | 0.938 |
| | 607 - 617 | + | GGAA g attcca | 0.947 |
| | 949 - 959 | + | AGAA g cttcac | 0.951 |

Table 3.2 continued.

| Gene Name | Position | Strand | Sequence | Core Similarity |
|---------------------------|-----------|--------|--------------|-----------------|
| Hsp90 | 64 - 74 | - | AGAAtggtccc | 0.982 |
| | 65 - 75 | + | GGAAcattcta | 0.956 |
| | 173 - 183 | - | AGAAaattcga | 0.982 |
| | 174 - 184 | + | CGAAtttctg | 0.938 |
| Hsp105 β | 415 - 425 | - | AGAActttcca | 0.965 |
| | 416 - 426 | + | GGAAagttctc | 0.960 |
| Calcyclin binding protein | 502 - 512 | - | GGAAccttcgc | 0.955 |
| | 503 - 513 | + | CGAAggttcca | 0.944 |
| Adrenergic receptor | 569 - 579 | + | AGAAggtccgg | 0.932 |
| Spermine oxidase | 139 - 149 | - | AGAAtgctcac | 0.931 |
| Formin Binding Protein | 139 - 149 | - | AGAAtgctcac | 0.931 |
| Annexin IV | 148 - 158 | - | AGAAggtatctg | 0.935 |
| α -spectrin | 148 - 158 | - | AGAAggtatctg | 0.935 |

Table 3.3: The presence of EGRF_SP1F_01 and SP1F_CEBP_01 promoter modules and their position on the – and + DNA strands of putative HSR genes.

| Gene Name | Position | Strand | Module | Model Score |
|-------------------------|----------|--------|--------------|-------------|
| Moesin | 204-173 | - | SP1F_CEBP_01 | 80.5 % |
| | 223-241 | + | EGRF_SP1F_01 | 89.3 % |
| | 269-241 | - | SP1F_CEBP_01 | 80.2 % |
| | 383-399 | + | EGRF_SP1F_01 | 89.0 % |
| | 423-439 | + | EGRF_SP1F_01 | 83.0 % |
| | 493-468 | - | SP1F_CEBP_01 | 80.5 % |
| | 649-674 | + | SP1F_CEBP_01 | 84.2 % |
| α -Spectrin | 117-145 | + | SP1F_CEBP_01 | 86.1 % |
| | 194-210 | + | EGRF_SP1F_01 | 89.0 % |
| ATIC/IMP cyclohydrolase | 405-436 | + | SP1F_CEBP_01 | 83.7 % |
| | 425-405 | - | EGRF_SP1F_01 | 86.2 % |
| | 451-467 | + | EGRF_SP1F_01 | 85.6 % |
| | 489-516 | + | SP1F_CEBP_01 | 91.8 % |
| | 505-489 | - | EGRF_SP1F_01 | 91.5 % |
| Proline-4 hydroxylase | 229-208 | - | SP1F_CEBP_01 | 83.2 % |
| | 229-208 | - | EGRF_SP1F_01 | 83.2 % |
| | 502-518 | + | EGRF_SP1F_01 | 84.6 % |
| Filamin | 264-282 | + | EGRF_SP1F_01 | 92.2 % |
| | 311-283 | - | SP1F_CEBP_01 | 82.4 % |
| | 364-346 | - | EGRF_SP1F_01 | 86.6 % |
| Karyopherin | 290-315 | + | SP1F_CEBP_01 | 80.3 % |
| | 354-338 | - | EGRF_SP1F_01 | 89.1 % |
| | 366-350 | - | EGRF_SP1F_01 | 83.5 % |
| | 673-657 | - | EGRF_SP1F_01 | 89.0 % |
| α B-Crystallin | 83-101 | + | EGRF_SP1F_01 | 98.4 % |
| | 1010-981 | - | SP1F_CEBP_01 | 82.5 % |

Table 3.3 continued.

| Gene Name | Position | Strand | Module | Module Score |
|------------------------|----------|--------|--------------|--------------|
| Hsp90 | 358-342 | - | EGRF_SPIF_01 | 84.6 % |
| | 394-368 | - | SP1F_CEBP_01 | 82.8 % |
| | 436-452 | + | EGRF_SPIF_01 | 83.2 % |
| Adrenergic receptor | 50-79 | + | SP1F_CEBP_01 | 84.6 % |
| | 599-583 | - | EGRF_SPIF_01 | 90.0 % |
| | 778-808 | + | SP1F_CEBP_01 | 83.2 % |
| Formin Binding Protein | 114-140 | + | SP1F_CEBP_01 | 82.4 % |
| | 121-103 | - | EGRF_SPIF_01 | 97.7 % |
| | 170-139 | - | SP1F_CEBP_01 | 83.4 % |
| Clathrin | 509-485 | - | SP1F_CEBP_01 | 81.5 % |
| | 612-596 | - | EGRF_SPIF_01 | 84.3 % |
| | 674-697 | + | SP1F_CEBP_01 | 80.5 % |
| Poly A binding Protein | 185-201 | + | EGRF_SPIF_01 | 91.9 % |
| | 441-457 | + | EGRF_SPIF_01 | 96.1 % |
| | 457-426 | - | SP1F_CEBP_01 | 84.8 % |
| | 730-710 | - | EGRF_SPIF_01 | 83.3 % |

3.5 Investigating the expression levels of genes containing conserved sequence motifs

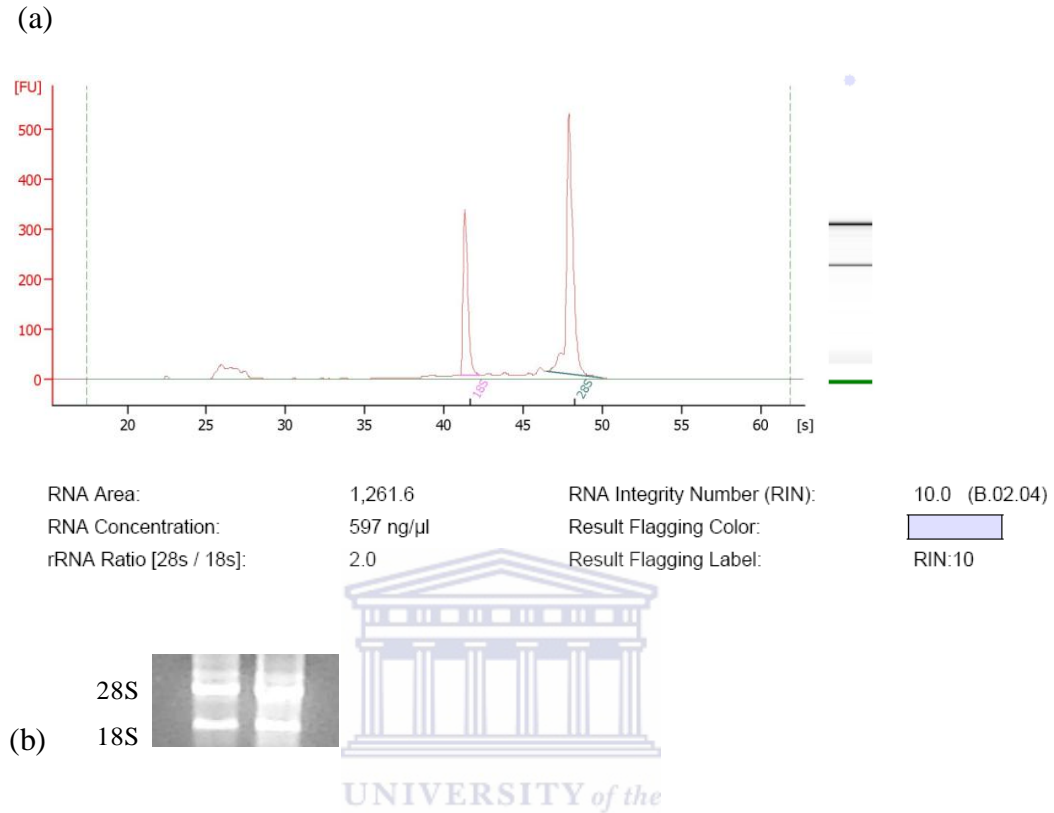
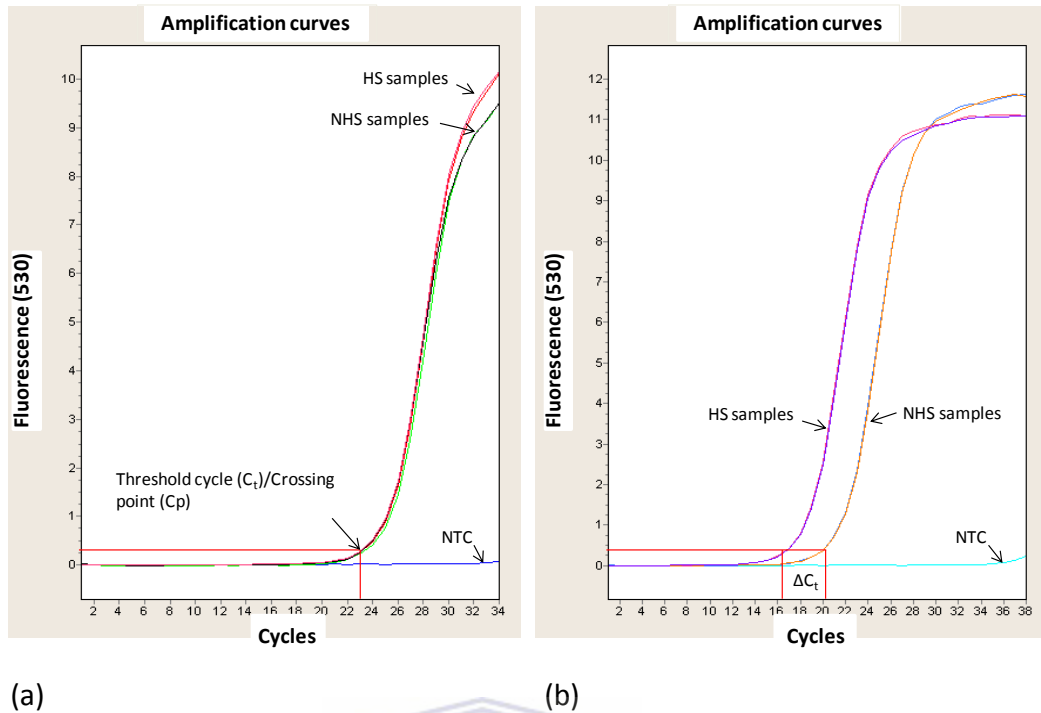


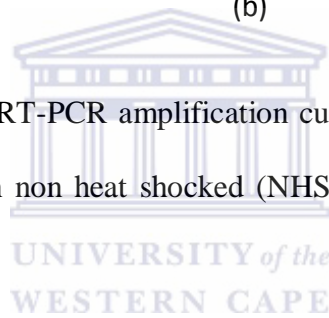
Figure 3.7: Electropherogram summary of an RNA sample extracted from H9c2 cells (a) and Gel electrophoresis image showing the 18S and 28S subunits of rRNA (b).

RNA was isolated as described in section 2.23 and RNA quality was analysed by using electrophoresis and the Agilent 2100 Bioanalyzer as described in section 2.23.6.

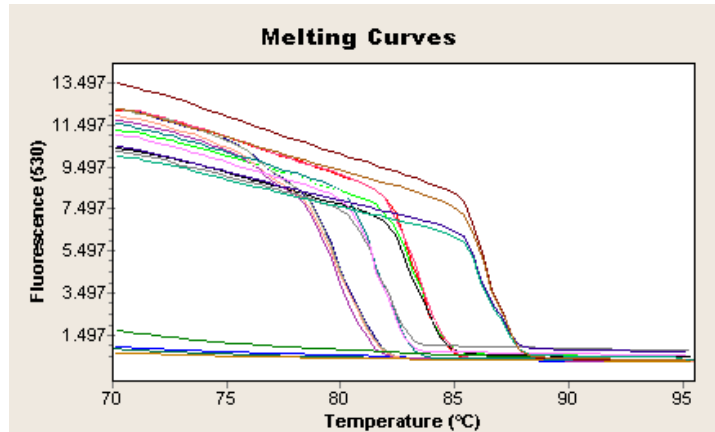


(a) (b)

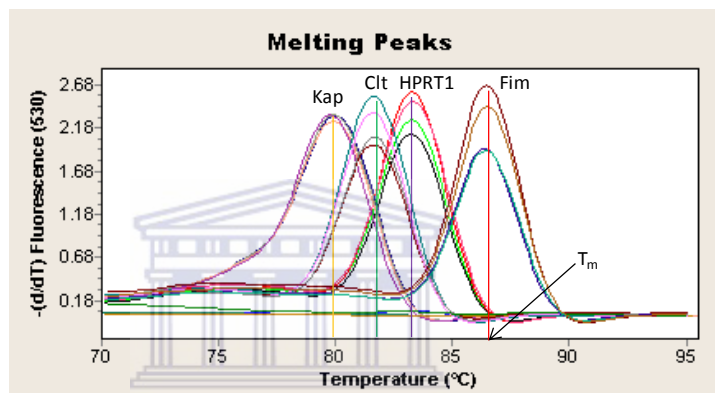
Figure 3.8: Real-time qRT-PCR amplification curves showing expression levels of *HPRT1* and *Hsp90* in non heat shocked (NHS) and heat shocked (HS) H9c2 cells.



The expression levels of *HPRT1* (reference gene) and *Hsp90* (a known heat shock responsive gene) were analysed by using qRT-PCR as described in section 2.25. A no template control (NTC) was included during the amplification for each target gene. HS, heat shocked; NHS, non-heat shocked; NTC, no template control; C_t , threshold cycle; C_p , crossing point; ΔC_t , difference in threshold cycles.



(a)

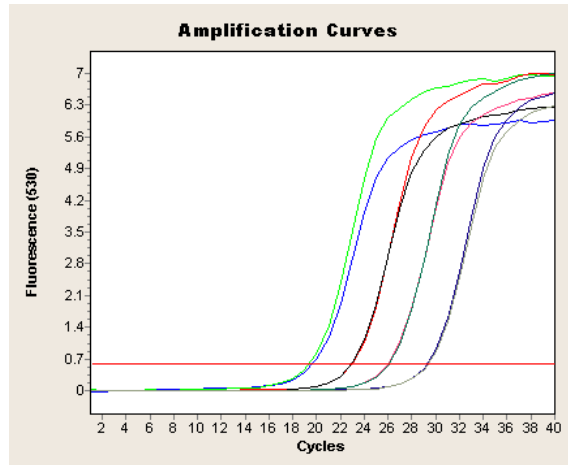


(b)

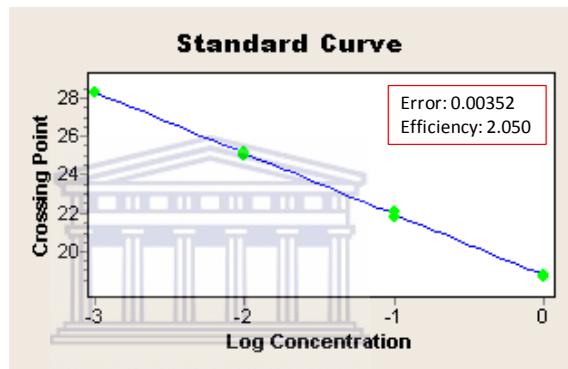
UNIVERSITY of the
WESTERN CAPE

Figure 3.9: Melting curves (a) and melting peaks (b) for *Karyopherin α -3*, *Clathrin*, *Hypoxanthine phosphoribosyltransferase 1* and *Filamin*.

A melting curve was automatically generated by using the LightCycler[®] software to plot fluorescence against temperature for each of the four genes. Plotting the reduction in fluorescence over time ($-dF/dT$) against temperature generated melting peaks for each PCR product from which T_m could be determined. Kap, *Karyopherin α -3*; Clt, *Clathrin*; HPRT1, *hypoxanthine phosphoribosyltransferase 1*; Fim, *Filamin- α* .



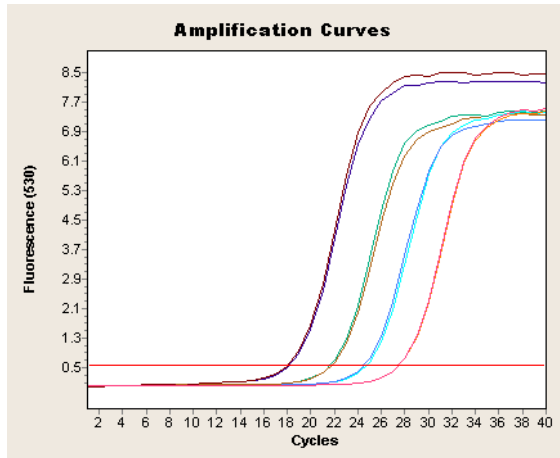
(a)



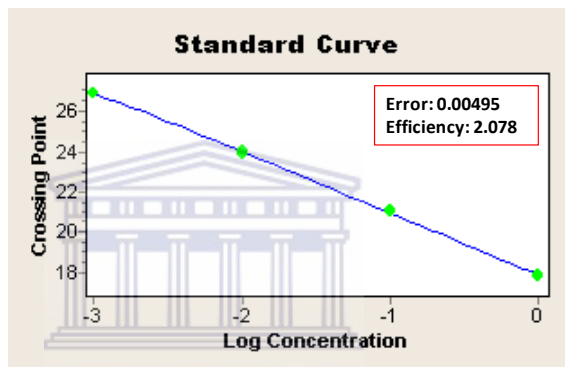
(b)

Figure 3.10: Amplification curves of standards (a) and the generated standard curve for *Atic* (b).

A calibrator sample was serially diluted and amplified by qRT-PCR as described in section 2.25.2. Mean C_t for each standard was plotted against log concentration to generate a standard curve for *Atic*.



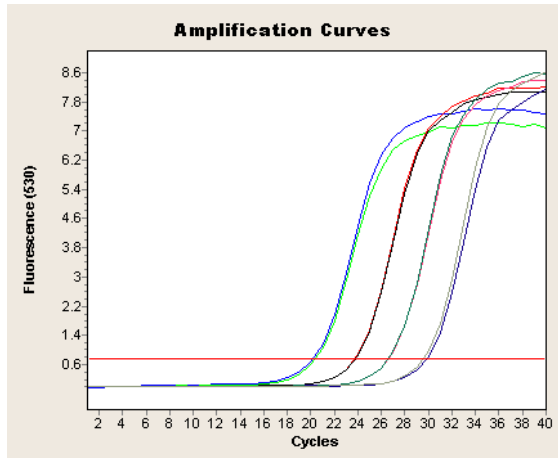
(a)



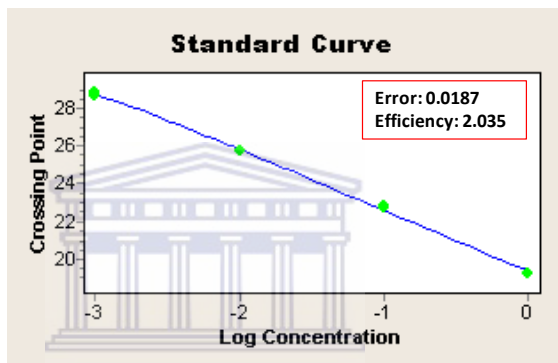
(b)

Figure 3.11: Amplification curves of standards (a) and the generated standard curve for *Cacybp* (b).

A calibrator sample was serially diluted and amplified by qRT-PCR as described in section 2.25.2. Mean C_t for each standard was plotted against log concentration to generate a standard curve for *Cacybp*.



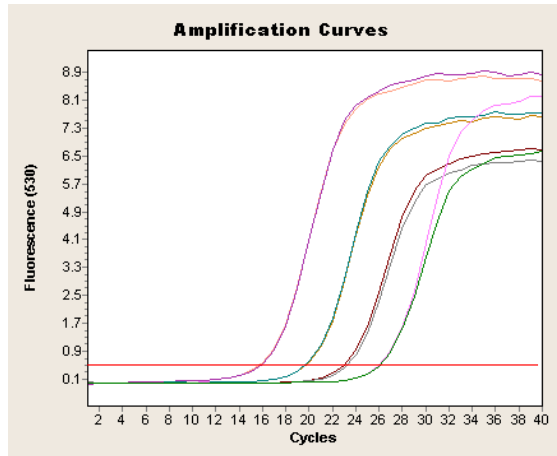
(a)



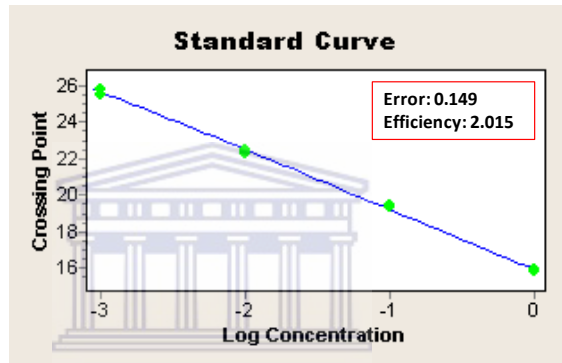
(b)

Figure 3.12: Amplification curves of standards (a) and the generated standard curve for *HPRT1* (b).

A calibrator sample was serially diluted and amplified by qRT-PCR as described in section 2.25.2. Mean C_t for each standard was plotted against log concentration to generate a standard curve for *HPRT1*.



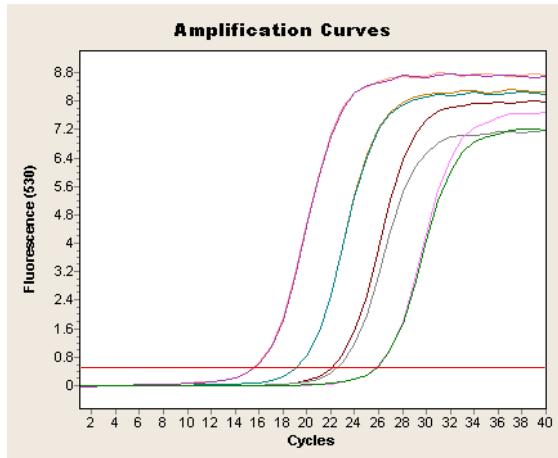
(a)



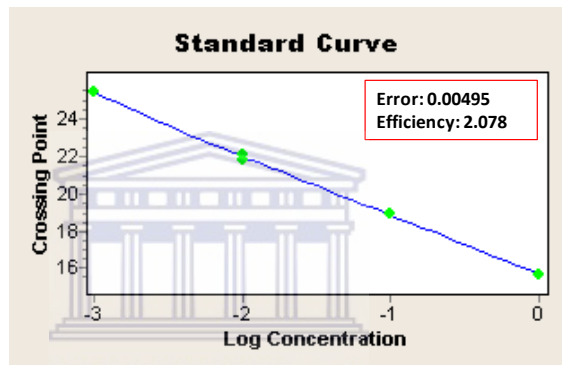
(b)

Figure 3.13: Amplification curves of standards (a) and the generated standard curve for *Hsp27* (b).

A calibrator sample was serially diluted and amplified by qRT-PCR as described in section 2.25.2. Mean C_t for each standard was plotted against log concentration to generate a standard curve for *Hsp27*.



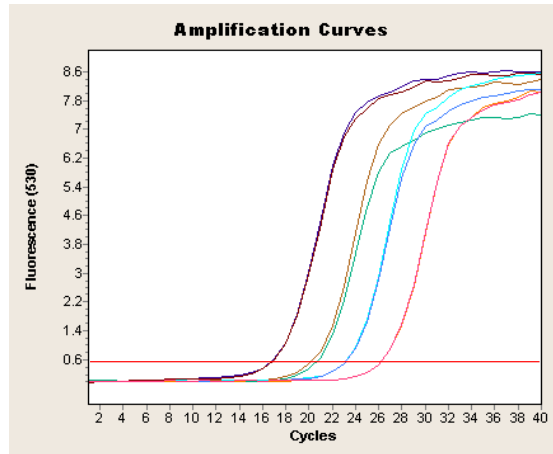
(a)



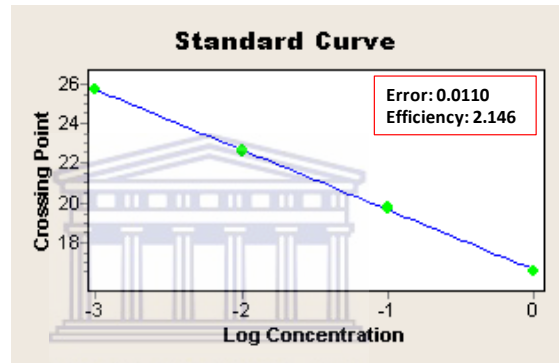
(b)

Figure 3.14: Amplification curves of standards (a) and the generated standard curve for *Pabpc1* (b).

A calibrator sample was serially diluted and amplified by qRT-PCR as described in section 2.25.2. Mean C_t for each standard was plotted against log concentration to generate a standard curve for *Pabpc1*.



(a)



(b)

Figure 3.15: Amplification curves of standards (a) and the generated standard curve for *RhoE* (b).

A calibrator sample was serially diluted and amplified by qRT-PCR as described in section 2.25.2. Mean C_t for each standard was plotted against log concentration to generate a standard curve for *RhoE*.

Table 3.4: Amplification efficiencies (E) of six target gene fragments that were amplified by qRT-PCR.

Amplification efficiencies of target gene were determined from their respective standard curves as described in section 2.25.3.

| Gene | Amplification efficiency (E) |
|---------------|--|
| <i>Atic</i> | 2.050 |
| <i>Pabpc1</i> | 2.078 |
| <i>Cacybp</i> | 2.117 |
| <i>RhoE</i> | 2.146 |
| <i>Hsp27</i> | 2.015 |
| <i>HPRT1</i> | 2.135 |



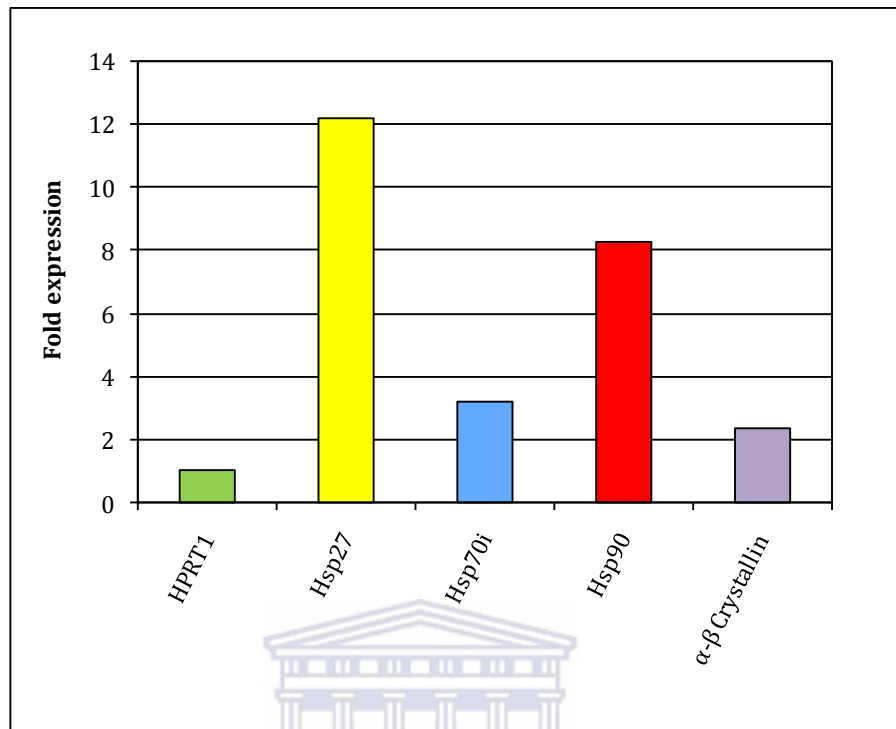


Figure 3.16: Expression levels of known Hsps in H9c2 cells following heat shock treatment.

Gene expression was measured after two hours of recovery from heat shock at 37 °C by using qRT-PCR (section 2.25.4). *HPRT1* was used as an endogenous reference gene.

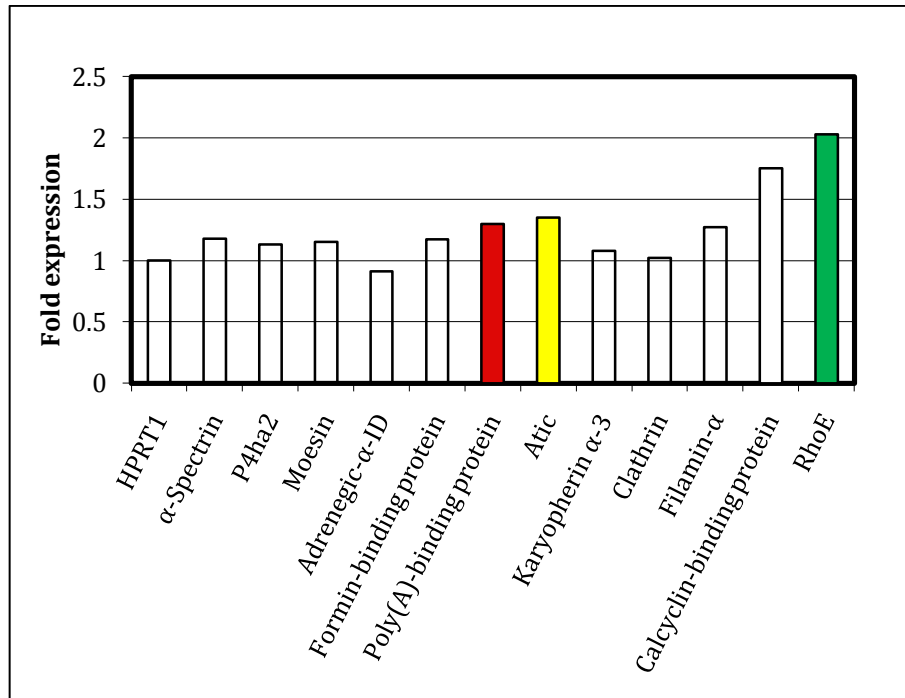


Figure 3.17: Expression levels of various target genes in H9c2 cells following heat shock treatment.

Gene expression was measured after two hours of recovery from heat shock at 37 °C by using qRT-PCR (section 2.25.4). *HPRT1* was used as an endogenous reference gene.

3.6 The over-expression of heat shock responsive genes in H9c2 genes

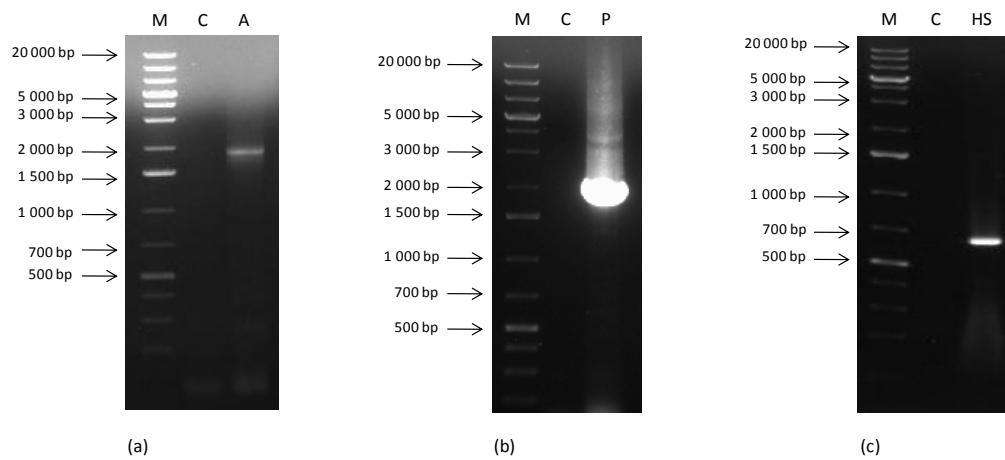


Figure 3.18: PCR amplification of full coding sequences of *Atic* (1 779 bp) (a), *Pabpc1* (1 911 bp) (b) and *Hsp27* (618 bp) (c) from cDNA.

Full coding sequences of *Atic*, *Pabpc1* and *Hsp27* were amplified from cDNA by PCR. PCR products were extracted by gel electrophoresis (section 2.14) and cloned into the MCS of pcDNA3.1(+) as described in section 2.15. A negative control (no DNA added) was included in each PCR to verify the template-specificity of the primers. **Lane M** represents the DNA size marker, **lane C** represents the negative control, **lane A** represents the PCR products of *Atic*, **lane P** represents the PCR product of *Pabpc1* and **lane HS** represents the PCR product of *Hsp27*.

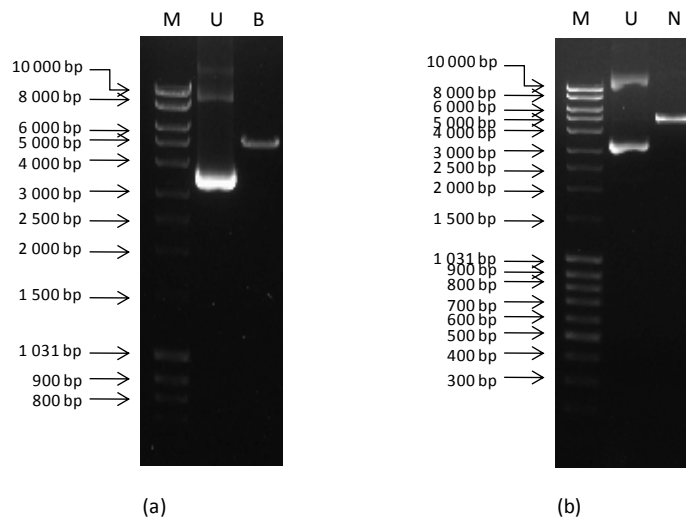


Figure 3.19: Agarose gel electrophoresis images of the undigested pcDNA3.1(+) vector (5 015 bp) and after digestion with *Bam*HI and *Not*I restriction enzymes.

Plasmid DNA was extracted as described in section 2.9.2 and digested by using *Bam*HI and *Not*I (section 2.10). Products of digestion were separated by agarose gel electrophoresis (section 2.14.2). **Lane M** represents the DNA size marker, **lane U** represents undigested pcDNA3.1(+), **lane B** represents pcDNA3.1(+) digested with *Bam*HI and **lane N** represents pcDNA3.1(+) digested with *Not*I.

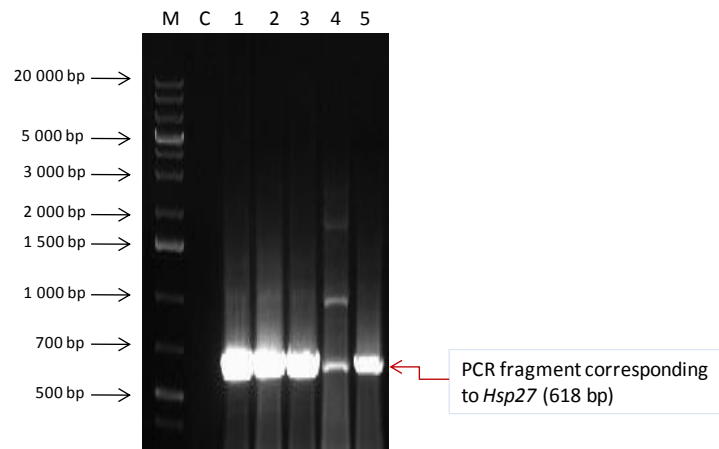


Figure 3.20: Colony PCR screen of bacterial colonies for clones containing *Hsp27*.

Bacterial colonies grown on L agar were used as a template in a PCR with gene-specific primers so as to identify colonies that contained the vector with the Hsp27 gene insert. **Lane M** represents the DNA size marker, **lane C** represents the negative control (no template added) and **lanes 1 to 5** represent bacterial colonies that were screened.

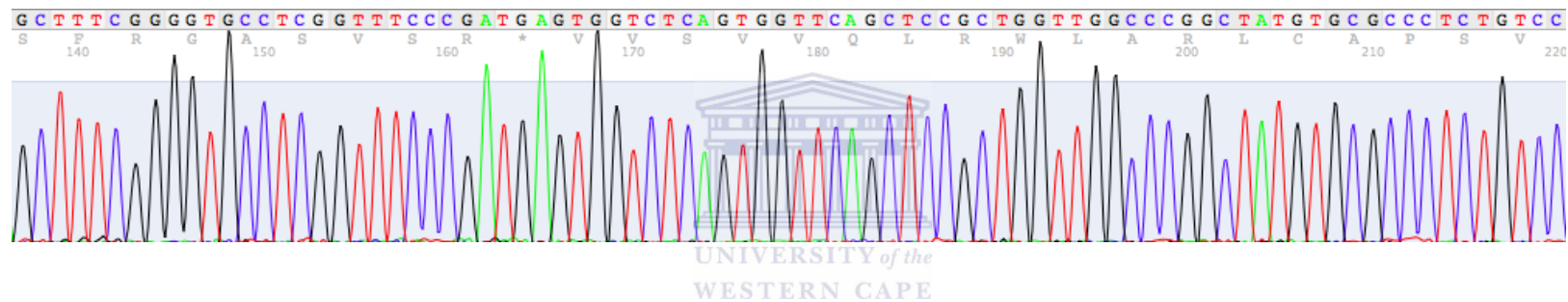




Figure 3.21: Graphic illustration of DNA sequence trace.

After successful cloning of *Atic*, *Pabpc1* and *Hsp27*, plasmid DNA samples were isolated from host cells and sent for automated sequencing

```
>  gb|M86389.1|RATHSP27A  Rattus norvegicus heat shock protein 27 (Hsp27) mRNA, complete cds
Length=787
```

```
GENE ID: 24471 Hspb1 | heat shock protein 1 [Rattus norvegicus]
```

```
Score = 1116 bits (604), Expect = 0.0
Identities = 617/623 (99%), Gaps = 2/623 (0%)
Strand=Plus/Plus
```

(a)

```
Query 30 CATGACCGAGCGCCGCGTGCCTTCTCGCTACTGCGGAGCCCCAGCTGGGAGCCGTTCCG 89
Sbjct 43 CATGACCGAGCGCCGCGTGCCTTCTCGCTACTGCGGAGCCCCAGCTGGGAGCCGTTCCG 102

Query 90 GGA CTGGTACCTGCCACAGCCGCTCTTCGATCAAGCTTTCGGGGTGCCTCGGTTTC 149
Sbjct 103 GGA CTGGTACCTGCCACAGCCGCTCTTCGATCAAGCTTTCGGGGTGCCTCGGTTTC 162

Query 150 CGATGAGTGGTCTCAGTGGTTCAGCTCCGCTGGTTGGCCCGGTATGTGCCCTCTGTG 209
Sbjct 163 CGATGAGTGGTCTCAGTGGTTCAGCTCCGCTGGTTGGCCCGGTATGTGCCCTCTGTG 222

Query 210 CGCCGCGACCGCCGAGGGCCCCGAGCAGTGACCTGGCC-GCGCCCGCCTTCAGCCGGG 268
Sbjct 223 CGCCGCGACCGCCGAGGGCCCCGAGCAGTGACCTGGCCAG-GCCCGCCTTCAGCCGGG 281

Query 269 CGCTCAACCGCAACTCAGCAGCGGTGTCTCAGAGATCCGACAGACGGCCGATCGCTGGC 328
Sbjct 282 CGCTCAACCGCAACTCAGCAGCGGTGTCTCAGAGATCCGACAGACGGCCGATCGCTGGC 341

Query 329 GCGTGTCCCTGGACGTC AACCACTTCGCTCCTGAGGAGCTCACAGTTAAGACCAAGGAAG 388
Sbjct 342 GCGTGTCCCTGGACGTC AACCACTTCGCTCCTGAGGAGCTCACAGTTAAGACCAAGGAAG 401

Query 389 GCGTGGTGGAGATCACTGGCAAGCACGAAGAAAGGCAGGATGAACATGGCTACATCTCTC 448
Sbjct 402 GCGTGGTGGAGATCACTGGCAAGCACGAAGAAAGGCAGGATGAACATGGCTACATCTCTC 461

Query 449 GATGCTTACCCGGAAATACACGCTCCCTCCAGTGTGGACCCCACTTGGTGTCTCTT 508
Sbjct 462 GGTGCTTACCCGGAAATACACGCTCCCTCCAGTGTGGACCCCACTTGGTGTCTCTT 521

Query 509 CCCTGTCCCTGAGGGCACACTCACGGTGGAGGCTCCGCTGCCCAAAGCAGTCACACAAT 568
Sbjct 522 CCCTGTCCCTGAGGGCACACTCACGGTGGAGGCTCCGCTGCCCAAAGCAGTCACACAAT 581

Query 569 CAGCGGAGATCACCATTCCGGTCACTTTCGAGGCCCGTGCCCAAATTTGGAGGCCAGAGT 628
Sbjct 582 CAGCGGAGATCACCATTCCGGTCACTTTCGAGGCCCGTGCCCAAATTTGGAGGCCAGAGT 641

Query 629 CGGAACAGTCTGGAGCCAAGTAG 651
Sbjct 642 CGGAACAGTCTGGAGCCAAGTAG 664
```

(b)

Figure 3.22: BLAST search results for the *Hsp27* sequence.

- (a) Gene identity and the quality of alignment.
- (b) Sequence alignment of *Hsp27* against the non-redundant nucleotide database using BLASTn.

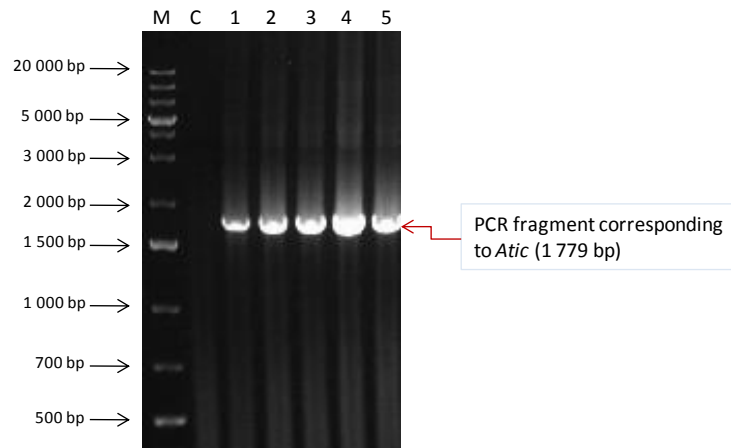


Figure 3.23: Colony PCR screen of bacterial colonies for clones containing *Atic*.

Bacterial colonies grown on L agar were used as a template in a PCR with gene-specific primers so as to identify colonies that contained the vector with the *Hsp27* insert. **Lane M** represents the DNA size marker, **lane C** represents the negative control (no template added) and **lanes 1 to 5** represent bacterial colonies that were screened.

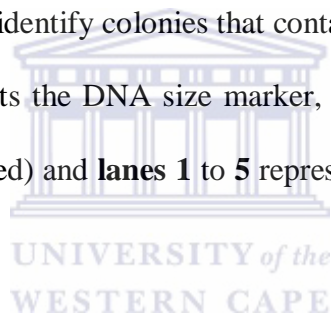





Figure 3.24: BLAST search results for the *Atic* sequence.

- (a) Gene identity and the quality of alignment.
- (b) Sequence alignment of *Atic* against the non-redundant nucleotide database using BLASTn.



>  [ref|NM_031014.2](#)  Rattus norvegicus 5-aminoimidazole-4-carboxamide ribonucleotide

formyltransferase/IMP cyclohydrolase (Atic), mRNA
[gb|BC072496.1](#)  Rattus norvegicus 5-aminoimidazole-4-carboxamide ribonucleotide
 formyltransferase/IMP cyclohydrolase, mRNA (cDNA clone MGC:91657
 IMAGE:7096880), complete cds
 Length=2505

[GENE ID: 81643 Atic](#) | 5-aminoimidazole-4-carboxamide ribonucleotide
 formyltransferase/IMP cyclohydrolase [Rattus norvegicus]
 (10 or fewer PubMed links)

Score = 1502 bits (813), Expect = 0.0
 Identities = 853/874 (97%), Gaps = 12/874 (1%)
 Strand=Plus/Plus

(a)



```

Query 28  CATGGCTTCCTCCAGCTTGCCCTGTTGAGTGTGTCTGACAAAACCTGGCCCTCGTGAATT 87
Sbjct 62  CATGGCTTCCTCCAGCTTGCCCTGTTGAGTGTGTCTGACAAAACCTGGCCCTCGTGAATT 121

Query 88  TGCCAGAAACCTCGCGTCTCTTGGTTTGGTTCGCTTCTGGAGGCACGGCAAAGC 147
Sbjct 122  TGCCAGAAACCTCGCGTCTCTTGGTTTGGTTCGCTTCTGGAGGCACGGCAAAGC 181

Query 148  GATCAGGGATGCTGGCCTGGCAGTGAGAGATGCTGTCTGAGCTAACTGGGTTCCTGAAAT 207
Sbjct 182  GATCAGGGATGCTGGCCTGGCAGTGAGAGATGCTGTCTGAGCTAACTGGGTTCCTGAAAT 241

Query 208  GTTAGGGGGCGTGTGAAAACCTTGCACTCCTGCAGTCCATGCTGGAATCTTAGCAGCAA 267
Sbjct 242  GTTAGGGGGCGTGTGAAAACCTTGCACTCCTGCAGTCCATGCTGGAATCTTAGCAGCAA 301

Query 268  TATTCAGAAGATGCTGCTGACGTGGCCAGGCTTGATTTCAACCTCATAAGAGTTGTTGT 327
Sbjct 302  TATTCAGAAGATGCTGCTGACATGGCCAGGCTTGATTTCAACCTCATAAGAGTTGTTGT 361

Query 328  CTGTAACCTGTACCCGTTTCGTGAAGACTGTGGCTTCTCCAGATGTAACCGTTGAGGCAGC 387
Sbjct 362  CTGTAACCTGTACCCGTTTCGTGAAGACTGTGGCTTCTCCAGATGTAACCGTTGAGGCAGC 421

Query 388  TGTTGAGCAAATTGACATTGGTGGCGTGACCTTACTGAGAGCTGCAGCCAAAACCATGC 447
Sbjct 422  TGTTGAGCAAATTGACATTGGTGGCGTGACCTTACTGAGAGCTGCAGCCAAAACCATGC 481

Query 448  TCGAGTGACAGTTGTGTGTGAGCCAGAGGACTATGGTGCGGTGGCTGCAGAGATGCAGGG 507
Sbjct 482  TCGAGTGACAGTTGTGTGTGAGCCAGAGGACTATGGTGCGGTGGCTGCAGAGATGCAGGG 541

Query 508  CTCTGGTAATAAGGACACCTCCCTGGAGACCAGGCGCCACTTGGCATTGAAGGCATTAC 567
Sbjct 542  CTCTGGTAATAAGGACACCTCCCTGGAGACCAGGCGCCACTTGGCATTGAAGGCATTAC 601

Query 568  GCATACCGCTCAATATGATGAAGCGATTCGGATTACTTCAGGAGACAGTACAGTAAAGG 627
Sbjct 602  GCATACCGCTCAATATGATGAAGCGATTCGGATTACTTCAGGAGACAGTACAGTAAAGG 661

Query 628  AATTTCTCAGATGCCCTTGAGGTATGGGATGAACCCCATCAGACTCCTGCCAGCTGTA 687
Sbjct 662  AATTTCTCAGATGCCCTTGAGGTATGGGATGAACCCCATCAGACTCCTGCCAGCTGTA 721
  
```

(b)

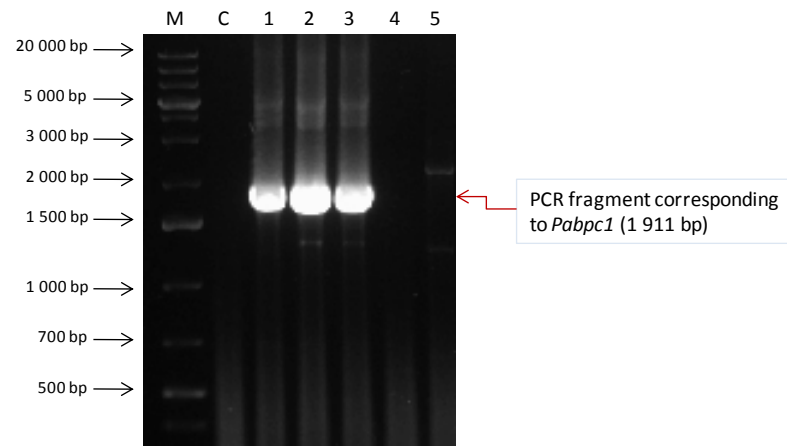


Figure 3.25: Colony PCR screen of bacterial colonies for clones containing *Pabpc1*.

Bacterial colonies grown on L agar were used as a template in a PCR with gene-specific primers so as to identify colonies that contained the vector with the *Pabpc1* insert. **Lane M** represents the DNA size marker, **lane C** represents the negative control (no template added) and **lanes 1 to 5** represent bacterial colonies that were screened.

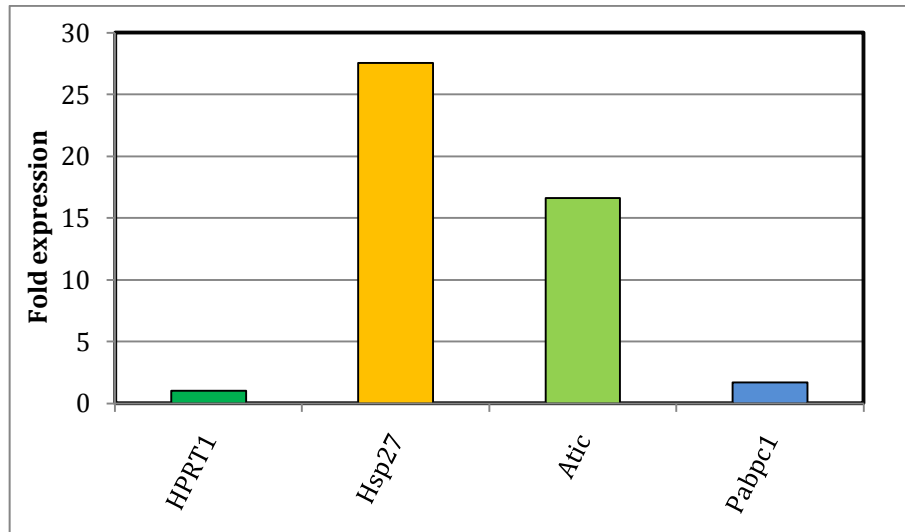


Figure 3.27: Relative expression of various target genes in transiently transfected H9c2 cells.

Real time quantitative PCR (section 2.25.4) was used to measure relative expression of *Hsp27*, *Atic*, *Pabpc1* and *RhoE* in H9c2 cells (section 2.25.4) 48 hours after being transfected with each expression construct. *HPRT1* was used as an endogenous reference gene.

CHAPTER 4.0: DISCUSSION

The overall objective of this study was to identify novel regulatory elements in the promoters of heat shock responsive genes. In order to achieve this objective and gain more insight into regulation of heat shock response in mammalian cells, both *in silico* and *in vitro* analyses were employed. Such an approach was considered very effective as it enabled experimental validation of some of the data generated by employing *in silico* tools.

4.1 Heat shock optimisation and cytoprotection

The initial phase of experimentation involved optimisation of the heat shock system. Rat heart-derived H9c2 myocytes were used as a simplified *in vitro* model of the myocardium and heat shock was used to induce cellular stress. Western blot analysis demonstrated that exposing H9c2 cells to 42 °C for one hour induced the expression of the Hsc70/Hsp70 complex (Figure 3.1). This increase in Hsc70/Hsp70 expression was observed after one hour of recovery at 37 °C following heat shock treatment. The Hsc70/Hsp70 polyclonal antibody that was used for Western blotting recognised both the constitutively expressed Hsc70 and the inducible Hsp70 isoforms. The observed increase in the Hsc70/Hsp70 protein complex abundance in H9c2 cells following heat shock was largely attributed to increased expression of Hsp70, which has been shown to be mostly absent under non-stress conditions but rapidly synthesised in response to exposure of cells to elevated temperatures (Mosser *et al.*, 2000).

After optimising experimental heat shock conditions, cytotoxicity assays were then carried out to investigate the cytoprotective effect of heat pre-conditioning of

H9c2 cell cultures against ethanol, a potent apoptosis-inducing agent. The APOPercentageTM apoptosis assay was used to detect and quantify apoptotic cells. The assay comprises of an anionic halogenated fluorescein dye which is taken up by apoptotic cells at the stage of plasma membrane phosphatidylserine (PS) externalisation (Martin *et al.*, 1995). Staining with this dye gives apoptotic cells a purple-red colour which can be detected by flow cytometric analysis. As shown in Figure 3.2 an increase in the apoptotic cell population (marker M2) was observed with increasing the concentration of ethanol. Figure 3.3 shows the effect of varying both the concentration of ethanol and time of exposure on H9c2 cells. The aim of this experiment was to establish a suitable combination of concentration and time of exposure that would cause between 60 – 80 % apoptosis. The rationale was that this percentage range would enable clear differentiation between cytoprotected and sensitive H9c2 cells in subsequent assays. A concentration of 10 % and an exposure time of four hours satisfied this experimental condition (Figure 3.4) hence were used in subsequent cytoprotection experiments. Additionally, a time dependent effect was only observed when using 10 % ethanol (Figure 3.3), which suggested improved consistency at this concentration compared to lower concentrations.

The cytoprotective effect of heat shock preconditioning against the pro-apoptotic effects of ethanol was demonstrated by subjecting H9c2 cells to heat shock at 42 °C for one hour prior to treating then with 10 % ethanol for four hours. As shown on Figure 3.5 heat shock pre-conditioned H9c2 cells were significantly ($p < 0.05$) protected from ethanol compared to control cells, more so after two hours of recovery from HS. The very low percentage cell death recorded for heat shocked

but non-ethanol treated cells ('0 hrs rec, tr') (Figure 3.5) indicated that the heat shock treatment itself did not cause any significant cell death. Thus the observed cell death after treatment with ethanol could confidently be attributed to the sole effects of ethanol.

Prior mild heat shock treatment (preconditioning) activates HSR genes which leads to increased synthesis of stress responsive proteins. This renders cells more resistant to a wide variety of subsequent, more severe insults, including apoptosis-inducing chemical substances through their chaperoning and anti-apoptotic effects as previously shown by Concannon *et al.* (2003), Paul *et al.* (2002) and Charette *et al.* (2000). However, caution must be taken when extrapolating results from such simplified *in vitro* models to human disease states because factors such as the unnatural cell environment, the number of cell passages, the degree of culture confluency, and the chemical composition of the media, may influence the outcome.

4.2 *In silico* analysis of gene regulation

Cellular decisions concerning processes such as survival, growth and differentiation are regulated at transcription level and are often reflected in altered levels of mRNA transcripts. Previous SSH data suggested differential expression of 127 mRNAs in rat cardiomyocytes exposed to 42 °C for one hour followed by recovery for two hours at 37 °C. Among the 127 genes, 91 were up-regulated whilst 36 were down-regulated. Up-regulated genes included known Hsp-genes (e.g., $\alpha\beta$ -crystallin, *Hsp90*, *Hsp105 β*), *Calcyclin binding protein/Siah-1 interacting protein (CacyBP/SIP)*, *RhoE*, and *Damage-specific DNA binding protein*, whilst down regulated genes included *Cyclophilin A*, α -tubulin,

Calgizzarin and *Formin binding protein*. Classification of these genes into functional groups revealed that they are involved in wide ranging cellular processes including transcription, protein synthesis, cytoskeletal organisation, calcium metabolism and signal transduction (Table 3.1). However, although SSH offers insight into the global gene expression profile, it is prone to significant levels of false positives. Thus, it is vital to validate the data generated by applying the technique. Accordingly an *in silico* strategy of analysing gene regulation was devised to complement the SSH data. The strategy was based on the hypothesis that HSR genes may be co-regulated by the same transcription factors and that their promoters share conserved sequence motifs representing binding sites for these factors.

Only up-regulated genes were considered for the analysis because genes that play crucial roles in heat shock response and cytoprotection are typically up-regulated following cellular perturbation. Additionally, only genes whose promoter sequences have been experimentally verified or that were supported by PromoterInspector (www.genomatix.de) predictions were considered in the analysis. This reduced the initial number of up-regulated genes to 60 (67 %). Interrogation of these putative HSR genes using MatInspector (www.genomatix.de) revealed that only 17 out of 60 genes (28 %) contained sequence motifs that were highly similar to the core sequence of the heat shock element (V\$HEAT) in their promoter regions. These included genes that had not been previously associated with the heat shock response such as *Moesin*, *Proline-4 hydroxylase*, *Eukaryotic translation factor-1*, *Cacybp* and *Adrenergic receptor* (Table 3.2).

Since only 28 % of the up-regulated genes were shown to contain HSE in their promoters it was subsequently hypothesised that additional heat shock responsive CAREs that are yet to be characterised are conserved in the promoters of HSR genes. In an effort to identify these consensus sequences, the promoter regions of *Hsp90*, *Hsp105 β* and *$\alpha\beta$ -crystallin* were interrogated using ModelInspector software (www.genomatix.de). Two modules were identified in all three genes, namely EGRF_SP1F_01 and SP1F_CEBP_01. The EGRF_SP1F_01 module comprise of two overlapping sites that bind the transcription factors early growth factor-1 (EGRF-1) and stimulating protein-1 (SP-1). On the other hand the SP1F_CEBP_01 module represents binding sites for SP-1 and CCAAT box/enhancer binding protein (CEBP) (www.genomatix.de). Screening the 60 up-regulated genes for the presence of EGRF_SP1F_01 and SP1F_CEBP_01 revealed that 12 genes (20 %) contained both modules in their promoter regions (Table 3.3). Among these *Moesin*, *Proline-4 hydroxylase*, *α -spectrin*, *$\alpha\beta$ -crystallin*, *Hsp90*, *Adrenergic receptor* and *Formin-binding protein* had previously been shown to also contain the HSE.

Previous studies have shown that SP-1 is essential for *Hsp70* gene expression (Bevilacqua *et al.*, 2000, Wilke *et al.*, 2000, Bevilacqua *et al.*, 1997, Morgan, 1989). Additionally, artificial promoter constructs containing multiple SP-1 binding sites have been shown to be highly responsive to exposure to ethanol (Wilke *et al.*, 2000). C/EBP has also been shown to bind the human *Hsp70* gene (Martínez-Balbas *et al.*, 1995). Thus based on this knowledge and the outcome of *in silico* analyses, it was proposed that SP-1/EGRF and/or SP-1/CEBP may act together to regulate the expression of HSR genes. Notably, a more complex

promoter module that would include binding sites for additional heat-activated transcription factors (e.g., HSF1) could not be identified during this study.

4.3 Real-time qRT-PCR analyses

The expression of the 12 putative HSR genes identified by SSH and *in silico* analysis was further investigated in H9c2 cells by using qRT-PCR (Ginzinger, 2002; Bustin, 2000). However, successful application of the technique is primarily dependent on isolation of RNA of the highest quality (Fleige and Pfaffl, 2006). As such the quality of the isolated total RNA was ascertained before it could be used for downstream applications (Figure 3.7). Only high-quality RNA was used to synthesis cDNA for qRT-PCR analysis.

The expression of target genes was normalised and expressed relative to that of *HPRT1* (an endogenous reference gene). Normalisation corrects for variation such as that arising from variable RNA or cDNA input. Thus careful selection of a reference gene is a vital component of qRT-PCR analysis. *HPRT1* was shown to be a suitable reference gene as its level of expression in H9c2 cells did not vary in response to HS treatment (Figure 3.8). SYBR[®] Green I fluorescent dye was used to detect and quantify the accumulating PCR product during qRT-PCR. This provides the simplest and most economic detection chemistry in qRT-PCR assays. However, the main disadvantage of using SYBR[®] Green I is that it binds indiscriminately to double-stranded DNA in the reaction mixture, including primer dimers and non-specific PCR products. This results in overestimation of the initial template concentration. To avoid this error, amplification specificity was verified by melting curve analysis. As shown on Figure 3.9, a single fluorescence peak representing one PCR product of *Karyopherin* (“Kap”), *Clathrin* (“Clt”),

HPRT1 and *Filamin- α* (“Fim”) was obtained when the reduction in fluorescence over time (-dF/dT) was plotted against temperature ($^{\circ}\text{C}$). The plateau of each melting peak coincides with the T_m of that specific PCR product, which enables confirmation of the identity of the amplified product.

Accurate quantification of relative gene expression requires that the E value of target genes be maximal. Accordingly E values of various genes were determined from their individual standard curves that were generated by plotting C_t s of 10-fold serial dilutions of the control cDNA template against $\log[10]$ template concentration (Figure 3.10 to Figure 3.15). The slope of the resulting standard curve is a function of amplification efficiency. E values were found to be maximal and comparable to that of the reference gene (Table 3.4). An E value of 2.0 (as determined by using the quoted variant of the equation for calculating E) indicates that at the log linear phase of amplification the amount of amplicon doubles after each PCR cycle. A low E value, which is often a result of using poor quality RNA or co-isolation of RT and/or PCR inhibitors, may contribute to a false-negative result.

Hsp27, *Hsp70*, *Hsp90* and *$\alpha\beta$ -crystallin* were significantly up-regulated following exposure of H9c2 cells to a mild thermal stress (Figure 3.16). These are well-characterised HSR genes that were used as positive controls in the HS assay. Generally the putative HSR genes (*Pabpc1*, *Atic*, *Filamin- α* , *RhoE* and *Cacybp*) showed slight (up to two-fold) induction whereas *adrenergic- α -ID* was down-regulated following HS treatment (Figure 3.17). It was noted that although *Moesin*, *Proline-4 hydroxylase*, *Formin binding protein* and *α -spectrin* contained the heat shock element in their promoters, these genes were only slightly (<1.25

fold) up-regulated in response to HS under these experimental conditions. However, it is possible that these genes may show higher levels of induction at time points other than that employed in this study. Conversely, the promoter of *RhoE*, a confirmed heat shock regulated gene (Ongusaha *et al.*, 2006) was shown not to contain V\$HEAT, EGRF_SP1F_01 and SP1F_CEBP_01 sequences, yet it showed the highest (two-fold) level of heat induction among the interrogated genes (Figure 3.17). Possibly this could be a case of indirect regulation as *RhoE* has been shown to be a pro-survival gene that is a transcriptional target of p53, which is in turn regulated by heat shock (Ongusaha *et al.*, 2006).

Several changes occur within the cell during heat shock response, including rapid changes in transcription and translation, alterations in cellular metabolism, cell cycle arrest, and cytoskeletal reorganisation (Cuesta *et al.* 2000; Liu *et al.*, 1992). Genes that were shown to be up-regulated following HS are associated with some of these processes.

The role played by *Pabpc1*, *Atic*, *RhoE* and *Cacybp* in stress response is not well established. Subsequent to *in silico* and qRT-PCR analyses, full-length coding sequences of two genes showing up-regulation following heat shock (*Atic* and *Pabpc1*) (Figure 3.18) were cloned into a mammalian expression vector (Figure 3.19) to facilitate further investigation into their potential cytoprotective roles. The successful cloning of each of the three sequences was confirmed by both colony PCR and automated sequencing (Figure 3.20 to Figure 3.26). Transient expression of each gene construct in H9c2 is shown on Figure 3.27. Interestingly no change in the quantity of the *Pabpc1* transcript was detected in transfected H9c2 cells. This

was attributed to the fact that very high levels of *Pabpc1* mRNA generally occur in mammalian cells (Ma *et al.*, 2009).



CONCLUSIONS AND FUTURE DIRECTIONS

The combination of *in silico* and *in vitro* analyses that was employed in this study proved to be a very effective approach as it enabled experimental validation of some of the data that were generated by *in silico* analyses. Two conserved modules, namely EGRF_SP1F_01 and SP1F_CEBP_01, were identified in the promoter sequences of three known Hsps and 12 putative HSR genes. These modules are believed to be involved in the regulation of HSR genes, in addition to known regulatory elements such as the HSE. However, there is a need to further investigate the role of these modules in regulating heat shock response using techniques such as co-immunoprecipitation.

Quantitative PCR analyses confirmed that the majority of the 12 genes predicted as heat shock responsive by *in silico* analyses were indeed slightly up-regulated in H9c2 cells following HS. These included *Atic*, *Cacybp* and *Pabpc1*. The role of these genes in regulation of heat shock response is not well known hence the full coding sequences of *Atic*, *Pabpc1*, and *Hsp27* were cloned in a mammalian expression vector to facilitate investigation of the potential cytoprotective roles of these genes in future.

Thus the conclusion drawn from this study was that EGRF_SP1F_01 and SP1F_CEBP_01 are regulatory elements that are preserved in promoter sequences of HSR genes. These modules are potentially involved in regulating the expression of genes in response to heat stress in H9c2 cells. These findings could significantly contribute towards a better understanding of regulation of cellular

defence mechanisms operating in stressed and/or injured cardiomyocytes and provide novel therapeutic targets against stress-induced tissue injury.



REFERENCES

- Arnaud C, Godin-Ribuot D, Bottari S, Piennequin A, Joyeux M, Demenge P, and Ribuot C (2003). iNOS is a mediator of the heat stress-induced preconditioning against myocardial infarction *in vivo* in the rat. *Cardiovascular Research*, **58**: 118-125
- Arya R, Mallik M, and Lakhota SC (2007). Heat shock genes-integrating cell survival and death. *Journal of Biosciences*, **32**: 595-610
- Beck SC, Paidas CN, Tan H, Yang J, and De Maio A (1995). Depressed expression of the inducible form of HSP70 (HSP72) in brain and heart after *in vivo* heat shock. *American journal of Physiology: Integrative and Comparative Physiology*, **269**: 608-613
- Beere HM, Wolf BB, Cain K, Mosser, DD, Mahboubi A, Kuwana T, Taylor P, Morimoto RI, Cohen GM, and Green DR (2000). Heat-shock protein 70 inhibits apoptosis by preventing recruitment of procaspase-9 to the Apaf-1 apoptosome. *Nature Cell Biology*, **2**: 469-475
- Bence NF, Sampat RM, and Kopito RR (2001). Impairment of the ubiquitin-proteasome system by protein aggregation. *Science*, **292**: 1552-1555
- Benjamin IJ and McMillan DR (1998). Stress (heat shock) proteins. Molecular chaperons in cardiovascular biology and disease. *Circulation Research*, **83**: 117-132
- Berridge MJ (1995). Capacitative calcium entry. *Biochemical Journal*, **312**: 1-11

Bevilacqua A, Fiorenza MT, and Magia F (1997). Developmental activation of an episomic *hsp70* gene promoter in two-cell mouse embryos by transcription factor Sp1. *Nucleic Acids Research*, **25**: 1333-1338

Bevilacqua A, Fiorenza MT, and Magia F (2000). A developmentally regulated GAGA box-binding factor and Sp1 are required for transcription of the *hsp70.1* gene on the onset of mouse zygotic genome activation. *Development*, **127**: 1541-1551

Birnboim HC and Dolly J (1979). A rapid alkaline extraction procedure for screening recombinant plasmid DNA. *Nucleic Acids Research*, **7**: 1513-1523

Black SC and Luchessi BR (1993). Heat shock proteins and the ischemic heart. An endogenous protective mechanism. *Circulation*, **87**: 1048-1051

Boyce N and Yuan J (2006). Cellular response to endoplasmic reticulum stress: a matter of life and death. *Cell Death and Differentiation*, **13**: 363-373

Brar BK, Stephanou A, Wagstaff MJD, Coffin RS, Marber MS, Engelmann G, and Latchman DS (1999). Heat shock proteins delivered with a virus vector can protect cardiac cells against apoptosis as well as against thermal or hypoxic stress. *Journal of Molecular and Cellular Cardiology*, **31**: 135-146

Brewer JW, Cleaveland J, and Hendershot LM (1997). A pathway distinct from the mammalian unfolded protein response regulates expression of endoplasmic reticulum chaperones in non-stressed cells. *The EMBO Journal*, **16**: 7207- 7216

Bruey J-M, Ducasse C, Bonniaud P, Ravagnan L, Susin SA, Diaz-Latoud C, Gurbuxani S, Arrigo A-P, Kroemer G, Solary E, and Garrido C (2000). Hsp27

negatively regulates cell death by interacting with cytochrome *c*. *Nature Cell Biology*, **2**: 645-652

Bucciantini M, Giannoni E, Chiti F, Baroni F, Formigli L, Zurdo J, Taddei N, Ramponi G, Dobson CM, and Stefani M (2002). Inherent toxicity of aggregates implies a common mechanism for protein folding diseases. *Nature*, **416**: 507-511

Bukau B and Horwich A (1998). Hsp70 and Hsp60 chaperone machines. *Cell*, **92**: 351-366

Butterfield DA, Howard BJ, Yatin S, Allen KL, and Carney JM (1997). Free radical oxidation of brain proteins in accelerated senescence and its modulation by *N-tert-butyl-alpha-phenylnitron*e. *Proceedings of the National Academy of Sciences of the United States of America*, **94**: 674-678

Cartharuis K, Frech K, Grote K, Klocke B, Haltmeier M, Klingenhoff A, Frisch M, Bayerlein M, and Werner T (2005). MatInspector and beyond: promoter analysis based on transcription factor binding sites. *Bioinformatics*, **21**: 2933-2942

Casadaban MJ and Cohen SN (1980). Analysis of gene control signals by DNA fusion and cloning in *Escherichia coli*. *Journal of Molecular and Cellular Biology*, **138**: 179-207

Cecconi F (1999). Apaf1 and the apoptotic machinery. *Cell Death and Differentiation*, **6**: 1087- 1098

Charette SJ, Lavoie JN, Lambert H, and Landry J (2000). Inhibition of Daxx-mediated apoptosis by heat shock protein 27. *Molecular and Cellular Biology*, **20**: 7602-7612

Concannon CG, Gorman AM and Samali A (2003). On the role of Hsp27 in regulating apoptosis. *Apoptosis*, **8**: 61-70

Cook SA, Sugden PH, and Clerk A (1999). Regulation of Bcl-2 family of proteins during development and in response to oxidative stress in cardiac myocytes: association with changes in mitochondrial membrane potential. *Circulation Research*, **85**: 940-949

Currie RW, Karmazyn M, Kloc M, and Mailer K (1988). Heat-shock response is associated with enhanced postischemic ventricular recovery. *Circulation Research*, **63**: 543-549

Currie RW (1987). Effects of ischemia and perfusion temperature on the synthesis of stress-induced (heat shock) proteins in isolated and perfused rat hearts. *Journal of Molecular and Cellular Cardiology*, **19**: 795-808

Dai Q, Zhang C, Wu Y, McDonough H, Whaley RA, Godfrey V, Li H, Madamanchi N, Xu W, Neckers L, Cyr D, and Patterson C (2003). CHIP activates and confers protection against apoptosis and cellular stress. *The EMBO Journal*, **22**: 5446-5458

Daniel NN and Korsmeyer SJ (2004). Cell death: Critical control points. *Cell*, **116**: 205- 219

Denasi M and Davies KJA (2003). Proteasome inhibitors induce intracellular protein aggregation and cell death by an oxygen-dependent mechanism. *FEBS letters*, **542**: 89-94

Diamond MI, Miner JN, Yoshinaga SK, and Yamamoto KR (1990). Transcription factor interactions: selectors of positive or negative regulation from a single DNA element. *Science*, **249**: 1266-1272

Donnelly TJ, Sievers RE, Vissern FLJ, Welch WJ, and Wolfe CL (1992). Heat shock protein induction in rat hearts. A role for improved myocardial salvage after ischaemia and reperfusion? *Circulation*, **85**: 769-778

Ellis RJ and van der Vies SM (1991). Molecular chaperones. *Annual Reviews of Biochemistry*, **60**: 321-347

Ferder ME and Hofmann GE (1999). Heat shock proteins, Molecular chaperones, and the stress response: Evolutionary and ecological physiology. *Annual Reviews of Physiology*, **61**: 243-283

Fessele S, Maier H, Zischek C, Nelson PJ, and Werner T (2002). Regulatory context is a crucial part of gene function. *TRENDS in Genetics*, **18**: 60-63

Fickett JW and Hatzigeorgiou AC (1997). Eukaryotic promoters? Recognition. *Genome Research*, **7**: 861-878

Fink AL (1999). Chaperone-mediated protein folding. *Physiological Reviews*, **79**: 425-449

Fleige S and Pfaffl MW (2006). RNA integrity and the effect on the real-time qRT-PCR performance. *Molecular Aspects of Medicine*, **27**: 126-139

Fleury C, Mignotte B, and Vayssiere JL (2002). Mitochondrial reactive oxygen species in cell death signalling. *Biochimie*, **84**: 131-141

Freude B, Masters TN, Robicsek F, Fokin A, Kostin S, Zimmermann R, Ullmann C, Lorenz-Meyer S, and Schaper J (2000). Apoptosis is initiated by myocardial ischaemia and executed during reperfusion. *Journal of Molecular and Cellular Cardiology*. **32**: 197–208

Gabai VL, Mabuchi K, Mosser DD, and Sherman MY (2002). Hsp72 and stress kinase c-jun N-Terminal kinase regulate the Bid-dependent pathway in tumour necrosis factor-induced apoptosis. *Molecular and Cellular Biology*, **22**: 3415-3424

Georgopoulos C and Welch WJ (1993). Role of the major heat shock proteins as molecular chaperones. *Annual Reviews of Cell Biology*, **9**: 601-634

Gething M-J and Sambrook J (1992). Protein folding in the cell. *Nature*, **355**: 33-45

Gill C, Meyer M, FitzGerald U, and Samali A (2006). The role of heat shock proteins in the regulation of apoptosis. Sreedah AS and Srinivas UK (eds.). *The role of heat shock proteins in the regulation of apoptosis*. Kerala, INDIA: 1-26

Gill C (2004). Thermotolerance and apoptosis in H9c2 cells: molecular and functional characteristics of the heat shock response. PhD thesis. Galway, National University of Ireland.

Gill C, Mestral R, and Samali A (2002). Losing heart: the role of apoptosis in heart disease- a novel therapeutic target. *The FASEB Journal*, **16**: 135-146

Ginzinger DG (2002). Gene quantification using real-time quantitative PCR: An emerging technology hits the mainstream. *Experimental Hematology*, **30**: 503-512

Gottlieb RA and Engler RL (1999). Apoptosis in myocardial ischemia-reperfusion. *Annals of the New York Academy of Science*, **874**: 412-426

Gottlieb RA, Burleson KO, Kloner RA, Barbior BM, and Engler RL (1994). Reperfusion injury induces apoptosis in rabbit cardiomyocytes. *The Journal of Clinical Investigation*, **94**: 1621-1628

Gupta S and Knowlton AA (2005). HSP60, Bax, apoptosis and the heart. *Journal of Cellular and Molecular Medicine*, **9**: 51-58

Hamacher-Brandy A, Brandy NR, and Gottlieb RA (2006). The interplay between pro-death and pro-survival signaling pathways in myocardial ischemia/reperfusion injury: apoptosis meets autophagy. *Cardiovascular Drugs and Therapy*, **20**: 445-462

Hargitai J, Lewis H, Boros I, Rácz T, Fiser A, Kurucz I, Benjamin I, Víg L, Péntes Z, Csermely P, and Latchman DS (2003). Bimoclomol, a heat shock protein co-inducer, acts by prolonged activation of heat shock factor-1. *Biochemical and Biophysical Research Communications*, **307**: 689-695

Hendrick JP and Hartl F (1993). Molecular chaperone functions of heat-shock proteins. *Annual Reviews of Biochemistry*, **62**: 349-384

Hescheler J, Meyer R, Plant S, Krautwurst D, Rosenthal W, and Schultz G (1991). Morphological, biochemical, and electrophysiological characterization of a clonal cell (H9c2) line from rat heart. *Circulation Research*, **69**: 1476-1486

Hightower LE and Hendershot LM (1997). Molecular chaperones and the heat shock response at COLD SPRING HARBOUR. *Cell Stress & Chaperones*, **2**: 1-11

Huang M, Wei J, Peng W, Liang J, Zhao C, Qian Y, Dai G, Yuan J, Pan F, Xue B, Sha J, and Li C (2009). The association of CaM and Hsp70 regulates S-phase arrest and apoptosis in a spatially and temporally dependent manner in human cells. *Cell Stress Chaperones*, **14**: 343-353

Hunt C and Calderwood S (1985). Conserved features of eukaryotic hsp70 genes revealed by comparison with the nucleotide sequence of human hsp70. *Proceedings of the National Academy of Sciences of the United States of America*, **82**: 6455-6459

Hutter MM, Sievers RE, Barbosa V, and Wolfe C (1994). Heat shock protein induction in rat hearts. A direct correlation between the amount of heat shock protein induced and the degree of myocardial protection. *Circulation*, **89**: 353-360

Jäättelä M (1999). Escaping cell death: survival proteins in cancer. *Experimental Cell Research*, **248**: 30-43.

James, TN (1998). The variable morphological coexistence of apoptosis and necrosis in human myocardial infarction: significance for understanding its pathogenesis, clinical course, diagnosis and prognosis. *Coronary Artery Disease*, **9**: 291-307

Jedlicka P, Mortin MA and Wu C (1997). Multiple functions of *Drosophila* heat shock transcription factor *in vivo*. *EMBO Journal*, **16**: 2452-2462

Jolly C, Konecyn L, Grady DL, Kutsikova YA, Cotto JJ, Morimoto RI, and Vourc'h C (2002). *In vivo* binding of active heat shock transcription factor 1 to human chromosome 9 heterochromatin during stress. *The Journal of Cell Biology*, **156**: 775-781

Jolly C and Morimoto RI (2000). Role of the heat shock response and molecular chaperones in oncogenesis and cell death. *Journal of the National Cancer Institute*, **92**: 1564-1572

Kalmar B and Greensmith L (2009). Induction of heat shock proteins for protection against oxidative stress. *Advanced Drug Delivery Reviews*, **61**: 310-318

Kaufman RJ (1999). Stress signalling from the lumen of the endoplasmic reticulum: coordination of gene transcriptional and translational controls. *Genes and Development*, **13**: 1211-1233

Kerr JFR, Willey AH and Currie AR (1972). Apoptosis: A basic biological phenomenon with wide-ranging implications in tissue kinetics. *British Journal of Cancer*, **26**: 239-257

Kiang JG and Tsokos GC (1998). Heat shock protein 70 kDa: molecular biology, biochemistry, and physiology. *Pharmacology and Therapeutics*, **80**: 183-201

Kimes BW and Brandt BL (1976). Properties of a clonal muscle cell line from rat heart. *Experimental Cell Research*, **98**: 367-381

Klemenz R, Andres A-C, Frohli E, Schefer R, and Aoyama A (1993). Expression of the murine small heat shock proteins hsp25 and $\alpha\beta$ -crystallin in the absence of stress. *The Journal of Cell Biology*, **120**: 639-645

Komarova EY, Afanasyeva EA, Bulatova MM, Cheetham ME, Marguli BA, and Guzhova IV (2004). Downstream caspases are novel targets for the antiapoptotic activity of the molecular chaperone Hsp70. *Cell Stress and Chaperones*, **9**: 265-275

Kozak M(1991). An analysis of vertebrate mRNA sequences: initiation of translation control. *Journal of Cell Biology*, **115**: 887-903

Kozak M (1990). Downstream secondary structures facilitate recognition of initiation codons by eukaryotic ribosomes. *Proceedings of the National Academy of Sciences of the United States of America*, **87**: 8301-8305

Kroemer G, Petit P, Zamzami N, Vayssiere JL, and Mignotte B (1995). The biochemistry of programmed cell death. *The FASEB Journal*, **9**: 1277-1287

Latchman DS (2001). Heat shock proteins and cardiac protection. *Cardiovascular Research* **51**: 637-646

Lee AS (1992). Mammalian stress response: Induction of the glucose-related protein family. *Current Opinion in Cell Biology*, **4**: 267-273

Lin KM, Lin B, Lian IY, Mestril R, Scheffler IE, and Dillmann WH (2001). Combined and individual mitochondrial HSP60 AND HSP10 expression in cardiac myocytes protects mitochondrial function and prevents apoptotic cell deaths induced by simulated ischemia-reoxygenation. *Circulation*, **103**: 1787-1792

Lindquist S and Craig EA (1988). The heat-shock proteins. *Annual Reviews of Genetics*, **22**: 631-677.

Lindquist S (1986). The heat shock response. *Annual Reviews of Biochemistry*, **55**: 1151-1191

Liu RY, Li X, Li L, and Li GC (1992). Expression of human Hsp70 in rat fibroblasts enhances cell survival and facilitates recovery from translational and transcriptional inhibition following heat shock. *Cancer Research*, **52**: 3667–3673

Livak KL and Schmittgen T (2001). Analysis of gene expression data using real-time quantitative PCR and the $2^{-\Delta\Delta ct}$ method. *Methods*, **25**: 402-408

Lum LSY, Sultzman LA, Kaufman RJ, Linzer DIH, and Wu BJ (1990) A cloned human CCAAT box-binding factor stimulates transcription from the human Hsp70 promoter. *Molecular and Cellular Biology*, **10**: 6709-6717

Lusardi TA, Farr CD, Faulkner CL, Pignataro G, Yang T, Lan J, Simon RP, and Saugstad JA (2010). Ischemic preconditioning regulates expression of microRNAs and predicted target, MeCP2, in mouse cortex. *Journal of Cerebral Blood Flow and Metabolism*, **30**: 744-756

Marber MS, Mestril R, Chi S, Sayen MR, Yellon DM, and Dillmann WH (1995). Overexpression of the rat inducible 70 kD heat stress protein in a transgenic mouse increases the resistance of the heart to ischemic injury. *Journal of Clinical Investigation*, **95**: 1446-1456

Marber MS, Walker JM, Latchman DS, and Yellon DM (1994). Myocardial protection following whole body heat stress in the rabbit is dependent on metabolic substrate and is related to the amount of inducible 70 kb Dalton heat shock protein. *Journal of Clinical Investigation*, **93**: 1087-1094

Marber MS, Latchman DS, Walker JM, and Yellon DM (1993). Cardiac stress protein elevation 24 hours after brief ischaemia or heat stress is associated with resistance to myocardial infarction. *Circulation Research*, **88**: 1264-1094

Marcu MG, Chadli A, Bouhouche I, Catelli M, and Neckers LM (2000). The heat shock protein 90 antagonist novobiocin interacts with a previously unrecognized ATP-binding domain in the carboxyl terminus of the chaperone. *Journal of Biological Chemistry*, **275**: 37181-37186

Martin JL, Mestril R, Hilal-Dandan R, and Brunton LL (1997). Small heat shock proteins and protection against ischemic injury in cardiac myocytes. *Circulation*, **96**: 4343-4348

Martin SJ, Reutelingsperger CPM, McGahon AJ, Rader JA, Van Schie RCAA, LaFace DM and Green DR (1995). Early distribution of plasma membrane phosphatidylserine is a general feature of apoptosis regardless of the initiating stimulus: Inhibition by overexpression of Bcl-2 and Ab1. *The Journal of Experimental Medicine*, **184**: 1545-1556

Martínez-Balbas MA, Dey A, Rabindran SK, Ozato K, and Wu C (1995). Displacement of sequence-specific transcription factors from mitotic chromatin. *Cell*, **83**: 90231-90237

Mattson MP, LaFerla FM, Chan LS, Leissring MA, Shepel PN, and Geiger JD (2000). Calcium signalling in the ER: its role in neuronal plasticity and neurodegenerative disorders. *Trends in Neurosciences*, **23**: 222-229

Maulik N, Engelman RM, Wei Z, Liu X, Rousou JA, Flack JE, Deaton DW, and Das DK (1995). Drug-induced heat shock preconditioning improves postischemic ventricular recovery after cardiopulmonary bypass. *Circulation*, **92**: 381-388

Meng X, Brown JM, Ao L, Banerjee A, and Harken AH (1996). Norepinephrine induces cardiac heat shock protein 70 and delayed cardioprotection in the rat through α_1 adrenoreceptors. *Cardiovascular Research*, **32**: 374-383

Morgan WD (1989). Transcription factor Sp1 binds to and activates a human hsp70 gene promoter. *Molecular and Cellular Biology*, **9**: 4099-4104

Morimoto RI (1998). Regulation of the heat shock transcriptional response: cross talk between a family of heat shock factors, molecular chaperones, and negative regulators. *Genes and Development*, **12**: 3788-3796.

Morimoto RI, Sarge KD, and Abravaya K (1992). Transcriptional regulation of heat shock genes. *The Journal of Biological Chemistry*, **267**: 21987-21990.

Morris SD, Cummings DVE, Latchman DS, and Yellon DS (1996). Specific inhibition of the 70 kDa heat stress proteins by the tyrosine kinase inhibitor herbimycin-A protects rat neonatal cardiomyocytes: a new pharmacological route to stress protein expression. *Journal of Clinical Investigation*, **97**: 706-712

Mosser DD, Caron AW, Bourget L, Meriin AB, Sherman MY, Morimoto RI, Massie B (2000). The chaperone function of Hsp70 is required for protection against stress-induced apoptosis. *Molecular and Cellular Biology*, **20**: 7146-7159

Nakai A, Tanabe M, Kawazoe Y, Inazawa J, Morimoto RI, and Nagata K (1997). HSF4, a new member of the human heat shock factor family which lacks

properties of a transcriptional activator. *Molecular and Cellular Biology*, **17**: 469-481

Nakai A and Morimoto RI (1993). Characterization of a novel chicken heat shock transcription factor, heat shock factor 3, suggests a new regulatory pathway. *Molecular and Cellular Biology*, **13**: 1983-1997

Nakagawa T, Zhu H, Morishima N, Li E, Xu J, Yankner BA, and Yuan J (2000). Caspase-12 mediates endoplasmic reticulum specific apoptosis and cytotoxicity by amyloid- β . *Nature*, **403**: 98-103

Nakayama K, Frew IJ, and Hagensen M (2004). Siah-2 regulates stability of prolyl-hydroxylases, controls HIF-1 α abundance, and modulates physiological responses to hypoxia. *Cell*, **117**: 941- 952

Narberhaus F (2002). α -Crystallin-type heat shock proteins: socializing minichaperones in the context of a multichaperone network. *Microbiology and Molecular Biology Reviews*, **66**: 64-93

Nicholson DW (1999). Caspase structure, proteolytic substrates, and function during apoptotic cell death. *Cell Death and Differentiation*, **6**: 1028- 1042

Nishimoto I, Okamoto T, Giambarella U and Iwatsubo T (1997). Apoptosis in neurodegenerative diseases. *Advances in Pharmacology*, **41**; 337-368

Nishitani Y and Matsumoto H (2006). Ethanol rapidly causes activation of JNK associated with ER stress under inhibition of ADH. *FEBS Letters*, **580**: 9-14

Nishizawa J, Nakai A, Higashi T, Tanabe M, Nomoto S, Matsuda K, Ban T, and Nagata K (1996). Reperfusion causes significant activation of heat shock transcription factor 1 in ischemic rat hearts. *Circulation*, **94**: 2185-2192

Ogata Y and Takahashi M (2003). Bcl-x_L as an antiapoptotic molecule for cardiomyocytes. *Drug News & Perspectives*, **16**: 446-459

Opie LH (1993). The mechanism of myocyte death in ischemia. *European Heart Journal*, **14**: 31-33

Pandey P, Saleh A, Nakazawa A, Kumar S, Srinivasula SM, Kumar V, Weichselbaum R, Nalin C, Alnemri ES, Kufe D, and Kharbanda S (2000). Negative regulation of cytochrome *c*-mediated oligomerization of Apaf-1 and activation of pro-caspase-9 by heat shock protein 90. *EMBO Journal*, **19**: 4310-4322

Parcellier A, Gurbuxani S, Schmitt E, Solary E, and Garrido C (2003). Heat shock proteins, cellular chaperones that modulate mitochondrial cell death pathways. *Biochemical and Biophysical Research Communications*, **304**: 505-512

Paul C, Manero F, Gonin S, Kretzy-Remy C, Viot S, and Arigo A (2002). Hsp27 as a negative regulator of cytochrome *c* release. *Molecular and Cellular Biology*, **22**: 816-834

Pearl LH and Prondromou C (2006). Structure and mechanism of the Hsp90 molecular chaperone machinery. *Annual Reviews in Biochemistry*, **75**: 271-294

Pfaffl MW, Horgan GW and Dempfle L (2002). Relative expression software tool (REST©) for group-wise comparison and statistical analysis of relative expression results in real-time PCR. *Nucleic Acids Research*, **30**: 1-10

Pfaffl MW (2001). A new mathematical model for relative quantification in real-time RT-PCR. *Nucleic Acids Research*, **29**: 2002-2007

Piot CA, Martini J, Bui SK, and Wolfe CL (1999). Ischaemic preconditioning attenuates ischaemia/reperfusion-induced activation of caspases and subsequent cleavage of poly(ADP-ribose) polymerase in rat hearts *in vivo*. *Cardiovascular Research*, **44**: 536-542

Pirkkala L, Nykänen P, and Sistonen L (2001). Roles of heat shock transcription factors in regulation of the heat shock response and beyond. *The FASEB Journal*, **15**: 1118-1131

Quigney DJ, Gorman AM, and Samali A (2003). Heat shock protects PC12 cells against MPP⁺ toxicity. *Brain Research*, **993**: 133-139

Rabindran SK, Giorgi G, Clos J, and Wu C (1991). Molecular cloning and expression of a human heat shock factor, HSF1. *Proceedings of the National Academy of Science of the United States of America*, **88**: 6906-6910

Rao RV, Hermel E, Castro-Obregon S, del Rio G, Ellerby LM, Ellerby HM, and Bredesen DE (2001). Coupling endoplasmic reticulum stress to the cell death program. *The Journal of Biological Chemistry*, **276**: 33869-33874

Rapoport TA (1992). Transport of proteins across the endoplasmic reticulum membrane. *Science*, **258**: 931-936

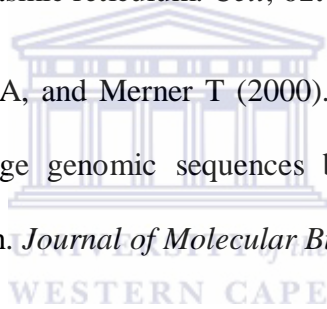
Ritossa F (1962). A new puffing pattern induced by heat shock and DNP in *Drosophila*. *Experientia*, **18**: 571-573

Ron D and Walter P (2007). Signal integration in the endoplasmic reticulum unfolded protein response. *Nature Reviews/Molecular Cell Biology*, **8**: 519-529

Salo DC, Donovan CM, and Davies KJA (1991). HSP70 and other possible heat shock proteins or oxidative stress proteins are induced in skeletal, heart, and liver during exercise. *Free Radical Biology and Medicine*, **11**: 239-246

Sambrook JF (1990). The involvement of calcium in transport of secretory proteins from the endoplasmic reticulum. *Cell*, **61**: 197-199

Scherf M, Klingenhoff A, and Merner T (2000). Highly specific localization of promoter regions in large genomic sequences by PromoterInspector: a novel context analysis approach. *Journal of Molecular Biology*, **297**: 599-606



Schröder M and Kaufman RJ (2005a). The mammalian unfolded protein response. *Annual Reviews of Biochemistry*, **74**: 739-789

Schröder M and Kaufman RJ (2005b). ER stress and the unfolded protein response. *Mutation Research*, **569**: 29-63

Schuetz TJ, Gallo GJ, Sheldon L, Tempst P, and Kingston RE (1991). Isolation of a cDNA for HSF2: evidence for two heat shock factor genes in humans. *Proceedings of the National Academy of Sciences of the United States of America*, **88**: 6911-6915

Schunkert H and Riegger GAJ (Eds.) (2000). Apoptosis in cardiac biology. Kluwer Academic Publishers, Massachusetts, USA.

Shan Y, Liu T, Sue H, Samsamshariat A, Mestril R, and Wang PH (2003). Hsp10 and Hsp60 modulate Bcl-2 family and mitochondria apoptosis signaling induced by doxorubicin in cardiac muscle cells. *Journal of Molecular and Cellular Cardiology*, **35**: 1135-1143

Sherman MY and Goldberg AL (2001). Cellular defences against unfolded proteins: a cell biologist thinks about neurodegenerative diseases. *Neuron*, **29**: 15-32

Shtutman M, Zhurinsky J, Simcha I, Albanese C, D'Amico M, Pestell R, and Ben-Ze'ev A (1999). The cyclin *D1* gene is a target of the β -catenin/LEF-1 pathway. *Proceedings of the National Academy of Sciences of the United States of America*, **96**: 5522- 5527

Snoeckx LHEH, Cornelussen RN, Van Nieuwenhoven FA, Reneman RS, and Van der Vusse GJ (2001). Heat shock proteins and cardiovascular pathology. *Physiological Reviews*, **81**: 1461- 1497

Sorger PK and Pelham HR (1988). Yeast heat shock factor is an essential DNA-binding protein that exhibits temperature-dependent phosphorylation. *Cell*, **54**: 855-864

Söti C, Nagy E, Giricz Z, Víggh L, Csemely P, and Ferdinandy P (2005). Heat shock proteins as emerging therapeutic targets. *British Journal of Pharmacology*, **146**: 769-780

Stephanou A, Brar B, Heads R, Knight RD, Marber MS, Pennica D, and Latchman DS (1998). Cardiotrophin-1 induces heat shock protein accumulation in cultured cardiac cells and protects them from stressful stimuli. *Journal of Molecular and Cellular Cardiology*, **30**: 849-855

Suzuki K, Sawa Y, Kaneda Y, Ichikawa H, Shirakura R, and Matsuda H (1997). *In vivo* gene transfection with heat shock protein 70 enhances myocardial tolerance to ischemia-reperfusion injury in rat. *The Journal of Clinical Investigation*, **99**: 1645-1650

Tanguay RM, Wu Y, and Khandjian EW (1993). Tissue-specific expression of heat shock proteins of the mouse in the absence of stress. *Developmental Genetics*, **14**: 112-118

Tannous P, Zhu H, Nemchenko A, Berry JM, Johnstone JL, Shelton JM, Miller Jr FJ, Rothermel BA, and Hill JA (2008). Intracellular protein aggregation is a proximal trigger of cardiomyocyte autophagy. *Circulation*, **117**: 3070-3078

Thornberry N A and Lazebnik Y (1998). Caspases: Enemies within. *Science*, **281**: 1312- 1316

Tissieres A, Mitchell HK, and Tracy UM (1974). Protein synthesis in salivary glands of *Drosophila melanogaster*: relation to chromosome puffs. *Journal of Molecular Biology*, **84**: 389-398

Travaria M, Gabriele T, Kola I, and Anderson RL (1999). A hitchhiker's guide to the human Hsp70 family. *Cell Stress and Chaperones*, **1**: 23-28

Travers KJ, Patil CK, Wodicka L, Lockhart DJ, Weismann JS, and Walter P (2000). Functional and genomic analyses reveal essential coordination between the unfolded protein response and the ER-associated degradation. *Cell*, **101**: 249-258

Umansky SR and Tomei LD (1997). Apoptosis in the heart. *Advances in Pharmacology*, **41**; 383-407

Vígh L, Literati PN, Horvath I, Torok Z, Balogh G, Glatz A, Kovács E, Boros I, Ferdinándy P, Parkas B, Jaszlits L, Jednákovits A, Korányi L, and Maresca B (1997). Bimoclomol: A non-toxic, hydroxylamine derivative with stress protein-inducing activity and cytoprotective effects. *Nature Medicine*, **3**: 1150-1154

Volloch V, Gabai VL, Rits S, Force T, and Sherman MY (2000). Hsp72 can protect cells from heat-induced apoptosis by accelerating the inactivation of stress kinase JNK. *Cell Stress and Chaperones*, **5**: 139-147

Von Harsdorf R, Li PF, and Dietz R (1999). Signalling pathways in reactive oxygen species-induced cardiomyocyte apoptosis. *Circulation*, **99**: 2934-2941

Webb SJ, Harrison DJ and Wyllie AH (1997). Apoptosis: An overview of the process and its relevance in disease. *Advances in Pharmacology*, **41**; 1-34

Werner T (2001). Target gene identification from expression array data by promoter analysis. *Biomolecular Engineering*, **17**: 87-94

Wilke N, Sganga MW, Gayer GG, Hsieh K, and Mills MF (2000). Characterization of promoter elements mediating ethanol regulation of *hsc70* gene transcription. *The Journal of Pharmacology and Experimental Therapeutics*, **292**: 173-180

World Health Statistics 2010. World Health Organisation

Wu C (1995). Heat shock transcription factors: structure and regulation. *Annual Reviews of Cell and Developmental Biology*, **11**: 441-469

Wytttenbach A, Carmichael J, Swartz J, Furlong RA, Narain Y, Rankin J, and Rubinsztein DC (2002). Effects of heat shock, heat shock protein 40 (HDJ-2) and proteasome inhibition on protein aggregation in cellular models of Huntington's disease. *Proceedings of the National AAcademy of Science of the United States of America*, **97**: 2898-2903

Yellon DM and Hausenloy DJ (2007). Myocardial reperfusion injury. *The New England Journal of Medicine*, **357**: 1121-1135

Yellon DM, Latchman DS, and Marber MS (1993). Stress proteins, and endogenous route to myocardial protection; fact or fiction? *Cardiovascular Research*, **27**: 158-161

Zheng TS, Hunot S, Kuida K, and Flavel RA (1999). Caspase knockouts: matters of life and death. *Cell Death and Differentiaion*, **6**: 1043-1053

Zhou BB and Elledge SJ (2000). The DNA damage response: Putting checkpoints in perspective. *Nature*, **408**: 433- 439

Zweier JL, Flaherty JT, and Weisfeldt ML (1987). Direct measurement of free radical generation following reperfusion of ischemic myocardium. *Proceedings of the National Academy of Sciences of the United States of America*, **84**: 1404-1407

Web references

<http://www.genomatix.de/>

<http://www.google.com/>

<http://www.ncbi.nlm.nih.gov/>

<http://openwetware.org/>

<http://www.speakingofresearch.files.wordpress.com/>

